Durham E-Theses

Disturbed weather measurements in atmospheric electricity using an instrumented van

Groom, Kenneth N.

ABSTRACT

Precipitation currents have been measured using an exposed receiver. Compensation for field currents has been achieved by subtracting the field currents to a probe, suitably amplified, from the total current to the exposed receiver. The potential gradient has been measured using a field mill, the theory of which has been rederived. Wind speed was also measured with a contact cup anemometer. The apparatus was installed in a Land Rover thus providing a mobile observatory.

The results obtained led to an analysis of the conditions in quiet rain when the inverse relation is not evident. The slope of the regression line between current and potential gradient is shown to depend upon the phase angle of the lag between the current-time and potential gradient-time records.

A method for deducing the lag or lead in records when the mirror image effect is not apparent has been evolved from consideration of the Lissajous plots first described by RAMSAY (1950). The method has been used to show some support for the ideas of CHALMERS (1965) concerning the behaviour of records taken beneath approaching and developing cloud systems. Both the approaching and developing situations have been observed.

An experiment has been described which conclusively shows the pylon to be the sourceof negative space charge associated with power lines in mist or fog. An explanation is offered in terms of the different mobilities of free electrons and positive ions which are supposed

to be formed byionisation due to tracking across the damp insulators. The electrons are shown during the negative phase of the line voltage to travel a distance before their capture which is greater than that from which they can be drawn back when the polarity of the alternating voltage changes.

Measurements of polar conductivities at two levels, above and below the $0^{o}C$ isotherm, have been made during steady snowfall with a Gerdien conductivity chamber. From these measurements the charge separation rate in the melting region has been estimated.

DISTURBED WEATHER MEASUREMENTS IN

ATMOSPHERIC ELECTRICITY USING AN

INSTRUMENTED VAN

by

KENNETH N. GROOM, M.Sc.,Grad.Inst.P.,F.R.Met.S.

Presented in Candidature for the Degree of Doctor

of Philosophy, in the University of Durham.

September 1966.

FOREWORD

The experimental work described herein was performed in an instrumental van. The vehicle used was a long wheel-base hard top Land Rover.

Being mobile, the van was suitable for investigations other than the main topic described. In fact, several minor investigations have been attempted, often in collaboration with a fellow research student, Mr. T. L. Ogden.

This Thesis has been written in two distinct parts. The first describes the main investigation of rain electricity. The minor investigations have been grouped together and appear in the second part.

Extensive use has been made of diagrams both in the description of apparatus and the presentation and discussion of results. It is felt that this procedure leads to a reduction in descriptive text.

The units of the work are rationalised M.K.S. The well known abbreviations such as μ for 10^{-6} and k for 10^{3} have been adopted and used without comment as to their meaning. Often in the construction of apparatus, dimensions do not have to be chosen by physical considerations; where this has been done no conversion from English to metric units has been made.

ABSTRACT

Precipitation currents have been measured using an exposed
receiver. Compensation for field currents has been achieved by
subtracting the field currents to a probe, suitably amplified,
from the total current to the exposed receiver. The potential
gradient has been measured using a field mill, the theory of which
has been rederived. Wind speed was also measured with a contact
cup anemometer. The apparatus was installed in a Land Rover thus
providing a mobile observatory.

The results obtained led to an analysis of the conditions in
quiet rain when the inverse relation is not evident. The slope of
the regression line between current and potential gradient is shown
to depend upon the phase angle of lag between the current-time and
potential gradient-time records.

A method for deducing the lag or lead in records when the
mirror image effect is not apparent has been evolved from consideration
of the Lissajous plots first described by RAMSAY (1960). The method
has been used to show some support for the ideas of CHALMERS (1965)
concerning the behaviour of records taken beneath approaching and
developing cloud systems. Both the approaching and developing situa-
tions have been observed.

An experiment has been described which conclusively shows the
pylon to be the source of negative space charge associated with
power lines in mist or fog. An explanation is offered in terms of
the different mobilities of free electrons and positive ions which

are supposed to be formed by ionisation due to tracking across the damp insulators. The electrons are shown during the negative phase of the line voltage to travel a distance before their capture which is greater than that from which they can be drawn back when the polarity of the alternating voltage changes.

Measurements of polar conductivities at two levels, above and below the $0^{o}C$ isotherm, have been made during steady snowfall with a Gerdien conductivity chamber. From these measurements the charge separation rate in the melting region has been estimated.

CONTENTS

PART I   Investigation of Precipitation Electricity

PART I

Chapters 1 to 6

Investigation of Precipitation Electricity

CHAPTER 1

Introduction

1.1 Note on the chapter's content

It is not the author's intention to give a survey of the

history and current state of Atmospheric Electricity. If he desires,

the reader can find such surveys in the literature e.g. WILSON (1950),

WORMELL (1953), CHALMERS (1957) and ISRAEL (1961).

Reference will be made to relevant previous work in the subject

where it is applicable. This introduction will be confined to a

brief discussion of the possible causes of the effects which the

investigation has attempted to measure.

1.2 Continuous Rainfall

For the purposes of electrical investigation GSCHWEND (1920) has

classified rainfall into three types: continuous or quiet rain,

shower or squall rain and electrical storm rain. The investigation

described was only concerned with continuous rain.

Continuous rain generally falls from Nimbo-stratus clouds,

although quite long periods of rain sometimes fall from Alto-stratus

clouds. For the purposes of this investigation both clouds can be

considered as only differing in altitude. The usual mode of formation

of these clouds is the warm front. In the warm front air rises slowly

up a gradient of about 1 in 100. The resultant cooling causes

condensation and cloud formation.

It is generally accepted that BERGERON (1933) has correctly accounted for the origination of most precipitation in temperate climates. Precipitation in frontal conditions will always start as snow which may or may not melt before reaching the ground.

In all stages of the history of a precipitation particle from its formation to its arrival at the ground there are some charging mechanisms which may be operating. These may be conveniently split up and the charging considered in distinct regimes. These are the solid and liquid phases and the transition from solid to liquid. To these three must be added any charging which occurs because of splashing at the ground.

CHALMERS (1959) has demonstrated that models of the electrical structure of nimbo-stratus clouds can be built without a detailed consideration of the charging mechanisms concerned. As such consideration is a huge field in itself, space does not permit its inclusion here.

1.3   The Electrical Structure of Nimbo-Stratus Clouds

CHALMERS (1959) considers the nimbo-stratus cloud as being of sufficient horizonal dimensions to render the edge effects negligible. The quasi-steady state, which for nimbo-stratus can be taken as observationally established, implies that the total vertical current density is independent of height. The components of the total current namely precipitation, conduction and convection currents vary in their contribution with height. (e.g. the total current will

be comprised completely of the conduction current above the cloud).

Although an analytical solution of the general proble.. is impossible Chalmers has worked out two limiting cases for both rain and snow clouds between which the true solutions are likely to lie. The result of Chalmers's analysis for rain clouds, which is reproduced in fig. 1.1, was a vertical profile of potential. Since the rain began as snow which is usually negative there must be a process of charging at or below the melting level to give the positive rain current usually observed e.g. CHALMERS (1956). The negative space charge liberated in such a separation accounts for the negative potential peak shown in the profile. The profile (c) is the case where the charge separation takes place at or near the ground by, as SMITH (1955) suggests, splashing for example. Profile (a) is the case where the separation takes place above the cloud base.

Chalmers believes that (c) is less likely than (a) to be near the true state of affairs because the space charge in the cloud is known to be everywhere negative. A negative space charge requires that the profile should be convex, viewed from the left, as a simple qualitative examination, fig. 1.2, of Poisson's equation shows. Hence it can be seen that (a) satisfies the requirement where (c) does not.

1.4 The Scope of the Present Work

Using a Land Rover apparatus to measure precipitation current and potential gradient has been rendered mobile. From Durham it is quite easy to reach places which are 1,000 - 2,000 ft. above sea level.

Often, particularly in nimbo-stratus conditions such places are within the cloud. It is thus possible to investigate the electrical nature of the cloud itself.

Mobile apparatus also affords the possibility of making comparisons of potential gradient and current at different levels in and below the same cloud. Such comparisons, in a quasi-steady state, could be of great importance in investigating the vertical profiles of electrical parameters, so adding further information to the work of CHALMERS (1959).

CHAPTER 2

The Design and Development of Apparatus

2.1 The Measurement of Precipitation Current Density

The choice between exposed and shielded receivers for the measurement of precipitation current has been discussed since the first measurements were made; with shielded collector by Elster and Geitel (1888) and WEISS (1906) with his exposed wire brush, which would almost certainly have been plagued by point discharge.

The main drawbacks of the exposed receiver is the displacement current which is also received due to changes in potential gradient. Compensation for displacement current is necessary if exposed receiver results are to be meaningful.

The shielded collector avoids displacement current by collecting the rain in a cone, usually, which is shielded from the potential gradient. This method is successful at all experimental sites except those at places with a very high exposure to potential gradient. The top of a metal mast causes a concentration of potential gradient such that adequate shielding of a receiver is quite impractical (see COLLIN and RAISBECK 1964). The shielded collector suffers from the drawback that not all the rain is collected. SCRASE (1938) reported that his collector only received half the amount of a standard rain gauge. Furthermore the sample collected is not usually typical of the rain falling. Since in the presence of wind the smaller drops are carried closer to the horizontal than are the larger. The

result is that a shielded collector will collect a greater proportion of larger drops than is typical of the rain.

This drawback was demonstrated quite dramatically in the present investigation. On one occasion a shielded collector was borrowed by the author during conditions of drizzle. The current measured was found to be less when the collector was vertical compared with when it was horizontal facing into the wind!

For this investigation it was decided that an exposed receiver would be more suitable as a greater collection area is possible. Thus facilitating a greater signal to noise ratio - an important consideration for apparatus which has to be carried, perhaps over rough country, in a Land Rover.

The first method to be considered was an adaptation of the method used by WILSON (1908) to measure air-earth current (see also CHALMERS 1962). The apparatus needed would simply have been an insulated plate with a covering mechanism.

As the general aim in the design of the apparatus was to make it suitable for eventual automatic recording, this method was not adopted as the mechanics of covering and uncovering a large plate would have been difficult to automate. The electronics are quite feasible as the timing could have been controlled by a stepping circuit. However, it was decided to have a separate plate for precipitation current and a field machine for potential gradient.

The collection plate

The plate constructed was circular. This shape was adopted in order to minimise the relative importance of edge effects. The signal from rain current is proportional to the area of the plate while the noise from edge effects is proportional to the perimeter. A circle, therefore, maximises the signal to noise ratio.

The maximum area which could be conveniently supported on the roof of the Land Rover was $0.5 \ m^2$. Walls of 3 inches were spot welded onto a circular plate of area $0.5 \ m^2$. The intervals between the spot welds were plugged with fibre glass compound to prevent leakage of water from the plate. Such leakage would give spurious results since the tray would behave as a water dropper; drops carrying away charge depending upon the potential gradient.

The plate was supported on five insulators, initially polystyrene (see later), distributed so as to bear the load equally.

The lead from the plate to the amplifier in the van below was a 1 cm diameter helix of stiff copper wire of diameter 2 mm. This construction allows the lead to be rigid during recording due to the stiffness of the wire, thus eliminating spurious piezoelectric currents; while the helix can take up any movement induced by the motion of the Land Rover in travelling which may have damaged a straight rigid conductor.

Guard ring

One of the main edge effects in these measurements is the charge which leaves the collector on a droplet produced by a drop splashing

on the collector tray. If such droplets stay in the air they give no cause for worry as this is a natural charge separation. If, however, they fall to earth off the tray they add a spurious component to the results. The effect can be compensated for by adding a guard ring, as suggested by WILSON (1916). Compensation is achieved since, in the presence of a guard ring there is on average an equal flux of droplets in and out of the collector tray.

Electronics

The order of magnitude of precipitation current density ranges from 10^{-12} to 10^{-10} Am^{-2} for continuous rain up to 10^{-8} Am^{-2} in showers, the highest ever recorded being 10^{-7} (CHALMERS and LITTLE 1947). The current density can be measured either by measuring the charge collected in an interval or by direct current measurement. For nimbo-stratus the range of interest will be that of continuous rain namely 10^{-12} to 10^{-10} A m^{-2}. For collection over periods of some minutes charges of the order 10^{-10} to 10^{-8} Coulombs would be collected.

Measurement of charges of this order is impractical with a ballistic galvanometer since the Land Rover's motion would upset the delicate levelling necessary. The charge would have to have been measured by the voltage it exerts across a capacitor. Since this voltage will be transitory it would be of dubious value for automatic recording unless the voltage was measured with a voltmeter of extremely high input impedance.

The best configuration for ultra high impedance valve voltmeters, the inverted triode, is described for example by ROWSON (1960) or

TRIMAR (1928)(see fig. 2.1). However for the use invisaged there is a fundamental drawback - there is no way of discriminating the sign of the voltage.

It was thought that a compromise may have been reached by using a normal electrometer valve even though the decay would have been more rapid. Although such circuits, fig. 2.2, work satisfactorily the decay was always found to be too rapid for automatic recording.

The voltage produced on a capacitor by a charge could alternatively be measured by a chopper type amplifier. A transistor chopper would not be suitable as it would, in the conduction regime, earth and so remove the charge being measured. However, a vibrating capacitor would be suitable if the A.C. amplification stage following it had a high input impedance. The sign of the charge would have to be determined by employing phase sensitive rectification.

The above is in fact a brief description of a vibrating reed electrometer (VRE) - the instrument which was in fact finally adopted for use. As a VRE was used it was possible to measure the current to earth from the plate directly, which is more useful than the discontinuous charge measurements.

The VRE which has been amply described elsewhere requires a power supply of 240 volts AC at 50 c/s. Such a supply was generated by a solid state transverter from a DC supply of 24 v from Lead-Acid Accumulators.
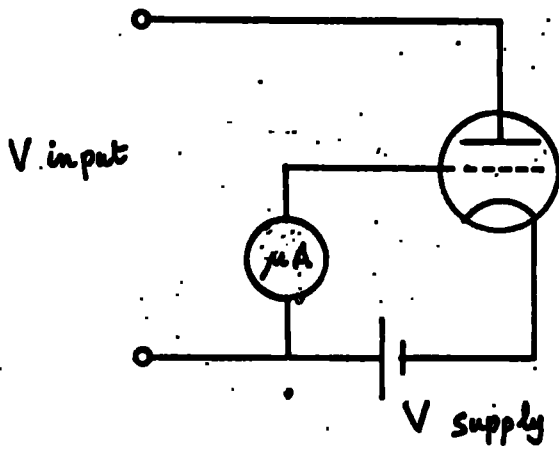
Fig. 2.1   Inverted triode voltmeter
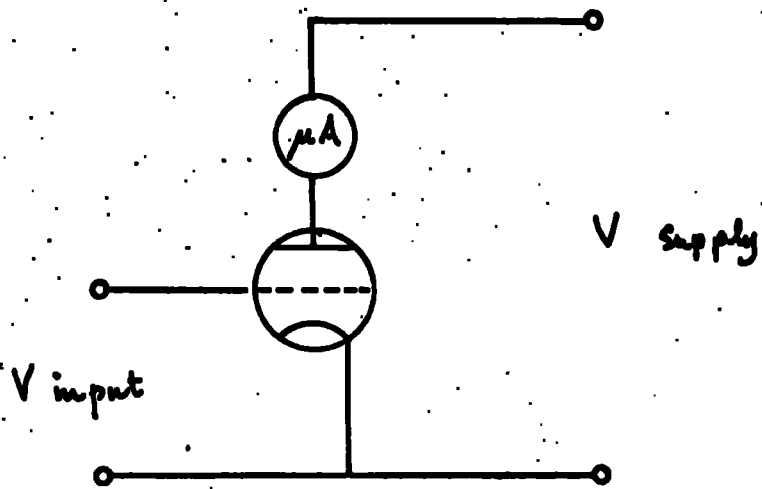
Fig. 2.2   Electrometer valve voltmeter

Insulation

The problem of the maintenance of high insulation in the lower atmosphere has always been difficult. DOLEZALEK (1956) has even been moved to the production of a publication on just this problem. The problem is to produce an insulator the resistance of which will not fall to an intolerable level under conditions of high humidity.

The best known insulating material readily available is polytetraflouroethelene (P.T.F.E.). The properties of P.T.F.E. are well documented in the various trade publications of the manufacturers. In the atmosphere the surface resistivity is most liable to failure due to the formation of a film of water over the insulator surface. An important and relevant property of P.T.F.E. is its angle of contact to water which is very close to 180°, causing any surface moisture to form droplets and roll off, thus keeping a dry surface. As the insulators were not readily accessible (see fig. 2.3) it was important that they should be reliable. A small scale test was conducted with a sample insulator. With the equipment at hand the highest measurable resistance was $10^{12}\Omega$. This is quite a convenient value as it coincides with the highest input impedance of the VRE. The experiment (fig. 2.4) consisted of placing the sample insulator in a controlled atmosphere the relative humidity of which was raised from 60 to 100%. Up to 85% RH the resistance was in excess of 10^{12} ohms decreasing to 4.10^{11} ohms at 100% RH.

It would seem that in using apparatus where the high input resistance was needed some heating of the insulators would be necessary

AMPLIFIER

10 cm.

FIG. 2.3   Collector plates and pulse pipe

I

Insulator under test in controlled environment.

E

$10^8 \Omega$

V   Valve Voltmeter
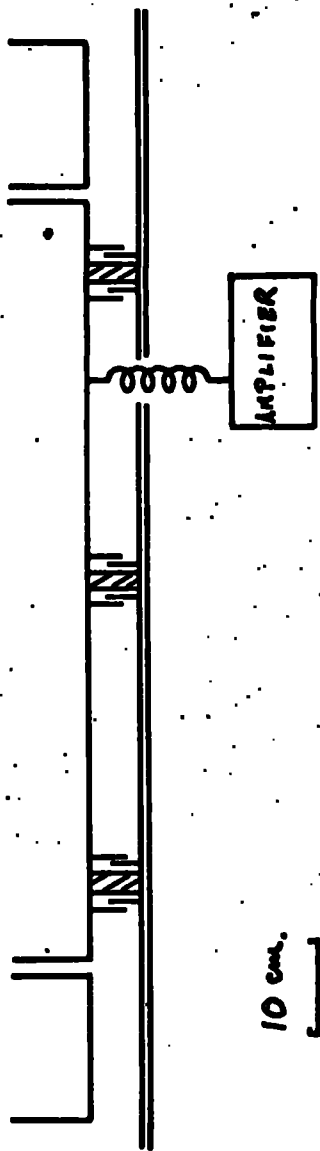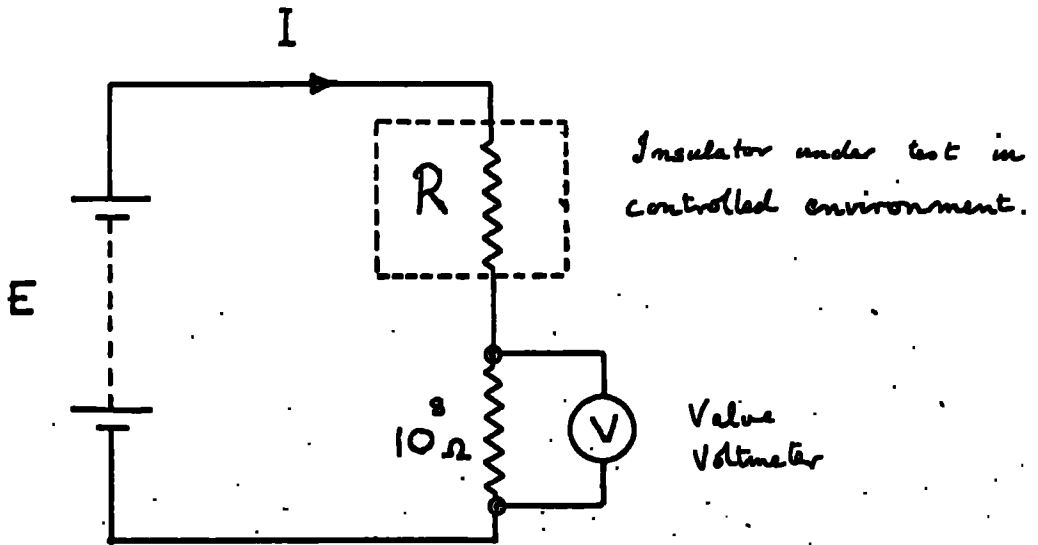
$I = \dfrac{V}{10^8} \simeq \dfrac{E}{R}$

$R \gg 10^8$

$R \simeq \dfrac{E}{V} \times 10^8 \; \Omega$

Fig 2·4   Setup for insulator test.

to keep the humidity low, whilst this would not be necessary for lower input impedance instruments.

Now since atmospheric water carries a large amount of impurity it was decided that it would be unwise to allow any condensation on the insulator in case a build up of surface dirt occurred which would have lowered the surface resistivity. It was decided that the plate insulators would have heating in spite of the foregoing paragraph just to be on the safe side.

The heating was done initially with a small coil of wire round each insulator each dissipating about $2\frac{1}{2}$ watts. As some trouble was experienced due to the low mechanical strength of the heater coils they were subsequently replaced by small 2.2 w bulbs which proved most reliable.

The configuration of the insulators and thin housing is shown in fig. 2.5. The insulator in the diagram can be seen to have grooves cut into it. These grooves increase the path for the surface breakdown and, more important, the grooves are cut on a lathe with a clean tool just before the insulators are mounted. It was found that the new cut surface had a very much higher surface resistance than a carefully cleaned old surface.

Compensation for displacement currents

With an exposed receiver the current measured is the sum of three components; the precipitation current, the conduction current and the displacement current i.e. for a plate area A

$$ I = A \left(j_p + \lambda F + \epsilon \frac{dF}{dt} \right) $$

Collector Plate

Protecting Cylinders

Base Plate

2.2 W heater bulb
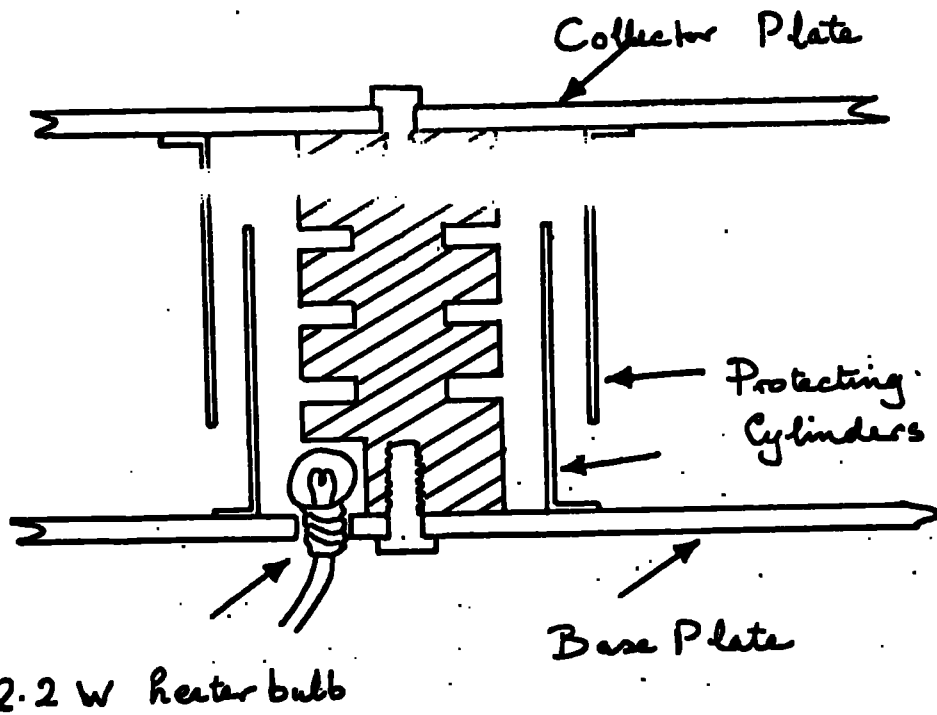
(Full Scale)

Fig. 2.5   The collector insulator housing

where λ is the appropriate polar conductivity at the plate

F is the potential gradient

A is the area of the collection plate

ϵ is atmospheric permittivity

The conduction current density (λF) will often, though not always, be negligible compared with the precipitation current density (j_p). However, the displacement current density $\epsilon \frac{dF}{dt}$ can quite easily be very much greater than and often of the same order as the precipitation current density. Fig. 2.6 shows the record of a displacement current superimposed upon an otherwise tolerably steady rain current. Since both the conduction and displacement currents are controlled by the behaviour of the electric field they can for convenience be lumped together and called "field currents".

ADAMSON (1960) has described apparatus to measure conduction current with compensation for displacement current. He took the differential output of a field mill and applied it to one grid of a double electrometer triode: the collector output was applied to the second grid. Amplification of the difference in anode voltages will, if the time constants are equally matched, be a measure of conduction current. The method which produced good results in all but very disturbed conditions follows SCRASE's (1933) vain attempt at compensation.

Application of Adamson's technique to the present problem involves interference with the input circuitry of the VRE which
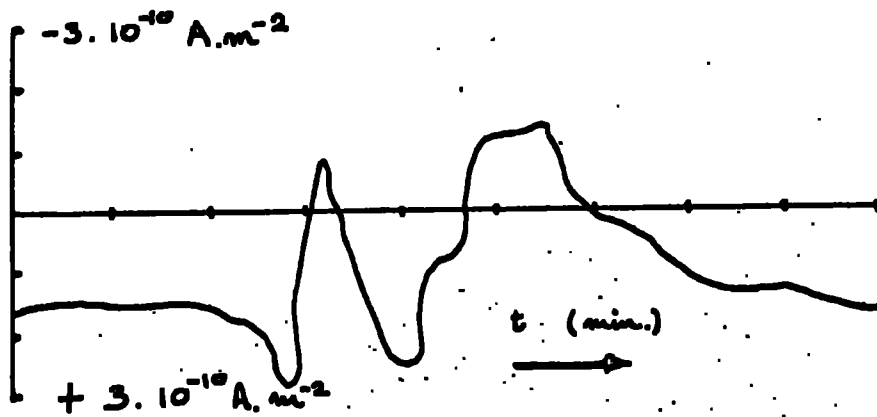
Fig. 2.6   Displacement currents

was not thought to be desirable.

MUHLEISSEN (private communication) has used earthed vertical conducting rods as shielding for a collector mounted in the plane of the earth's surface. Such shieldings which would only interfere with the precipitation to a small extent, was found to eliminate the potential gradient at the collector. Such a method would give the desirable properties of both exposed and shielded receivers.

Electrolytic tank experiments

The plausibility of Muhleissen's idea for a collector mounted on the roof of a van was investigated in two dimensions for various models in an electrolytic tank.

The models under test were attached to an earthed plate. The equipotential surfaces between the plates were plotted by selecting a voltage with the potential dividing resistance boxes R_1 and R_2 (see fig. 2.7) and adjusting the position of the probe with the loud speaker registers minimum sound.

Two shapes of model were investigated, fig. 2.8, which approached Muhleissen's use in the plane of the earth's surface and the possible configuration on the van. In practice shielding posts would have to be separated by about 1.3 m. Any post height in excess of 2 m would be quite impractical, so the maximum height: separation ratio worth investigation was 3:2. The equipotential diagrams in fig. 2.9 show evidence of good shielding for high ratios.

In the second model the potential of the plate was determined by placing the probe on the collector and adjusting R_1 and R_2 until
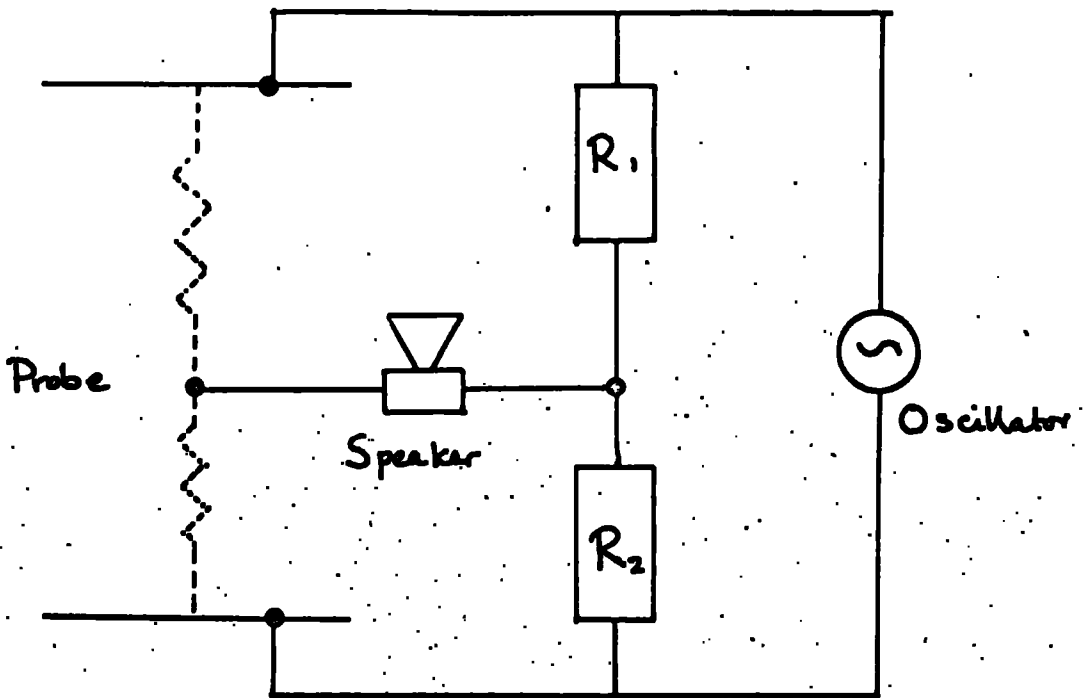
Fig. 2.7 Schematic arrangement of electrolytic tank
experiments
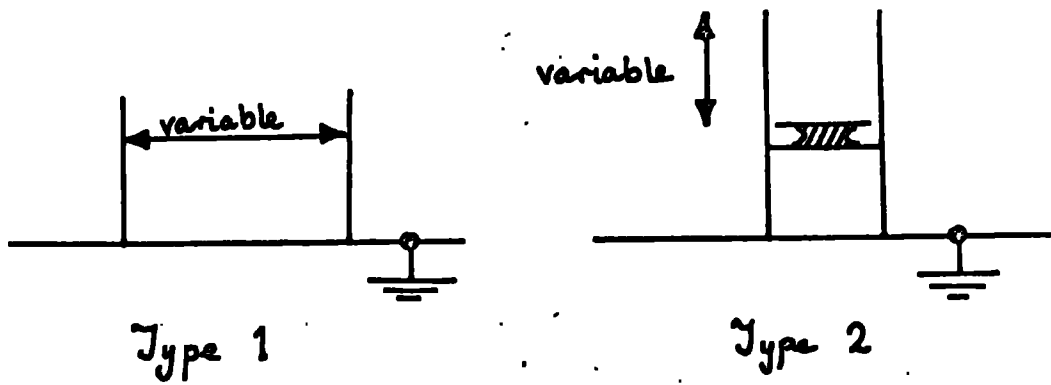
Fig. 2.8   Model shapes investigated
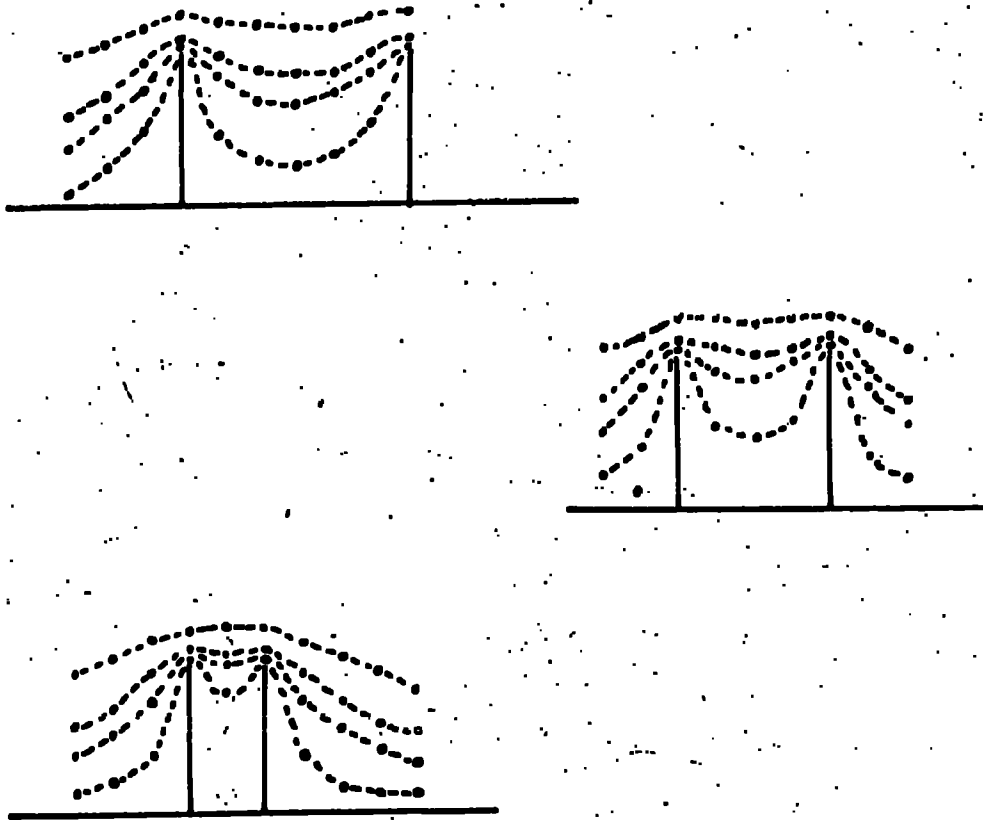
Fig. 2.9   Results with type 1 model

a balance point was found. The ratio of $\dfrac{R_2}{R_1+R_2}$ gives the ratio of the voltage of the collector to the total potential difference applied. The reduction factor can be defined as the ratio of the potential with shielding to that without. From a graph of reduction factor against shielding height (fig. 2.10) it was deduced that a height of about 2 m would give a 1% reduction factor.

Field trials of post shielding

Three posts, (2 m high of $\frac{1}{2}$ inch diameter brass rod) were erected symmetrically about the collector plate. The tip of each rod was turned to a hemisphere.

The testing procedure consisted of placing a portable field mill in the centre of the collector and comparing the reading in the presence and absence of the shielding posts. A fine day was chosen and the ambient potential gradient monitored with a second field mill. Unfortunately no significant reduction in the field mill reading was observed, indicating that the posts provided negligible shielding. The project was dropped forthwith.

Compensation by direct measurement of field current

An obvious method of compensation is to subtract the field current from the total current. To do this it is necessary to measure the field current arriving in an area equal to that of the collecting plate. Ideally, what is required is a second plate adjacent to the first which can be "persuaded" not to accept any rain. As this cannot be done what is required is some device which will accept the same number of lines of force as the total current collecting
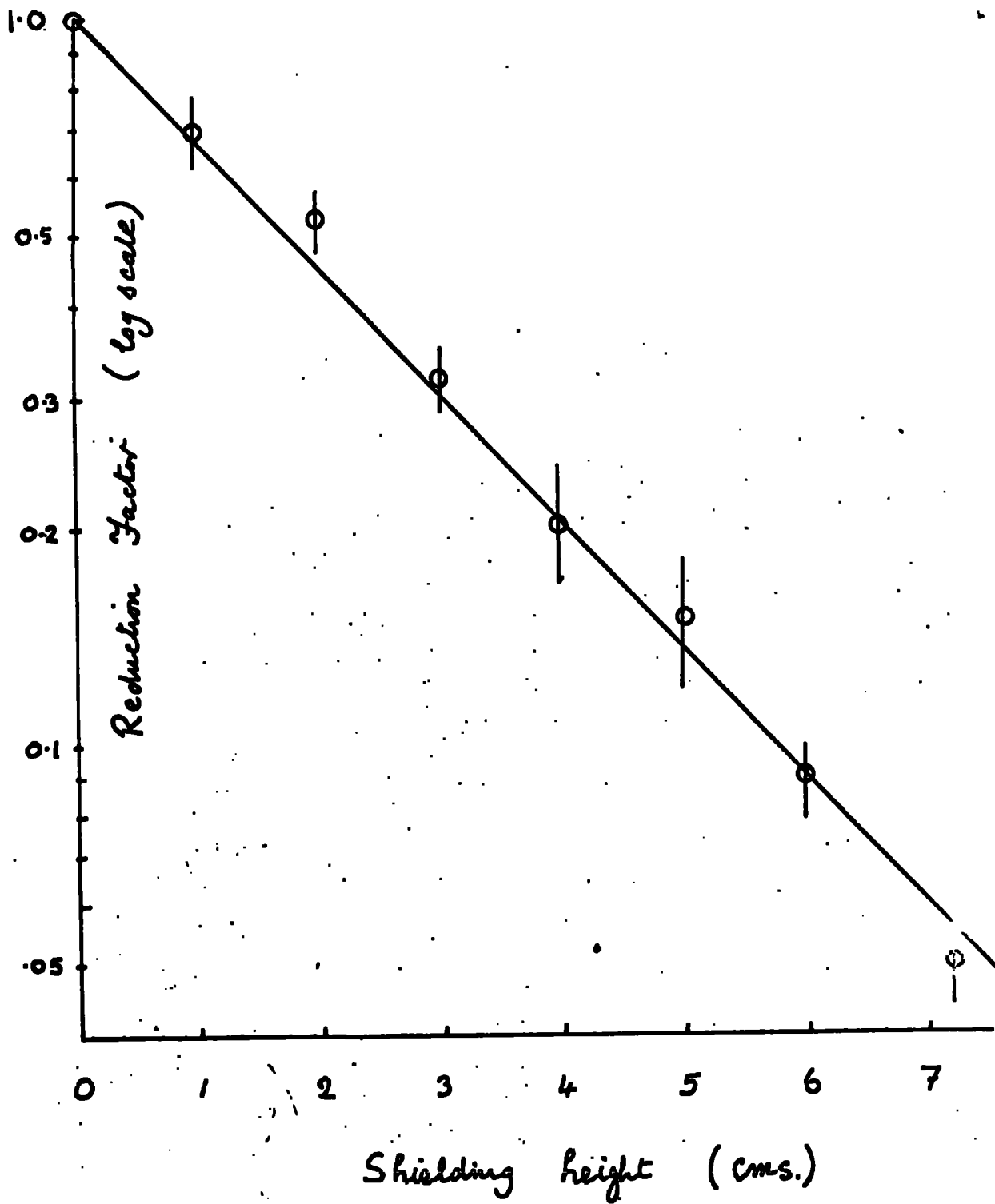
Fig. 2.10   Type 2 model results

plate, but will not accept any rain. This could be done by inverting a plate so that the rain cannot enter; lines of force would, however, reach the plate in the same way as they reach an inverted field mill.

Experience with field mills has shown that some exposure is lost when they are inverted. Thus it would seem that the area of the inverted plate needed to collect the same number of lines of force would have to be greater than the 0.5 m^2 area of the original collector plate.

If the exposure could be increased the size could be reduced. It was decided that perhaps an inverted point could be used instead of an inverted plate as this would have a greater exposure to the field. This method was adopted in the hope that the position of the point could be so adjusted that the point would have an equivalent plane area equal to that of the plate.

Measurement showed that this could not easily be done. However, it was realised that the output of the probe could be amplified up before the subtraction was performed.

The field current probe was constructed from a small rounded point protected by a brass umbrella fig. 2.11.

A second V.R.E. had by this time been requested for the other van-borne experiment by Mr. T.L. Ogden. It was decided that the D.C. amplifier KE 503B made by Rank Nucleonics should be suitable for the measurements of precipitation current although not sensitive enough for the space charge measurements as initially planned by Mr. Ogden.

Insulators

Heaters

Umbrella

1 inch
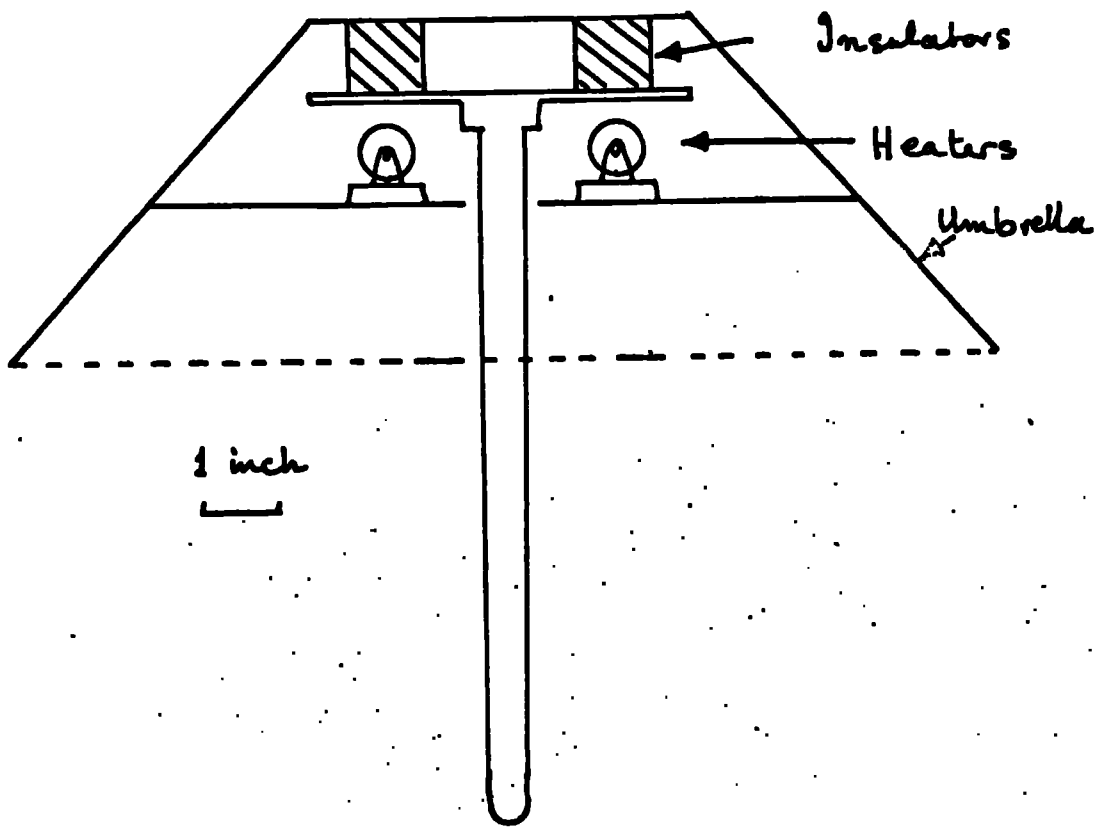
Fig. 2.11   The field current probe

The obvious course of an exchange was taken. Two TM 503B amplifiers were purchased and employed for the measurement of the plate and probe currents.

The difference between the plate and probe currents would give the precipitation current if the equivalent plane area of the probe is equal to that of the plate.

The probe was attached to the back of the van, the point being about 6 ft. above ground level. Now if the equivalent plane area is not equal to the plate area; the gain of the amplifier can be adjusted to give an output which can be matched with the output from the probe in non precipitating conditions.

To determine the equivalent plane area of the probe the outputs of the two amplifiers were recorded on a chart, a section of the record of which is reproduced in fig. 2.12. Values of current from both records were plotted on a graph shown in fig. 2.13. The small non zero intercept was due to an incorrect zero setting of the chart. This, however, was not of importance as it is the slope of the line which gives the quantity of interest. The slope was found to be $\frac{3.04}{2.63}$ x 10^{-2}. As the area of the plate was 0.5 m^2 the equivalent plane area of the probe is 0.5 x $\frac{3.04}{2.63}$ x 10^{-2} m^2 = $\frac{1.52}{1.31}$ x 10^{-2} m^2. It was found that, and can be discerned from fig. 2.12, that there was a difference in the time constants of the two amplifiers. As the makers strongly discouraged the interference with the input circuitry it was decided to measure the difference with apparatus having a long time constant - the idea being that the differences due to the mis match
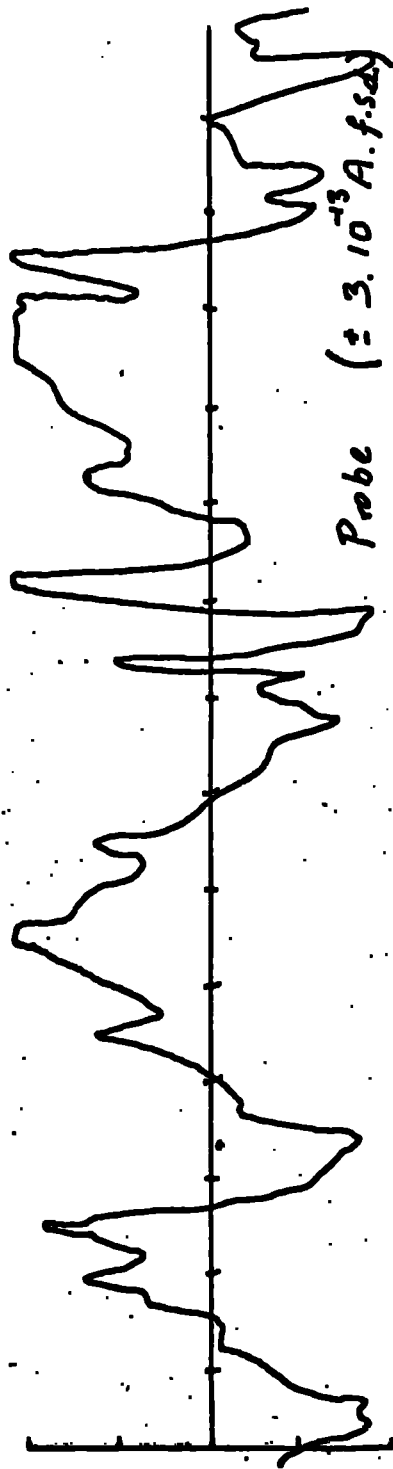
Fig. 2.12 Displacement currents to plate and probe 3.2.66

Plate $(\pm 8.10^{-12} A.f.s.d.)$

Probe $(\pm 3.10^{-13} A.f.s.d.)$

t axis
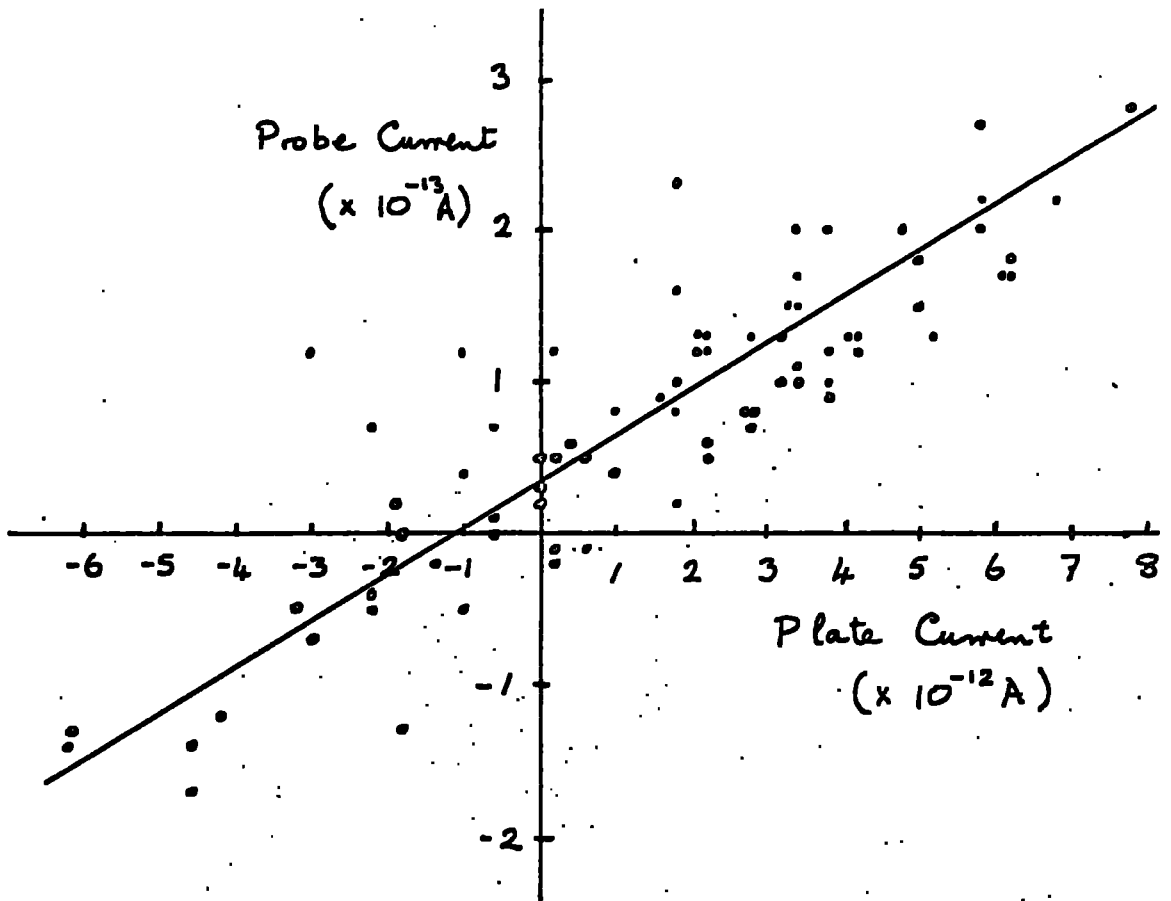
Fig. 2.13 Scatter diagram for displacement currents 3.2.66

of time constants would be smoothed out.

The device used to indicate the difference had to have a time constant of about 30 sec. The output of each NE 503B feeds a low impedance so the value of capacitor necessary is prohibitively large. What was needed was a device with a low input impedance and a high output impedance. The device,used fig. 2.14, was what is known as a long tailed pair and is often used for temperature compensation in D.C. amplifiers. Each transistor deals with one signal and the difference between the two is indicated on the voltmeter. The capacitor of 1000μF imposes a time constant of 30 sec. The setting controls RV1 and RV2 are used to set the zero under open and short circuit conditions respectively.

The gain of the probe's amplifier was adjusted until no difference could be detected between the plate's and the probe's output during non precipitating conditions. This system worked satisfactorily in nimbo status weather when conditions are not generally violent. The system could not compensate for displacement currents caused by small local space charges which influence the probe and plate at different times and possibly to different amounts. This was probably the cause of the scatter shown in fig. 2.13.

A direct calibration of the difference amplifier was performed, the results of which are shown in fig. 2.15. It was not thought necessary to calibrate the Rank D.C. amplifiers.
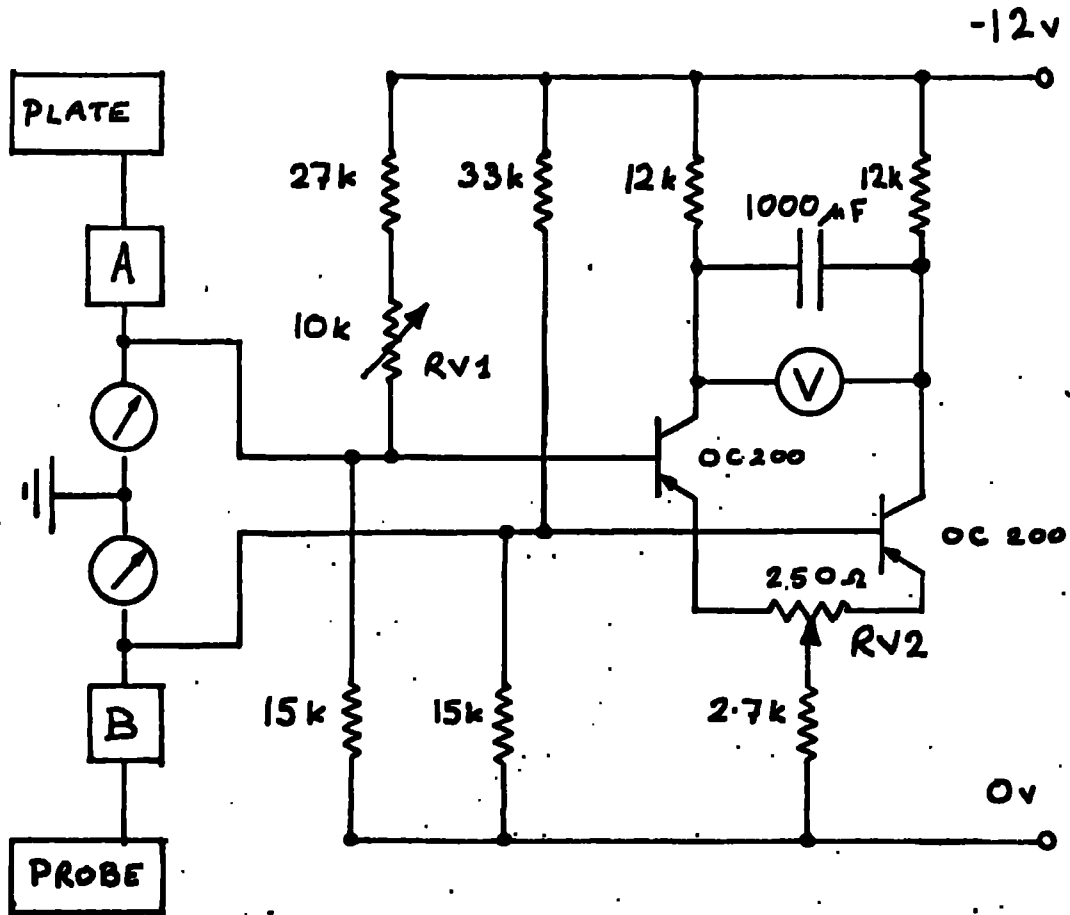
Fig. 2.14   The difference amplifier
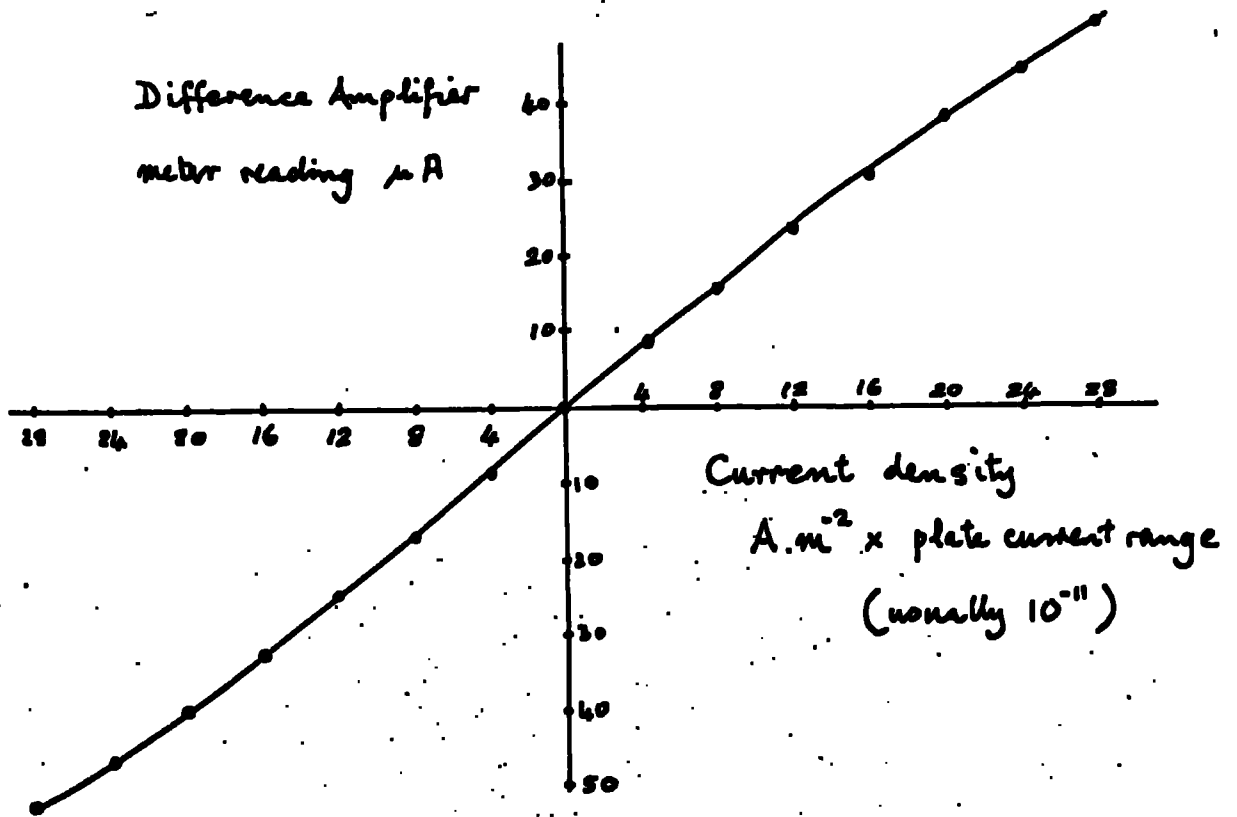
Fig. 2.15 : Difference amplifier calibration

2.2 The Measurement of Potential Gradient

The vertical potential gradient can be measured directly with potential equalisers at different heights. This method usually involves a long period for equalisation unless radioactive equalisers are used. However, as the radioactivity may distort the measurement of other parameters the indirect method is usually preferred. (The passive probe antenna described by CROZIER (1963) is not convenient for portable apparatus).

Coulomb's law gives the surface charge density σ bound onto a plane conducting surface by a potential gradient F as

$$\sigma = - \epsilon F$$

where ϵ is the permittivity of the medium. In the case of the atmosphere ϵ can be taken as ϵ_o, the permittivity of free space 8.85×10^{-12} F m^{-1}. For a typical fine weather potential gradient of 100 v m^{-1} the surface charge density is of the order of 10^{-9} coulombs per square metre.

This charge density is measured with field machines by shielding some conductor which has been exposed to the potential gradient whereupon the charge is no longer bound and flows in the direction of earth. The shielding exposure cycle is achieved by moving the shielding so as to alternately expose and shield the sensing plate, or to move the sensing plate beneath the shielding. The field mill is of the former type whilst the agrimeter (CHALMERS 1953) and the electrostatic voltmeter (MATHIAS 1926) are of the latter.

The outputs of the agrimeter and electrostatic voltmeter are both proportional to the surface charge density and the frequency of the exposure-shielding cycle. Suppose an electrostatic voltmeter has an area of 50 cm^2 exposed to a potential gradient of 100 v m^{-1}. Then for a frequency of 50 c/s the output current will be about 5×10^{-10} Amps. (The detailed theory of the electrostatic voltmeter can be found in KASEMIR 1944). In view of the difficulty of amplifying direct as opposed to alternating currents a field mill was used.

The theory of the field mill

Signal amplitude

The exposure-shielding cycle in a field mill is usually achieved by rotating a vane which is cut into segments of a circle over a similar sensing plate (fig. 2.16). For a vane of N sectors the apex angle of each vane is π/N.

The exposable area of the vane is $(r_2^2 - r_1^2)\pi/2$ which can be written as

$$\left(r_2^2 - r_1^2\right) N \phi / 2$$

Now the charge bound to an area A by a potential gradient F is

$$q = - \epsilon A F$$

If the charge on the plate when screened is q_o then the charge q_t in an intermediate position is given by

$$q_t = q_o - \epsilon_o A F \frac{\omega t}{\pi}$$

where ω is the angular velocity of the rotor and t is the time elapsed

$$\phi = \pi/N$$
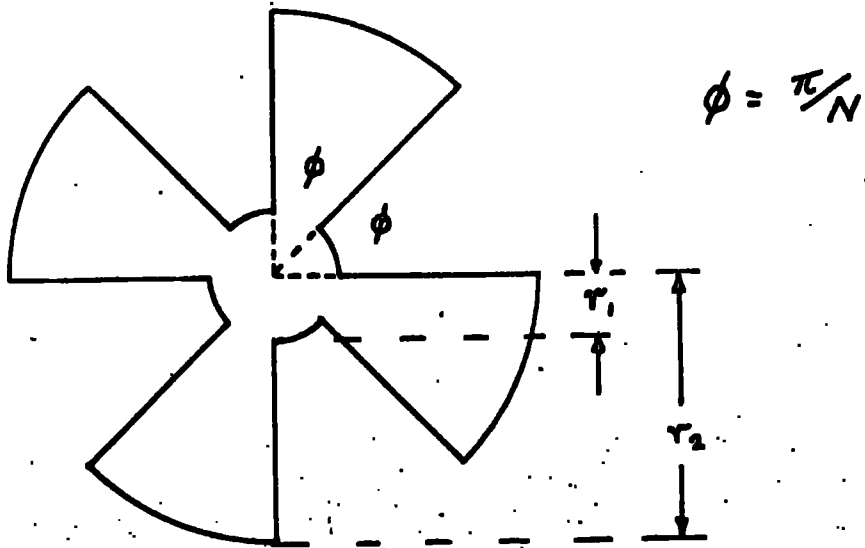
Fig. 2.16 A four sector field mill vane
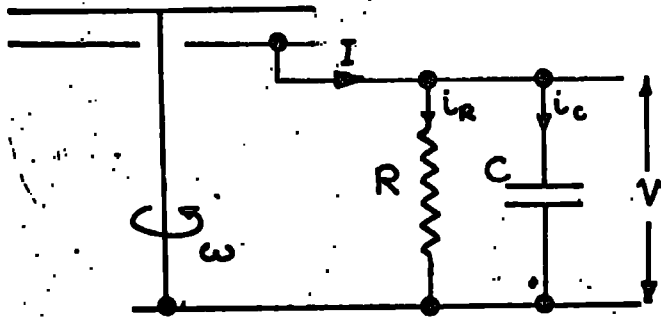
Fig. 2.17 The stator-rotor assembly

since the last instant of total screening.

The displacement current is given by

$$\frac{dq}{dt} = I = - \epsilon_0 A F \frac{\omega}{\pi} \qquad \dots \text{(1)}$$

The equivalent circuit, including leaks and stays, of the rotor-stator assembly is shown in fig. 2.17. Now at time t the voltage **V** across the capacitance C is given by

$$V = \frac{1}{C} \int_0^t i_c \, dt$$

since $I = i_R + i_C$

$$V = \frac{1}{C} \int_0^t \left(I - V/R \right) dt$$

differentiating

$$\frac{dV}{dt} = \frac{I}{C} - \frac{V}{RC}$$

Solution of this differential equation with the boundary condition that $V = K$ when $t = 0$ yields

$$V = IR \left(1 - e^{-t/RC}\right) + K e^{-t/RC} \qquad \dots \text{(2)}$$

To evaluate this expression a boundary condition which gives K is needed. This condition is that at the beginning of the n th half cycle, when t is taken as zero, the voltage will be equal to the (n-1) the peak value, V_{n-1} say. Equation 2 for $t = \frac{1}{2f}$ (the half period) becomes

$$V_n = IR \left(1 - \exp\left(-1/2fRC\right)\right) + V_{n-1} \exp\left(-1/2fRC\right)$$

$$\dots \text{(3)}$$

The successive expansion of equation 3 for all n from 1 to N gives a power series for V_N. The alternation of signs is due to the alternation of the sign of I with successive half cycles of its square wave

$$V_N = (-1)^N IR(1-\alpha)\left(1-\alpha+\alpha^2\ldots(-\alpha)^{n-1}\right) + (-\alpha)^N V_0 \quad \ldots\ldots (4)$$

where $\quad \alpha = exp(-1/2fRc)$

If, for definiteness, the first half cycle is taken as being one of exposure then V_0 will be zero as no charge will be bound on the stator when it is screened from the potential gradient. The power series in equation 4 with the last term, $(-\alpha)^N V_0$, being zero is converging if $\alpha < 1$; which is the case.

Summation of 4 now gives

$$V_N = \frac{(-1)^{N-1} IR(1-\alpha)\left(1-(-\alpha)^N\right)}{(1+\alpha)} \quad \text{for N finite}$$

$$V_\infty = \pm \frac{IR(1-\alpha)}{1+\alpha} \quad \text{for N infinite} \left.\right\} \ldots(5)$$

The ambiguity of sign in equation 4 is removed if the amplitude, but not the sign of the output is considered for V_N and V_∞.

Response time

It is desirable to know at what time V_N is a good approximation to V_∞ for operational use of a field mill.

The response time can be defined to be the time taken for the ratio $(V_n - V_\infty)/V_\infty$ to become equal to $1/e$. Where, as above, V_n is

the peak voltage amplitudo n half cycles after an instantaneous increase
of potential gradient from zero to F. For equation 5 the ratio is,
in terms of amplitude only,

$$\left| \frac{V_N - V_\infty}{V_\infty} \right| = \left| \frac{\frac{IR(1-\alpha)(1-(-\alpha)^N)}{(1+\alpha)} - \frac{IR(1-\alpha)}{(1+\alpha)}}{\frac{IR(1-\alpha)}{(1+\alpha)}} \right|$$

$$= \left| 1 - (-\alpha)^N - 1 \right| = \alpha^N$$

The value of N for which $\alpha^N = e^{-1}$ will lead to the defined response
time. Since $\alpha = \exp(-1/2fRC)$ the said condition is satisfied when
N = 2f RC. A number of half cycles N corresponds to a time N/2f
seconds. Thus the defined response time is equal to RC, the relaxa-
tion time of the stator rotar assembly.

It should be noted that to solve the condition laid down, N
will not in general be an integer which the treatment strictly requires.
However, V_E for non-integral values of N can be considered as lying
on the envelope of the peak values of V and the response time can be
considered as being also referred to this curve.

Dependence upon frequency

If RC is suitably small then the amplitude of the mill signal
can be taken as $\left| V_\infty \right|$. Substituting for α, equation 5 gives

$$|V_\infty| = \frac{IR(1 - \exp(-1/2fRC))}{(1 + \exp(-1/2fRC))} \quad \dots \quad (5a)$$

Expansion of $\dfrac{1 - e^{-x}}{1 + e^{-x}}$ gives

$$\frac{1 - 1 + x - \frac{1}{2}x^2 + \frac{1}{6}x^3 - \dots}{1 + 1 - x + \frac{1}{2}x^2 - \frac{1}{6}x^3 + \dots}$$

$$= \frac{x}{2}\left(1 + \frac{x}{2}\right) \quad \text{neglecting terms of order } x^2 \text{ and higher}$$

$$= x/2 \quad \text{'' '' '' '' '' '' ''}$$

Thus the expansions of (5a) gives

$$|V_\infty| = \frac{IR}{4fRC} \qquad \text{provided } \frac{1}{2fRC} \ll 1$$

Substituting for I from equation (1)

$$|V_\infty| = \frac{\epsilon AF\omega}{4\pi fC} = \frac{\epsilon AF}{2C} \quad \dots \quad (6)$$

Thus it can be seen that the output of the mill is directly proportional to the potential gradient and independent of the frequency provided that $2fRC \gg 1$.

Choice of component values

Value of C

From equation 6

$$C = \frac{\epsilon AF}{2|V_\infty|}$$

For convenience of amplification an output of ~ 0.1 m. for 1 V/m would be suitable. With a normal size portable mill r_2 = 7.5 and r_1 = 2.5 cm giving an area of 25 π cm^2.

These figures yield

$$C = \frac{8.85 \times 10^{-12} \times 25 \times \pi. 10^{-4} \times 1}{2 \times 10^{-4}}$$

$$= 348 \text{ pF}$$

This represents the maximum acceptable value for C required to give a large enough signal for amplification. It should be recalled that this capacitance includes the capacity of rotor-stator assembly (typically 30 pF) and the input capacity of the first stage of the amplifier (say, 3 or 4 pF).

Value of R

It has been shown in equation (6) that the output amplitude is independent of the resistance, however, the resistance value does have considerable effects upon the mill's performance. In the equivalent circuit (fig.2.17) R represents the resistive combination of the grid-cathode leakage (or solid state equivalent) of the amplifier input stage and the parallel leakage resistor which is incorporated.

The grid current in the input valve will develop a potential drop across R which will put the stator at a D.C. potential different from that of earth. Clearly the higher R is allowed to be the greater this effect will be. Such a D.C. potential will give rise to two effects. The first is the unequal exposure of the field mill to fields

of opposite sign. The second and more important is that a spurious signal of the same frequency as the true signal will arise due to the varying capacity of the stator-rotor capacity.

The potential drop across the resistor, R_1 due to grid current I_g is of course

$$V = I_g R$$

This voltage is also across the capacitance which consists of a constant capacity C and a variable component due to the change of capacity, $\widetilde{\Delta C}$, with the rotor's movement the maximum value of which is ΔC. The amount of charge held on the capacitance will vary $\widetilde{q}$ being equal to $V \widetilde{\Delta C}$. The peak voltage of spurious signal $\widetilde{V} = \dfrac{\widetilde{q}}{C} = \dfrac{V \Delta C}{C} = IR \dfrac{\Delta C}{C}$. It is necessary for this spurious signal to be smaller than that due to 1 v/m, say, i.e.

$$\frac{\Delta C}{C} R I_g \ll 10^{-4}$$

Now $C = 350$ pF as determined and ΔC is typically ~ 4 pF. An electrometer valve has a grid leakage current of the order of 10^{-12} A

$$\text{Hence } R \ll \frac{350 \times 10^{-12} \times 10^{-4}}{10^{-12} \times 4 \times 10^{-12}}$$

$$\ll 10^{10} \text{ ohms.}$$

This condition is well satisfied by a value of $10^8 \, \Omega$.

A component value of 200 pF for the capacitor which, together with the intrinsic capacity of the vanes, gives 230 pF, which is well within the requirements for C.

Once R and C have been fixed the frequency can be chosen with reference to the condition for non-dependance of output upon frequency, f, and resistance, R i.e. that which requires

$$x = 1/(2f\ RC) \ll 1$$

It will be recalled that this is the condition for the approximation that

$$\frac{1 - e^{-x}}{1 + e^{-x}} = \frac{x}{2}$$

In fact fig. 2.18 shows that this condition need not be taken to too extreme lengths. Fig. 2.19 shows the functions $y = x/2$ and $y = \dfrac{1-e^{-x}}{1+e^{-x}}$ plotted for values of x between 0 and 1. It can be seen that for x as large as 0.5 the differences between the functions is barely discernible (1 part in 500).

Thus the frequency condition is easily satisfied, for, in practical terms, the condition becomes

$$2f\ RC > 2$$
$$\text{i.e. } f > (RC)^{-1}$$

which for the values quoted yields

$$f > \text{about } 40$$

Hence, for almost any practical motor, the frequency presents no theoretical problem. This allows the choice to be made for electronic convenience.

As audio frequency amplification is probably the easiest to achieve, a 3000 rpm motor driving a 4 vane mill yielding 200 c/s would be quite suitable.
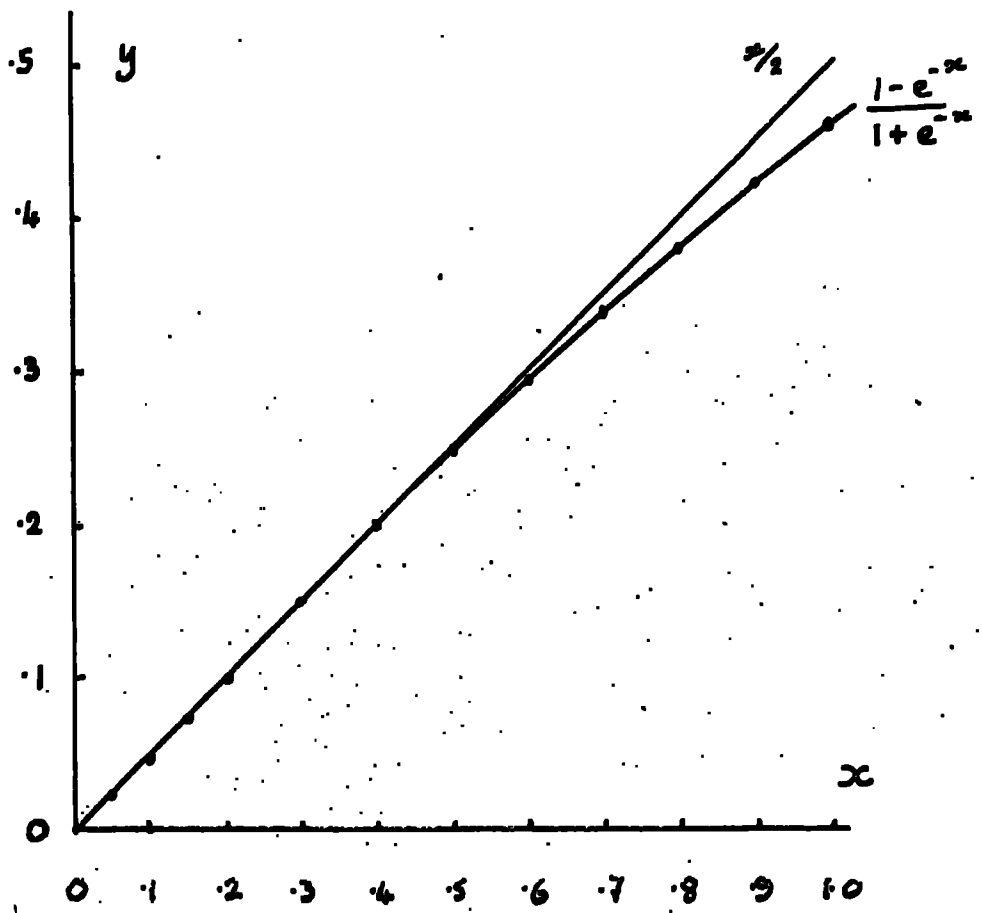
Fig. 2.18 The functions $x/2$ and $\dfrac{1-e^{-x}}{1+e^{-x}}$

Sign discrimination

Since in the investigation proposed no very high potential
gradients were likely to be encountered, it was decided that a single
potential gradient range would be adequate. This being the case, the
simplest method of sign discrimination was that of displacing the zero.
An auxiliary field is best produced by a high voltage over a small
area of the stator, rather than a low voltage over a large area. This
procedure reduces the proportionate error introduced by contact
potentials due to surface deterioration. It was decided that this
could be best achieved by applying a voltage to an insulated guard
ring.

The field mill design

The power available to drive the 3000 rpm motor was 24v D.C.
Such a motor inevitably produces sparking at its commutator. Adequate
screening of the electromagnetic radiation from such a spark requires
special metals of low permeability. It was thought that a better
solution would be to isolate the motor from the mill by employing a
flexible drive shaft. The use of such a shaft meant using a higher
power motor than may have otherwise been necessary. The torque
required to begin turning the vane when transmitted through the flexible
drive was found to be 3.4 ounce-inches. This necessitated obtaining
a 4 ounce-inch motor to do the job.

The mill head unit was mounted on an outer wall of the van in
dovetail slides so that it could be easily removed for travelling and
stowed similarly inside the van. The motor was mounted inside the van,

the flexible drive passing through the van wall to the head unit.

To reduce noise and vibration due to the motor, anti vibration mountings were employed. These consist of a solid rubber cylinder, on to each end of which is bonded a threaded rod. The rubber thus affords a flexible link which reduces the transmission of vibrations.

On an initial test it was found that the mill was receiving pick up which had the same frequency as that of the motor. It was felt that this may well have been transmitted from the motor to the shaft inside and then conducted along the flexible drive to the head unit. To prevent such conduction, a rubber bonded bush was used to link the motor with the flexible drive. Such a link is also flexible which obviated the need to line up accurately the flexible drive with the motor shaft. It was found that this measure eliminated the pick-up described.

To protect the cathode follower from the vibration of the moving parts of the mill, the whole moving part unit is separated from the mill chassis by anti-vibration mountings. The construction of the moving part unit is shown in the exploded diagram comprising fig. 2.19.

In fig. 2.19 P represents the outer case of the flexible drive which terminates in a solid bush, H, and the central rotating drive shaft, M. The bush H is rigidly fixed into a brass cylinder, L. To facilitate lining up the shaft, M, accurately a ball race, K, is fitted into the upper end of L. The plate, G, which screws onto L is the base for the mounting of the guard ring, A, on its insulators, E, and the stator, C, on its insulators, D. The rotor, B, is carried by a brass

A

B

C

D

E

F

G

H

J

K

L

M

N

P

2 cm
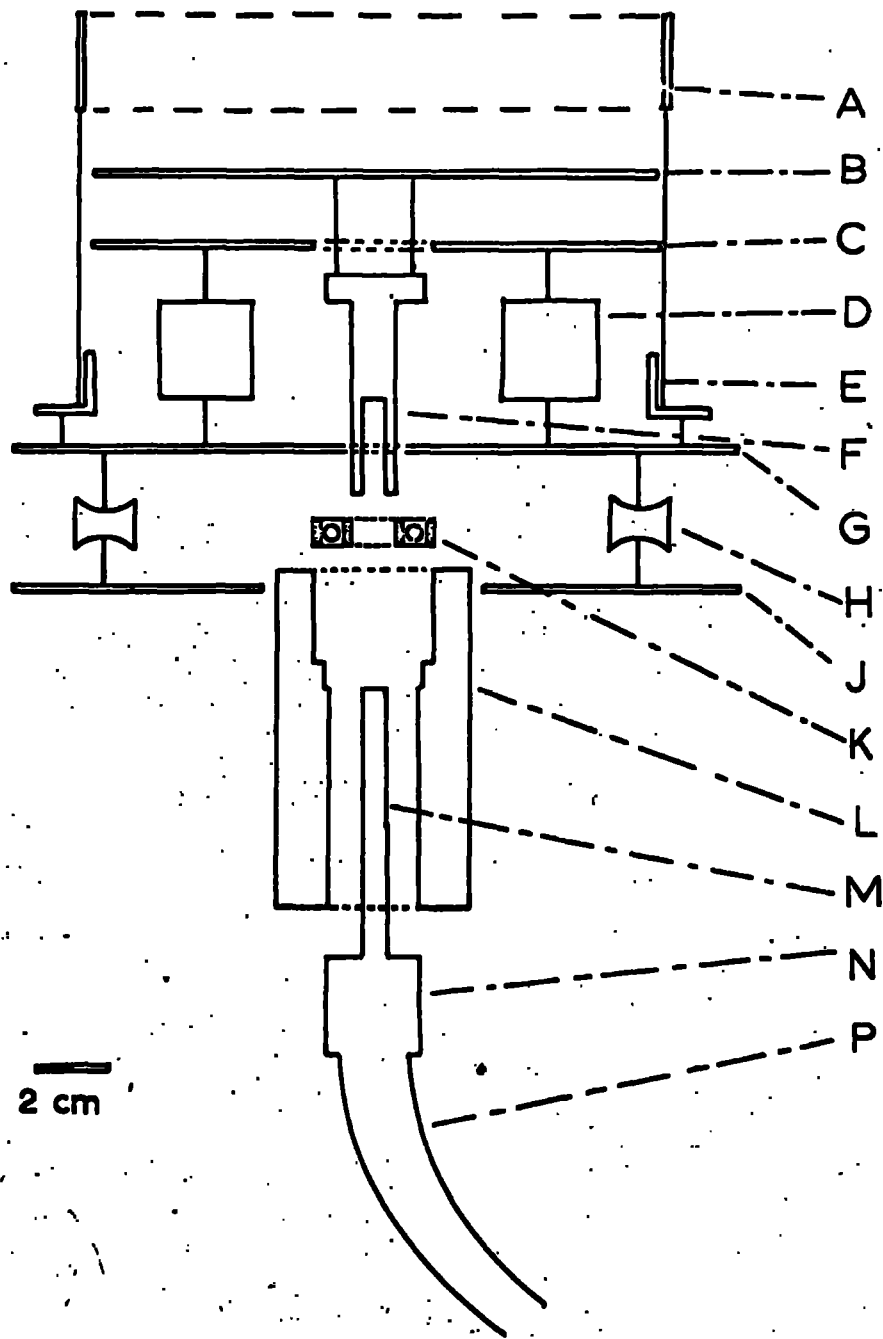
Fig. 2,19 FIELD MILL moving part unit.

bush, F, which locates over the drive shaft, M. The whole unit/ is

linked to the chassis by the flexible mountings, H, which join the

base plate, G, to the anchor plate, J.

The insulators, D, were constructed originally of polystyrene –

a good insulator is necessary to maintain the insulation of the input

of the cathode follower stage. For the same reasons as for the collector

plate the polystyrene insulators were subsequently replaced by P. T. F. E.

insulators.

Field mill electronics

Rough calculation showed that the magnitude of the signal to

be amplified would vary between 1 and 400 mv.

The shortage of available power made the use of solid state

circuitry an attractive proposition.

After a brief flirtation with an all transistor circuit ("Texas")

which proved too much for the author's knowledge of electronics, a

hybrid circuit was decided upon. This consisted of a low dissipation

sub-miniature electrometer triode ME 1404 as a preamplifier followed

by straightforward transistorised audio amplifier. The amplifier

circuit is shown in fig. 2.20. The circuitry of the head unit is

mounted on a small piece of veroboard as shown in fig. 2.21 and linked

to the chassis by two pieces of sponge rubber. The cathode follower

circuit is quite standard and needs no explanation. The two supply

voltages were obtained from dry batteries kept inside the van. The

input signal is passed from the stator by a lead through one of the

Fig. 2.20   The field mill electronics
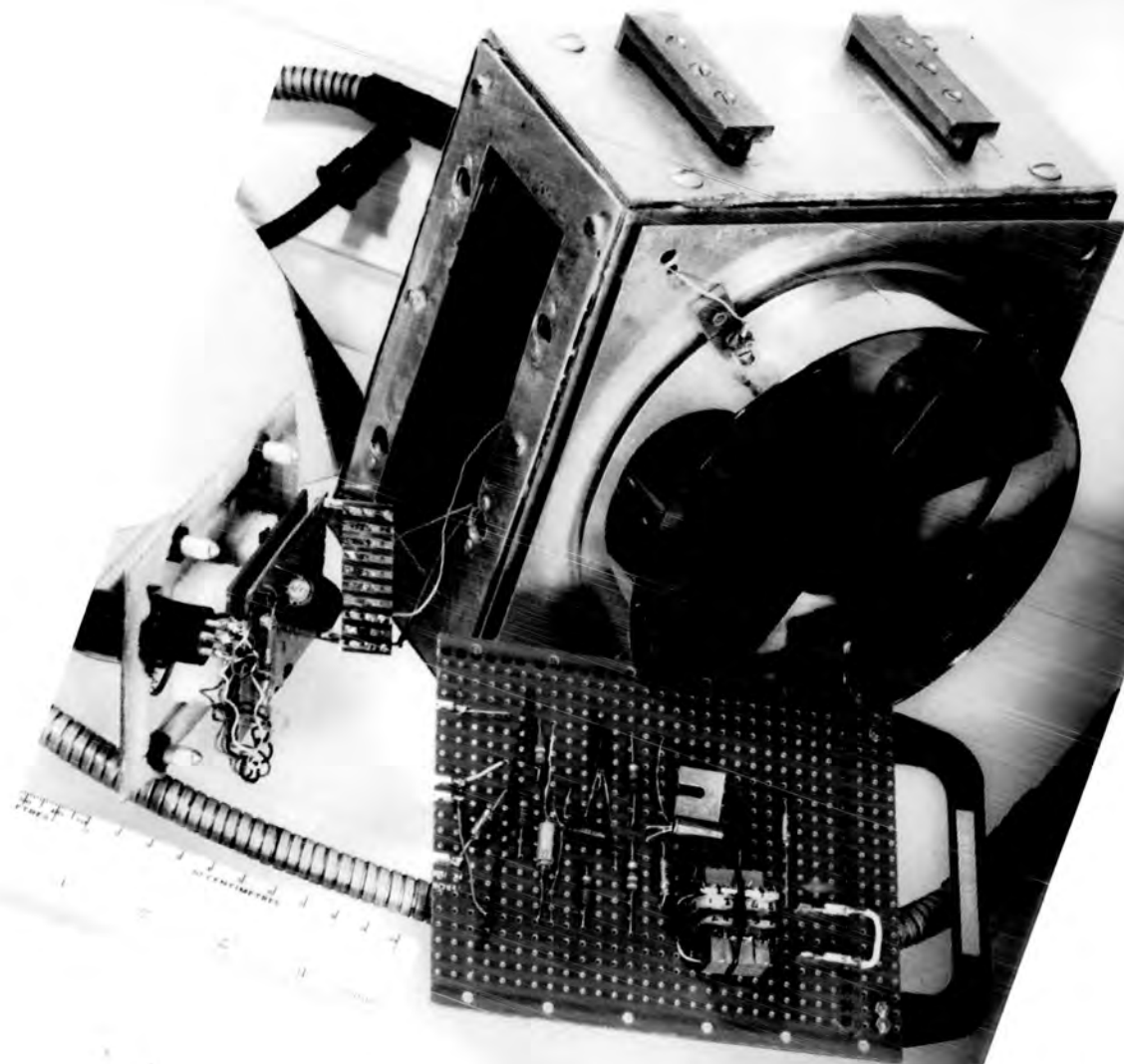
insulators. The rotor is maintained at earth potential by an earthed carbon brush which contacts the rotor's bush.

The potentiometer shown between the head unit and the remainder of the amplifier acts simply as an attenuator to cut down the input to avoid saturating the amplifier. A preset potentiometer was used and it served as a gain control.

The amplifier employed had a high current gain and was insensitive to actual transistor parameters (CHERRY 1963). A current feedback pair was used for the first stage. Such a pair fig. 2.22 works with low (theoretically zero) input resistance and high output resistance. The gain of the pair is given by approximately R_3/R_4. This amplifier was designed to have a gain of 100 as can be seen from the ratio 2.2k to 22 Ω. The bias components R_1 and R_2 were chosen to suit, according to the theory given by Cherry. The output consists of an emitter follower and a transformer coupled rectifying stage. The large, 10μF, smoothing capacitor served also to suppress rapid fluctuations of potential gradient. The final output of 0 to -12v was displayed on a 0-500 μA meter with series resistor.

Calibration of field mill

As can be seen in fig. 2.20 a variable series resistor RV3 is used with a microammeter to form a voltmeter. Before calibration could be done the value of this resistor must be set. This was done by applying the output of a signal generator at the frequency of the mill, actually 183 c/s, of the amplitude which would just pass undistorted
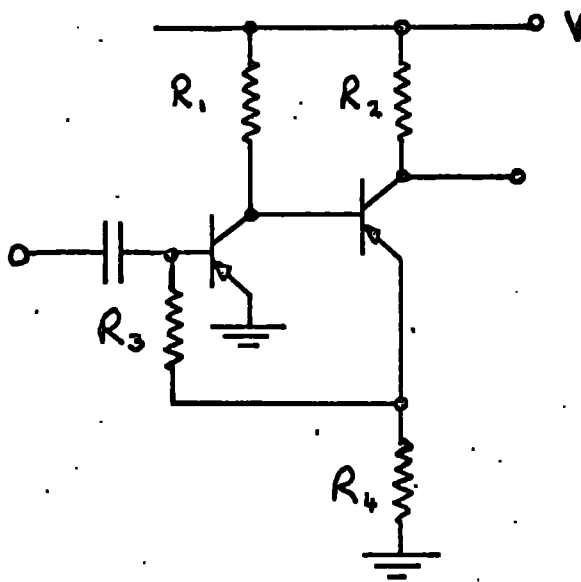
Fig. 2.22   A current feed-back pair
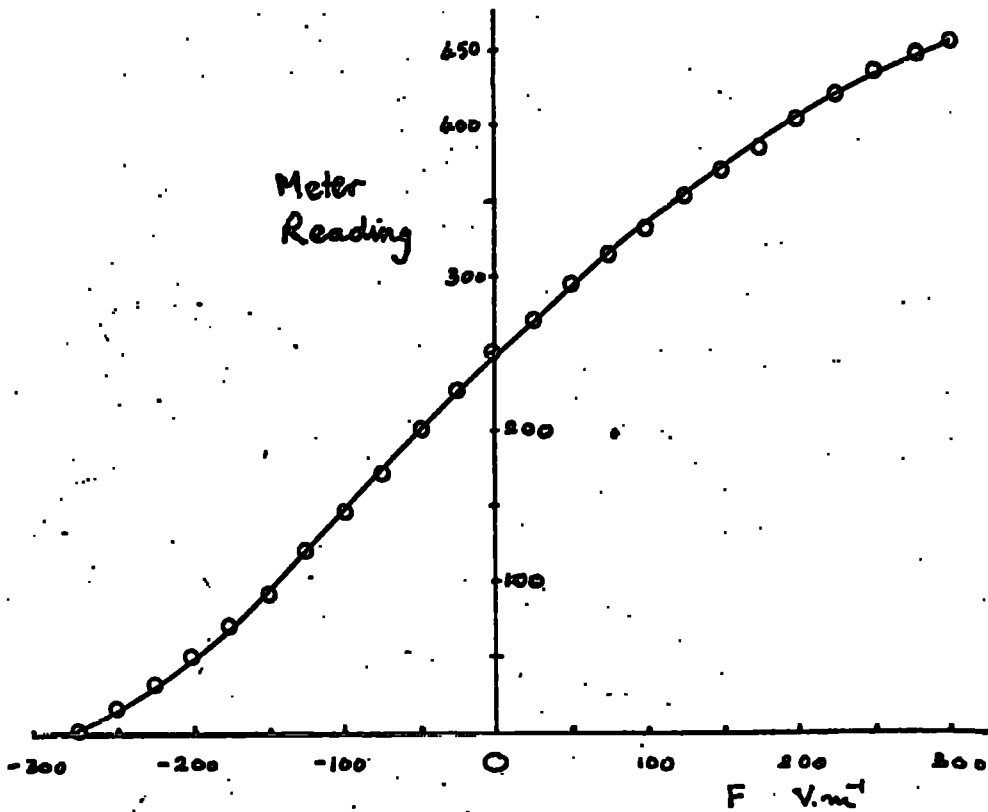
Fig. 2.23   The field mill calibration

through the amplifier. The value of RV3 was then adjusted to allow the maximum measurable current, 500. μA, to flow through the meter.

For easy calibration a plate was constructed which could be readily fixed over the vanes by insulators attached to the base plate of the moving part unit described above. In the photo fig. 2.21 the calibration plate can be seen on the left whilst the holes to which its insulation pillars are fixed are clearly visible in the corners of the mill's base plate. The separation of the calibration plate and the stator was 4.5 cm.

So that the calibration of the instrument could be kept constant it was decided to instigate a check on each occasion that the mill was to be used. This procedure was designed to eliminate drift of the calibration due to deterioration of batteries. With the calibration plate in place a voltage of 215v from the power supplies of the VRE installed for Mr. Ogden's experiment, was applied to the plate. The attenuator gain control RV2 was adjusted, if necessary, to give a reading of 450 in the absence of any bias voltage.

To check the zero the calibration plate was now earthed and the bias voltage applied. If necessary, the set zero potentiometer RV1 was adjusted to give the zero reading of 250. The actual calibration was performed in two stages: the first, to get a calibration curve in arbitrary units of potential gradient, and the second, to fix this calibration curve to an absolute value of potential gradient.

The curve was obtained by setting the system as described

above then applying voltages to the calibration plate and noting the
reading. The voltage applied to the plate ~~being~~ was an arbitrary unit of
potential gradient as the exposure of the mill on the side of the van
was not known.

This curve was fixed to absolute potential gradient by com-
paring the readings of this mill with those of a calibrated mill
mounted in the plane of the earth's surface. The author is indebted
to Dr. K.A. Higazi and Mr. R.R. Darsley for their assistance in
providing the standard field mill on the two occasions this procedure
was carried out. The calibration curve in terms of meter reading
and absolute potential gradient is shown in fig. 2.23.

2.3 The Measurement of Rainfall Amounts

ADKINS (1959) described an instrument to measure the rate of
rainfall. His instrument collected rain in a normal rain gauge and
allowed it to pass through a nozzle at the apex of the collection cone.
The nozzle was constructed such that the water left the cone in large
drops of constant size. These drops fell through a wire grid whose
alternate strands were connected together. In passing through the
grid the drops make a circuit thus triggering a monostable multi-
vibrator (one shot). The output of this one shot is fed into a Millar
integrator giving a final output suitable for a pen recorder.

The quantity and rate of rainfall can be determined from one
instrument if a record of volume of rain against time is taken. This

can be done with apparatus similar to that of Adkins. Instead of

integrating the drop count as Adkins did the drop count itself was

recorded. The drops making the circuit across at grid produce a

signal which actuates an electromagnetic counter.

The cone and drop former

ADKINS (1959) and RAISBECK (1963) constructed their nozzles

from brass with a taper of such dimensions as to be sure that water

would always bridge the throat of the nozzle. An oxide film was

produced to reduce the angle of contact in order to wet the surface

easily.

In this investigation a glass tube was tried as a nozzle in

the first instrument produced, the "Mark I". The use of glass presented

no drawbacks and has the advantage of having a suitable angle of

contact without special treatment.

The cone of the mark I instrument was made of zinc sheet. This

material proved in trials to be too rough especially at the joint

to the glass tube. The roughness caused a good deal of water to

lodge on the surface in light rain; there being an appreciable delay

of some minutes before the surface became sufficiently wet to function

satisfactorily.

To avoid this serious drawback the mark II instrument employed

an 8" glass filter funnel as collection cone. The drop former was

produced by drawing the $\frac{3}{4}$" funnel outlet into a taper. The taper was

cut at a suitable place to give an outlet of approximately the desired

size. This method of making a hole of size which is critical to the instrument is not as unsatisfactory as it may seem, since the nozzle has in any case to be calibrated. This procedure of forming the cone and nozzle from the same piece or glass removes all water holding joints without introducing any further complications.

The desired drop size can be worked out from considerations of the resolution required for normal rates of rainfall with a restriction imposed by the maximum possible counting rate of the electronics. Clearly, for accurate resolution, as great a number of drops as possible should be counted while the maximum rate of interest should not saturate the counter or it will be underestimated.

In meteorology rates of rainfall are classified as follows:

Rate mm/hr

a) very light   drops do not completely wet surface

b) light   trace ≤ 2.54

c) moderate   2.54 to 7.6

d) heavy > 7.6

(see for example Glossary of Meteorology page 464).

In this investigation a rate of 2.54 mm hr^{-1} had to be readily measurable. For a cone of aperture of the order of 300 cm^2 a rate of 2.5 mm hr^{-1} would give 1.25 cm^3 per min. Sufficient resolution would be achieved for a count of about 20 drops for this rate. It can be seen that a drop size of 0.0625 cm^3 would achieve this. Such a drop size would indicate for the maximum counting rate of 3 drops per second, a rate of rainfall of 22.5 mm hr^{-1}. This limitation is

obviously of no practical importance.

The nozzle on the cone used had an outlet diameter of 2 mm which resulted in a drop size of 0.0593 cm^3 which gave slightly better resolution than required.

Determination and constancy of drop size

Before considering the determination of the drop size, it is necessary to prove its constancy. Drops were allowed to fall from the nozzle onto moving filter paper, the grid having been removed. The water used was stained with black ink to render the drops visible. The relative drop sizes were measured by placing the stain under a graticule and counting the number of squares covered or partially covered. Since all partially covered squares are counted the area was overestimated. However, since absolute values were not of interest in this constancy test, this was not regarded as serious. The reliability of this counting procedure was tested by measuring one drop many times at different orientations to the graticule. The 25 measurements taken had a mean of 93.84 and standard deviation of 1.76. This gives the 95% confidence interval for a measurement of the area of this stain as 93.84±3.45 i.e. 93.84 ±3.7%. It was assumed that the others would vary similarly meaning that it was 95% certain that the measurements are within 4% of the true value.

Four drops at each of eleven different drop frequencies were caught, fig. 2.24, and measured, the results showed no serious variation in drop size. The change in drop size from light to moderate rates of rainfall amounts to 3.7% of the mean which is within the

1

2

3

the estimated error of measurement.

Having established that the drop size was sufficiently constant, its absolute size was determined. This was done by allowing measured volumes of water to fall from a burette into the collection cone. The resulting drops were counted with the aid of the electronics described below. The water was fed from the burette at differing rates to allow for the slight variation in size with rate. The drop size was calculated from the quotient of the total volume of water passed and the total number of drops counted. The determination gave a drop size of 0.0593 cm^3 as has been mentioned above. The cone and drop former are shown in fig. 2.25.

The grid

The grid has to be constructed so that alternate wires are connected together while being insulated from their neighbours. Adjacent wires must be sufficiently close for the drops to be sure of bridging the gap, but not so close that water will remain to bridge the gap when the drop has passed through the grid. The maximum permissible separation is clearly the drop radius. For 0.0593 cm^3 drops the radius is 2.46 mm. Allowing for the finite width of the grid wires a nominal separation of 0.1" was adopted. This fairly large value was used to minimise the chance of remnant water bridging the gap.

The first grid was constructed from parallel wires of tinned copper. This grid at first performed satisfactorily, but the electrolysis
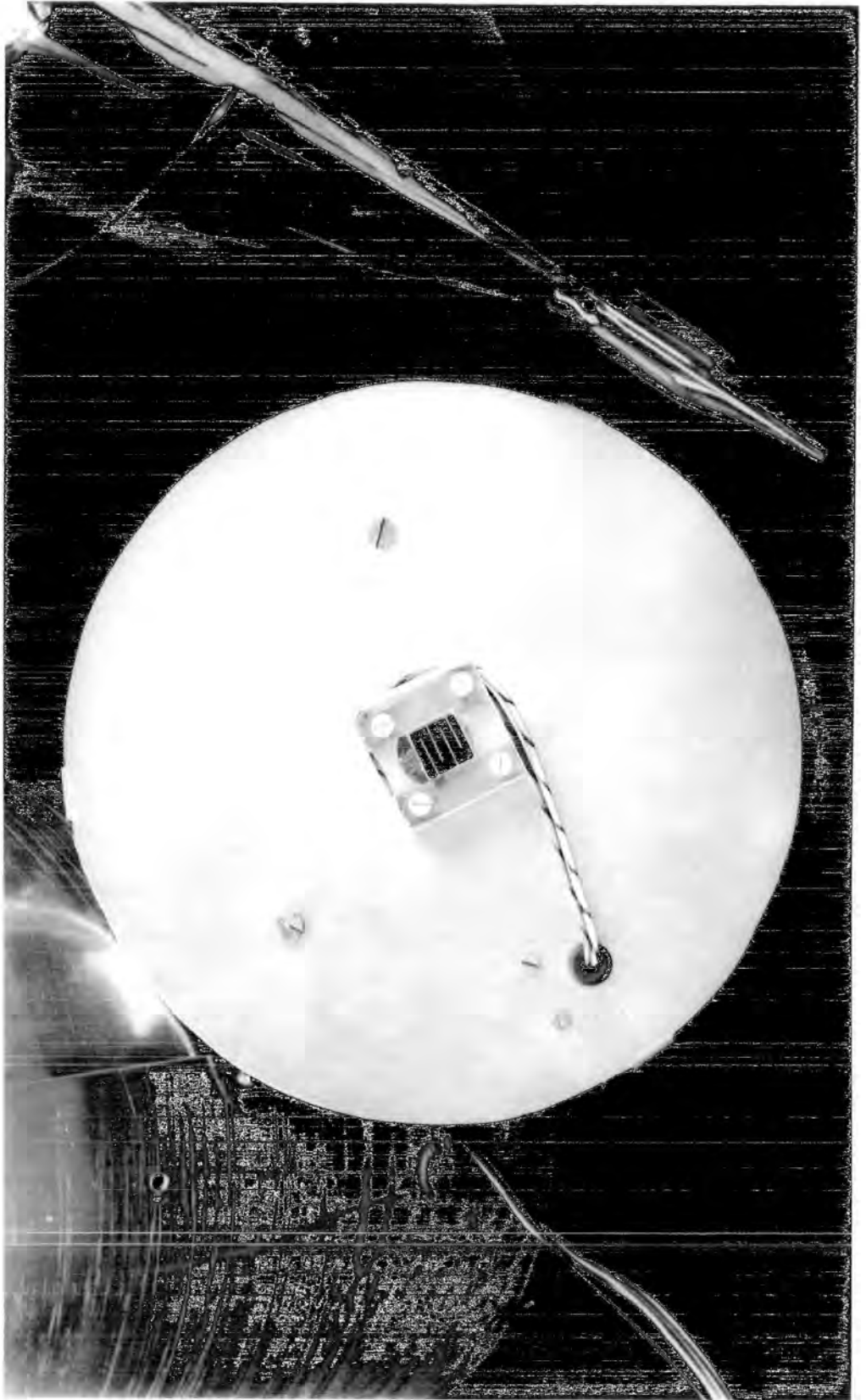
which occurred during occasional accidential bridging produced a deposit which eventually impaired its effectiveness.

It was decided to use an inert material for the second grid. This was constructed similarly from gold wire. However, it was difficult to maintain sufficient tension during construction. This resulted in a variation in spacing allowing bridging of remnant water in places and only single wire contact in others.

The final grid, shown in fig. 2.25, was made with stainless steel sewing needles (diam. 0.5 mm). These were chosen as being inert electrodes to the electrolysis of water and rigid.

The electronics

The simplest feasible arrangement is shown in fig. 2.26. It was found to work but not well. The pulses produced by the drops passing through the grid were very ragged; often causing the counter to register two counts for one drop and occasionally being too short to be registered at all. Also the current required to energise the counter was large enough to shorten appreciably the life of the transistor.

It was decided to use the initial pulse to trigger a one shot multivibrator. This enables the pulse to be converted into a "clean" pulse of any desired length.

The maximum counting rate of the electromagnetic counter available was three counts per second. There was, therefore, no point in designing the one shot to be much faster than this. The pulse length adopted was about 100 msec given approximately by 0.7 RC shown
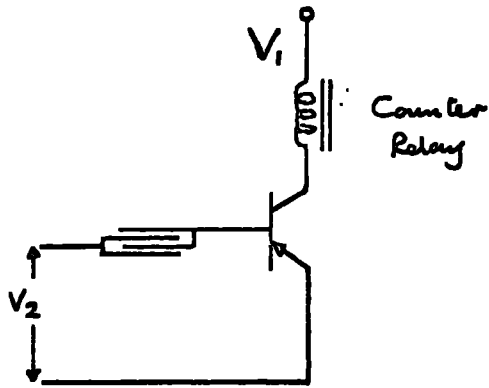
Fig. 2.26   A simple drop counter
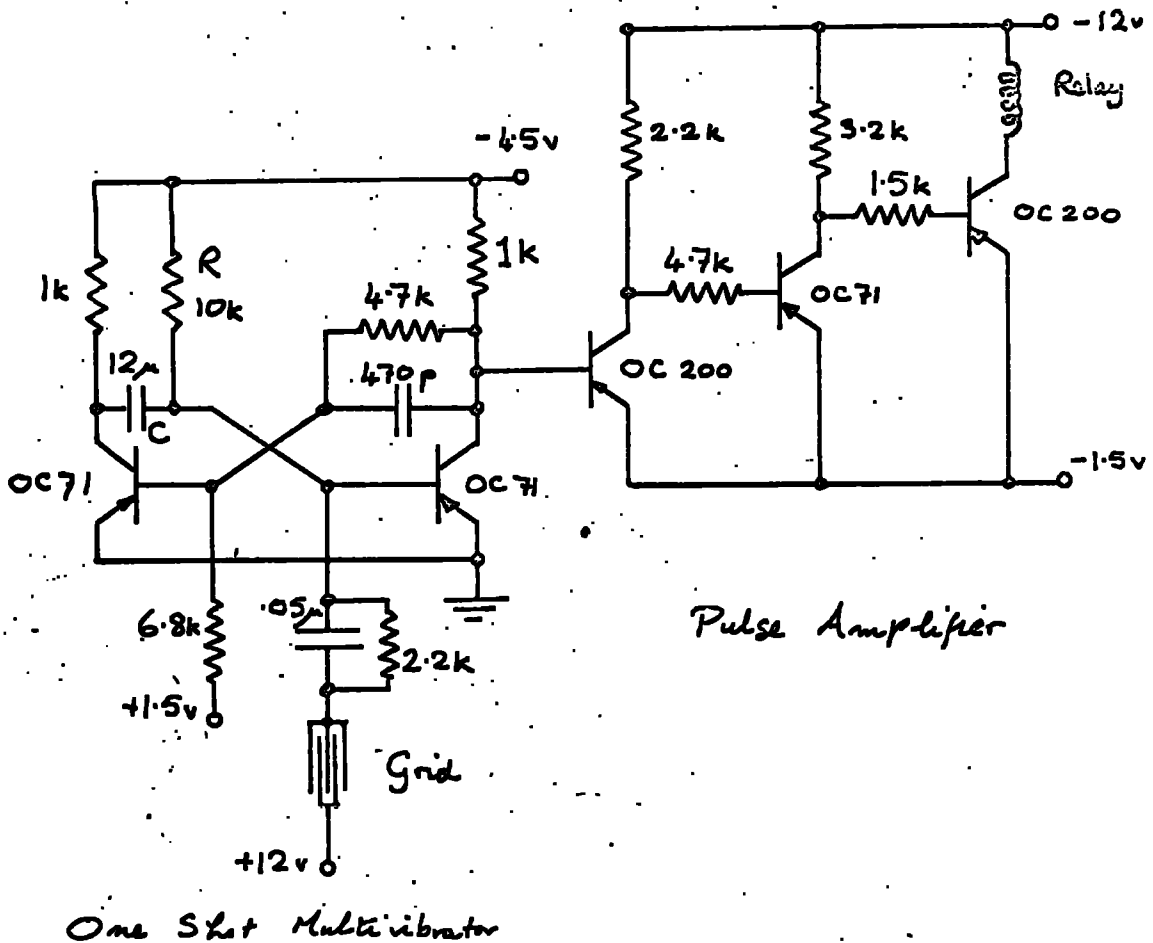
Fig. 2.27   Electronics of the rainfall recorder

in the circuit diagram fig. 2.27. A potential difference of 12 v had to be applied across the grid to enable a drop to trigger the one shot. Since the counter required a large current it was switched by a relay which, in its turn, was energised by the one shot pulse after suitable amplification.

Application to subsequent automatic recording

The system proposed (Chapter 10) requires each instrument to give a voltage output between 0 - 12 volts. This was achieved with a rotary stepping relay. This is a relay device, in which each action causes a wiper arm to sweep one step round a circle of 48 contacts in the manner of a uniselector. The contacts were wired onto a resistor chain and the wiper acted as the slider of a potentiometer dropping the 12 volts in 48 steps. When the wiper passed from position 47 to 0 the output was less than the previous value. This fact would be used to in preparing a computor programme so that it would correct for the lack of continuity of the output see fig. 2.28.

A suggestion for improving the electronics

Since the rainfall recorder was built, the author has become aware of magnetic reed relays. These are new devices which consist of a reed switch, a pair of magnetically operated contacts mounted in a hermetically sealed glass envelope, which, when surrounded by a coil, forms a miniature relay. Such a relay coil could be wired in place of the collector resistor in a one shot. This technique would allow the amplification stages to be dispensed with hence reducing costs while increasing reliability.
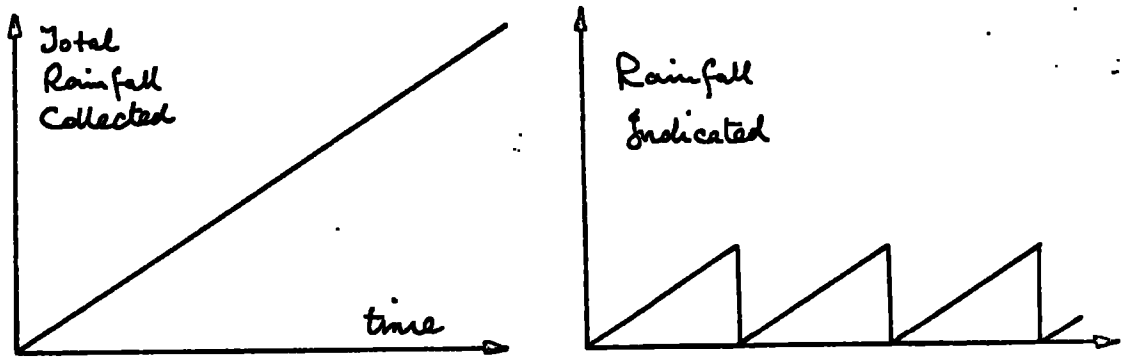
Fig. 2.28   Characteristic of automated recorder
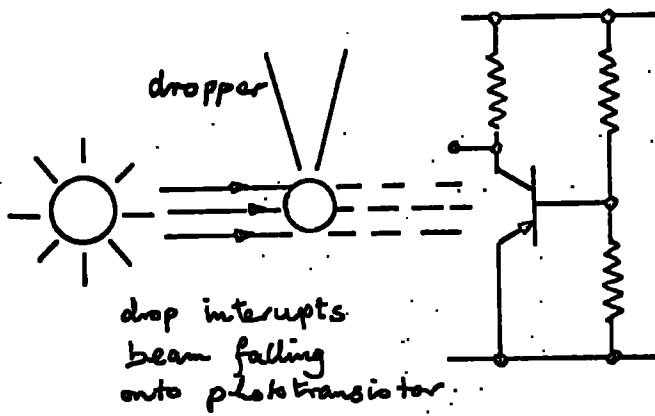
Fig. 2.29

Drop detection with

a photo transistor
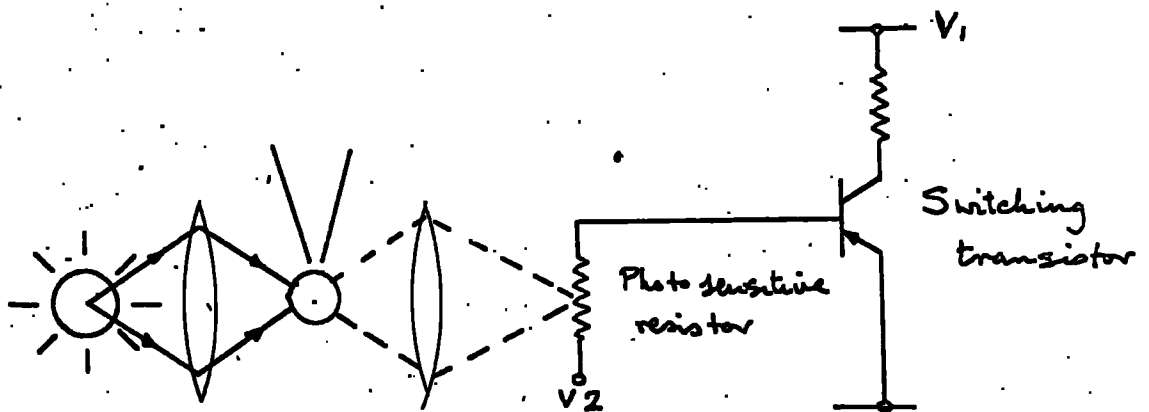
Fig. 2.30   Drop detection with a photo resistor

A further thought on the grid

Using a grid involves dropping drops through a grid and getting a ragged pulse which requires amplification while risking the possibility of remnant water bridging the insulator. Both drawbacks could be avoided by using a photoelectric device to give a pulse when a light beam is intercepted by a drop. Two small experiments were tried along these lines. The first, fig. 2.29, using a phototransistor OC71P produced a 1.5v voltage pulse which without amplification is insufficient to energise a relay. The second, fig. 2.30, employing a photosensitive resistor and a more precise optical arrangement, was more promising as an appreciable resistance change was observed. However, since the grid system previously described functioned satisfactorily, further development along photoelectric lines was not undertaken.

2.4 The Measurement of Wind Speed

In examining the earlier records it was felt that an indication of wind speed would have been useful. A three cup anemometer was in the author's possession having been used in an earlier investigation. This anemometer was generator type having a bar magnet rotating in a plane perpendicular to its axis between two relay coils. In the earlier work the current induced in coils had been measured with a sensitive moving coil galvanometer.

In the van such an operation would have proved most inconvenient. It was decided to convert the instrument into a contact anemometer.

This was achieved by mounting a reed switch beside the rotating magnet. Now whenever the magnetic field direction was parallel to the reed the contacts were closed, opening again when the field direction was perpendicular to the reed. Thus two contacts were made for each revolution of the anemometer affording adequate resolution for quite low wind speeds.

The reed switch was wired in series with an electromagnetic counter the registration of which indicated the run of wind. The wind speed itself could be computed by differentiation of the run of wind. The whole arrangement is shown schematically in fig. 2.31.

Calibration was performed by comparison with a calibrated meteorological office pattern anemometer whilst the two were operated side by side on the 4 ft. mast used for the anemometer in the investigation. The author is indebted to Mr. M.J. Smith for the loan of the M.O. anemometer. The calibration curve shown in fig. 2.32 shows that an onset of ~ 1.4 m/s is required to set the anemometer in motion. However, this was not regarded as a serious drawback in an instrument measuring a parameter of secondary importance.

In operation the run of wind was observed at 30 sec intervals calculation giving the mean wind speed over the interval.

2.5 The Power Supplies

There is little of physical interest in the system of power supplies used, so this section will only give a brief sketch of what

Wind driven cups

Magnet

−24 v

Reed switch

Counter Relay
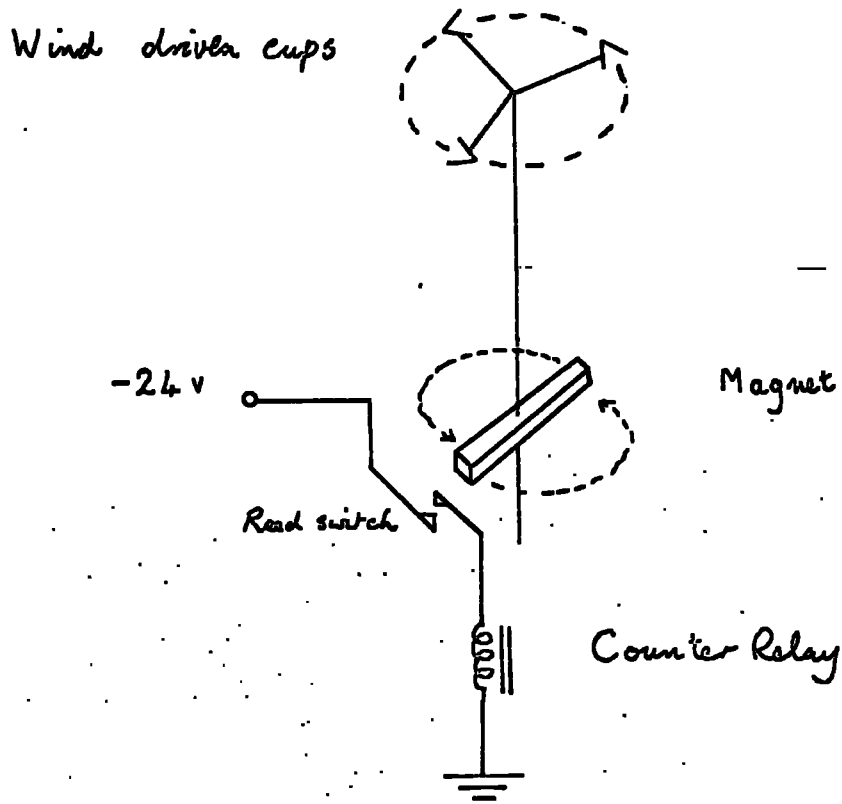
Fig. 2.31 Contact cup anemometer
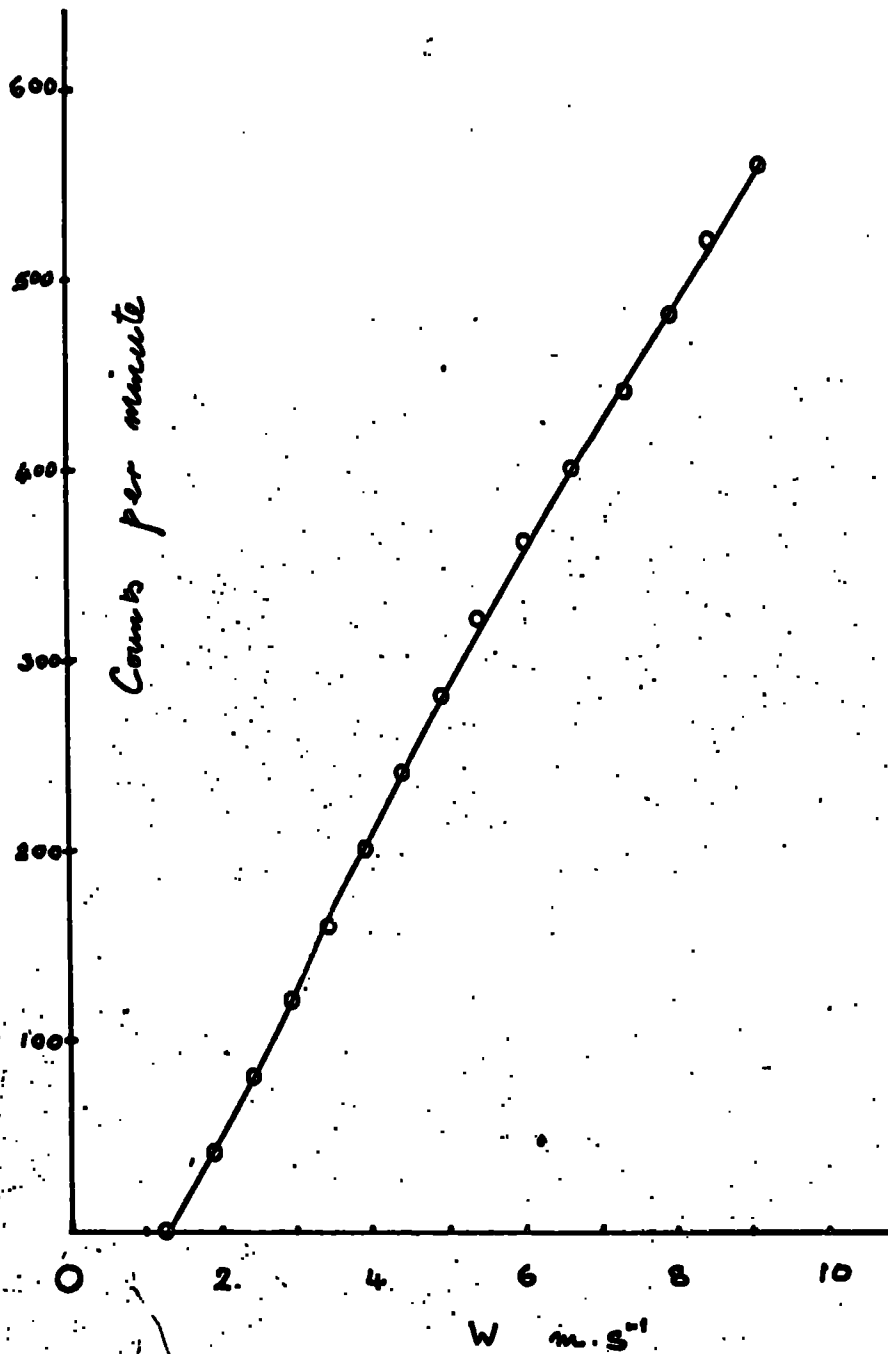
Fig. 2.32   Anemometer calibration

was done. Briefly the low currents were supplied by dry batteries and
the high currents by chargeable accumulators.

A heavy current drain was made by three items. The transverter,
type 24/120T by Valradio, required 6.3 amps at 24 volts D.C. The
field mill motor required 3 amps at 24 volts. The insultator heaters
ran from 1 amp at 12 volts. These were supplied from two pairs of
two 12 volts heavy duty-lead-acid accumulators. With such a power
drain (234 watts) it was necessary to have very frequent recharging.
It was decided that this could be best achieved by installing battery
chargers in the van and plugging these into the mains overnight. In
this way the accumulators were kept in a fully charged state. As it
is also desirable not to switch off the Rank amplifiers and the V.R.E.
they were run off the mains overnight, whilst the accumulators were
being recharged. The state of the electrolyte was checked from time
to time and topped up when necessary.

That part of the electronics which required a stabilised power
supply was fed by a -12 volt supply, stabilised by a Zenner diode,
also taken from the accumulators.

All the low current supplies the level of which was not
critical were taken from dry batteries of the appropriate value. These
batteries were checked periodically and replaced whenever necessary.

In all the circuit diagrams, the supplies are from dry batteries
with the exception of the -12 v line which is zenner stabilised from
the accumulators.

CHAPTER 3

The Use of the Apparatus

3.1 The Performance of the Apparatus

3.1.1 The collector

Occasionally during heavy rain the gap between the cylindrical walls of the tray and the guard ring was bridged by water. This resulted in an effective short circuit of the input resistance of the electrometer. The contact potential due to the different states of the surfaces became apparent when the resistance was so reduced. Thus the effect on the electrometer of the gap being bridged by water was a massive negative deflection.

The trouble was always cleared by removing the offending water with a piece of adsorbent paper. The trouble could have probably been eliminated if the tray and guard ring had had inclined edges meeting at the apex of an inverted "V". In such a system the drops would not have been trapped on a vertical wall where they tended to accumulate until a short took place well below the rim of the tray.

Neither arrangement would have helped in snow in which the collector was found to be quite useless due to the bridging of the gap at the rim by snowflakes.

For use in snow the gap between the guard ring and the collector would need to be greater than the $\frac{1}{8}$ to $\frac{1}{4}$ inch used. A gap of about one inch would have probably been adequate. It was not possible to alter this dimension without rebuilding the apparatus. It was felt that the incidence of snow did not justify such rebuilding.

Measurements could have been taken if the guard ring had been removed altogether. However, it was not convenient to remove and replace the guard ring so no precipitation currents were measured in snow.

During snow attention was focussed elsewhere, see chapters 7 and 9.

3.1.2 The compensation system

Occasionally it was necessary to adjust the balance of the compensation arrangement. At about fortnightly intervals the van was taken out on a fine day, when the precipitation current was zero, and the null balance of the probe and plate amplifiers checked and adjusted if necessary. There were, unfortunately, times when a record had been taken before the balance was discovered to be in need of adjustment. On these occasions there was found to be a significant correlation between the current and the differential of the potential gradient, as will be shown in chapter 4 (table 4.2).

It has been mentioned in section 2.1 that local space charges were expected to give a statistical scatter to the results. Such a scatter was observed before the long 30 sec time constant was imposed on the difference amplifier's output. On occasions when diesel lorries passed close to the apparatus it was possible to see on the probe and plate amplifiers a difference in time of arrival of the field change. The effect was not, however, detectable on the smoothed output of the difference amplifier.

On one occasion recording had to be abandoned because the wind was blowing raindrops onto the probe. This rendered invalid the assumptions about the probe current being only field current. On all other recording attempts the umbrella provided sufficient protection.

On a further occasion the probe was set into vibration by a strong gusty wind. The violent motion set up what were presumed to be piezoelectric currents in the probe circuit. Fortunately these wind effects were sufficiently rare to be tolerated without redesign of the apparatus.

3.1.3 The field mill

The calibration procedure described in section 2.2 was performed every time the mill was used. Some slight adjustment of the gain and/or the set-zero control was usually found to be necessary. However, tests showed that the calibration remained constant over periods of a few hours. It was not therefore necessary to check the calibration at the end of every recording period.

The only trouble experienced with the mill was a mechanical failure in the flexible drive. This was found to have been due to the loosening of a threaded link which was easily rectified.

3.1.4 The rainfall collector

It soon became clear that the operation of the rainfall collector was not satisfactory. Initially the cone was dry so that water entering stayed as drops on the surface until it became almost entirely wet. At this stage a drop's arrival caused a virtual

avalanche of water into the drop former. After a few avalanches the cone was restored to a state of being nearly dry again so the process began again. The record of rainfall collected was thus a characteristic of the apparatus as well as the rate of rainfall. No way was devised of keeping the state of the cone's surface the same all the time. It was eventually decided that the results were not worthy of inclusion so none have been given.

3.1.5 The anemometer

Originally the anemometer was mounted on the roof of the van. However, in this position the plate recorded a current which had a rapidly varying component. This was clearly a displacement current due to the motion of the cups. When the anemometer was moved to a 4 ft. stand away from the van the trouble disappeared.

Within the limits of its calibration $(1.4 - 10 \text{ ms}^{-1})$ the anemometer functioned without problems. Outside these limits the stand was once blown down!

3.2 Recording Sites

The criteria for a recording site was that it should be flat with no trees, telegraph poles, etc. to distort the potential gradient and that the run of wind should be as far as possible undisturbed. It had also to be off the road yet readily accessible.

Such a site was found at Sunniside (Ordinance Survey reference NZ136366). This site is in fact a Durham County Council road gravel

storage tip. Although adjacent to the road it was found that a

separation of about twenty yards rendered effects of passing vehicles

negligible.

The Sunniside site was 300 m above mean sea level. Although

higher sites could have been found by travelling further afield it

was decided that more comparable information could be gathered at a

single station than at an assortment of different sites.

The author realised that more measurements actually inside

clouds may have been made if more travelling had been done, but felt

that constancy of site was more important in a limited investigation.

Sometimes it was found to be useful to have measurements at

the Observatory either before or after the Sunniside record to serve

as a comparison. Measurements made at the Observatory must be treated

with caution if direct comparisons are to be made between sites. This

is because it was not possible at the Observatory to take the van

to a place of similar exposure to its position at Sunniside.

Two other sites, Hamilton Row (NZ177405) and Broompark

(NZ245418) were each used once to give low level comparisons with

Sunniside readings.

3.3 The Collection of Data

The proposed system of automatic data collection (chapter 10)

was not completed so the author had to rely on visual recording. At

half minute intervals readings were entered on a duplicated record

sheet. The long time constants of the outputs allowed each reading to be checked after its entry.

Although this method was most laborious there was the compensation of immediate fault detection. This allowed a fault, such as water bridging the collector gap, to be rectified without any great loss in recording time.

The recording was normally continued until the precipitation ceased or until a steady state had been recorded for 30 min. In the latter case the van was moved to a different level and recording recommenced in the hope of finding information about the vertical electrical profile.

3.4 Collection of Meteorological Information

The University Observatory keeps records of the usual meteorological parameters. The values of any parameter needed was taken from the Observatory's records.

The general weather situation on a wider scale was found by examination of the Daily Weather Report.

CHAPTER 4

Results

4.1 Obtaining Absolute Values from the Raw Data

It was intended that the University's Elliot 803 computer be used to perform the calculations for the data analysis. It was unnecessary to consult the calibration curves in producing data tapes for the computer as the computer could also perform this task.

The raw data consisted of meter readings for potential gradient and precipitation current and an integer from 0 to 999 to represent the run of wind. The values of potential gradient and precipitation current were found by direct reference to the calibration curves. The wind speed was found by calculation of the count in a $\frac{1}{2}$ minute interval by subtraction of successive readings then reference to the calibration curve.

The calibration curves were fitted to third degree polynomials using a library program which is described by FORSYTHE (1957). (The abbreviated spelling "program" has become accepted with reference to computers so is adopted here).

There is little to be gained by giving the full programs used. Each was written in the Autocode language which is too specialised to describe without lengthy explanations. The programs written by the author will be described with reference to what they did rather than how they did it.

The raw data were punched onto paper tape by the secretarial staff of the computer unit, to whom the author is indebted. Each

tape was headed by a number code defining the record number, the date, starting time and finishing time. Where blanks occurred in the record of any parameter a code symbol was punched so that the computer would recognize the blank.

The "absolute values from raw data program" read in the raw data and produced, by evaluation of the appropriate polynomial, an output of the absolute values for each parameter. Where the code symbols were encountered they were reproduced on the output tape. Thus the output tape was suitable for direct entry as a data tape for subsequent programs. To eliminate the possibility of confusion the number code was reproduced at the head of each output tape.

At the end of each record a summary of the data was produced giving the mean, standard deviation and number of observations of each parameter. Table 4.1 was compiled from these data summaries but does not give all the information contained on the summaries.

4.2 Simulated Charts

With the records having been taken by hand there was no chart available for visual inspection. This was regarded as a drawback as inspection of charts can often give birth to ideas for analysis which are not apparent from lists of numbers. As the work involved in plotting the results by hand would have been very tedious it was decided to get the computer to perform the task.

The teleprinter used had a carriage width of 69 characters so no great resolution was possible. However, as the chart was only

Record Number	NUMBER CODE Date	Time of Start	Finish	Potential Gradient V.m^{-1} Mean	Std.devn.	Precipitation Current x 10^{11} A.m^{-2} Mean	Std.devn.	Wind Speed m.s^{-1} Mean	Std.devn.
2.0	22.4	1000	1020	81.8	9.89	-0.054	1.53	-	-
2.1	22.4	1050	1133	21.6	38.7	-1.41	2.48	-	-
3.0	22.4	1401	1415	78.6	13.8	-0.765	1.95	-	-
4.0	4.5	1423	1558	-105	42.5	-3.64	4.23	-	-
6.0	11.5	1348	1515	-67.5	49.8	0.35	4.52	4.53	1.27
7.0	17.4	1338	1527	46.0	10.1	7.32	2.83	4.29	0.90
7.1	17.4	1600	1611	25.1	2.05	3.72	0.233	-	-
8.0	19.5	1601	1715	-36.1	107	2.47	10.8	3.50	7.33
9.0	24.5	1324	1430	-22.5	31.2	0.835	0.671	4.04	0.50
10.0	25.5	1205	1245	49.9	10.5	0.216	0.415	4.55	0.47
11.0	12.6	2047	2124	114	25.7	0.566	1.45	1.79	0.58
13.0	23.6	1306	1312	44.0	2.80	5.91	1.28	-	-
13.1	23.6	1335	1345	16.8	41.5	-0.189	0.895	-	-
14.0	24.6	1000	1132	49.9	9.07	0.226	0.534	-	-
15.0	24.6	1154	1212	46.5	2.80	0.312	0.284	-	-
16.0	27.6	1308	1345	16.1	24.5	1.54	4.16	-	-
17.0	28.6	1100	1115	-23.0	5.32	0.973	0.827	8.73	1.12
18.0	7.7	1028	1034	114	5.35	-15.6	2.24	3.07	0.82
19.0	10.7	1525	1615	83.4	9.49	4.87	1.89	5.17	7.86
20.0	10.7	1631	1643	52.2	5.52	2.57	0.803	-	-

Table 4.1

required for a visual aid, from which no measurements were to be taken, a high degree of resolution was quite unnecessary.

The program read in tapes of absolute values. For each parameter the ratio of the value to the full scale deflection was calculated. A number of spaces proportional to the ratio were punched on the output tape before a character F,-I or W to signify potential gradient, precipitation current or wind speed. Allowance was made for F and I being centre zero functions. After each set of F, I and W a new line was output signifying 30 seconds of time. After every 20 sets (10 minutes record) zero markers were printed on the chart to aid examination.

After the simulated charts had been printed out the like symbols were joined with coloured ink lines so producing charts which served as valuable visual aids.

4.3 Pair Sorting

Before detailed analysis of correlation coefficients could begin it was necessary to produce tapes with data in the pairs required. The original absolute values tapes could not be used because of the interference of the third parameter. A separate program was, therefore, written to sort the data into the pairs required.

The pair sorting program read the data in sets and punched out on the output tapes the required pairs if complete. (Often there were blanks so that only one half of the pair appeared on the absolute values tape). The computer punched two outputs one on each of its

output channels with the two sets of pairs required I, F and I, W.

To test for the effect on the precipitation current of displacement current it was necessary to have pairs of $\frac{dF}{dt}$ and I. Since the time intervals were constant a correlation test of $F(t)-F(t-30) = \Delta F$ with I was all that was necessary.

A small modification of the program allowed it to give an output of pairs of ΔF and I.

4.4 Correlation Coefficients

The basis of the analyses performed was the correlation coefficient. A program to compute this coefficient was written.

The program read in the tapes of pairs and formed the sum and sum of squares of each parameter together with the sum of the product of the pairs. When all the pairs had been read the final calculation was performed yielding the mean and standard deviations of each parameter together with the correlation coefficient. The mean and standard deviation were not necessarily the same as those produced in the initial data summary because of the blanks having reduced the data which was formed into pairs. However, the difference was never appreciable.

The results of the correlation coefficient computations are given in table 4.2.

4.5 Regression Coefficients

MORGAN (1960) has described how the best straight line must be

CORRELATION COEFFICIENTS

Record Number	F - I	ΔF - I	I - W
2.0	-0.087	-0.006	-
2.1	0.359	0.355	-
3.0	0.157	0.929 *	-
4.0	0.124	0.821 **	-
6.0	0.146	0.720 **	-0.099
7.0	-0.054	-0.039	-0.015
7.1	-0.051	0.327	-
8.0	0.155	-0.442	0.189
9.0	-0.304	-0.179	0.115
10.0	0.191	-0.177	0.117
11.0	0.731 *	-0.075	-0.465
13.0	0.138	0.607	-
13.1	0.671	-0.223	-
14.0	0.060	-0.063	-
15.0	- 0.163	0.323	-
16.0	0.395	0.760 *	-
17.0	0.400	0.021	0.412
18.0	-0.737	0.114	-0.200
19.0	0.541 *	0.114	-0.121
20.0	-0.435	0.533	-

*   denotes coefficient significant at 95% level

**   denotes coefficient significant at 99.5% level

Table 4.2

calculated from pairs of data (x, y) when both x and y are subject to error. The slope, c, of the line

$$\frac{y - \bar{y}}{\sigma_y} = c \frac{x - \bar{x}}{\sigma_x} \qquad\qquad 4.1$$

lies between the slopes of the regression lines of x on y and y on x. The actual value of the slope depends upon the correlation coefficient of x and y and a parameter k which is related to the relative errors in x and y. Figure 5.3 in the next chapter shows how sensitive the slope is to the relative error of x and y. The figure shows the slope varying from that of the regression of y on x (when x is free from error) to that of x on y (when y is free from error).

The relative error is taken as $\frac{e_x}{\sigma_x} / \frac{e_y}{\sigma_y}$ where e denotes the actual error and σ the standard deviation. Now for precipitation current and potential gradient, since σ_I and σ_F vary considerably from record to record, the relative error ratio cannot be taken as a constant. The errors e_I and e_F were taken as 0.25 x the range of the plate current amplifier and 2.75 v/m. These measurements both correspond to the minimum resolution of the output meters. The relative error is thus $D = 11 \, \sigma_I / \sigma_F$. Using the method of MORGAN (1960) the slope c was calculated. Table 4.3 shows the results of the calculations. The regression coefficients a and b of the equation

$$I = a + bF \qquad\qquad 4.2$$

are also shown in table 4.3 having been calculated from a transformation of equation 4.1 in terms of F and I for x and y.

Record No.	$D = \dfrac{\sigma_I}{\sigma_F}$	k	c	$I = a + bF$		Place	Notes
				$a \times 10^{11}$	$b \times 10^{11}$		
2.0	1.725	− 1.42	−	−	−	O	
2.1	0.71	− 0.71	0.82	− 2.6	0.053	S	
3.0	1.58	− 1.37	1.46	− 17.3	0.210	S	
4.0	−1.803	− 1.07	1.08	8.0	0.108	S	*
6.0	0.988	− 0.99	0.95	6.06	0.085	S	*
7.0	2.93	− 1.66	−	−	−	S	
7.1	0.956	− 0.96	−	−	−	S	
8.0	1.275	− 1.22	1.21	9.2	0.140	S	
9.0	0.25	− 0.25	0.53	0.54	− 0.012	S	
10.0	0.534	− 0.53	0.67	− 1.35	0.032	S	
11.0	0.592	− 0.59	0.89	− 3.3	0.034	S	
13.0	4.77	− 1.79	2.46	− 40.6	1.060	B	
13.1	0.238	− 0.24	0.69	− 0.48	0.015	S	
14.0	0.732	− 0.73	−	−	−	S	
15.0	1.00	− 1.00	− 1.00	4.54	− 0.091	O	p
16.0	1.84	− 1.46	1.33	− 2.0	0.222	O	p*
17.0	1.72	− 1.42	1.30	5.8	0.208	S	
18.0	4.91	− 1.80	− 1.26	48.4	− 0.560	S	
19.0	2.2	− 1.55	1.31	− 17.1	0.262	S	
20.0	1.63	− 1.39	− 1.26	12.3	− 0.187	H	

Blank rows occur where c is indeterminable using MORGAN 1960

Symbols and abbreviations

O - Observatory   S - Sunniside   B - Broompark   H - Hamilton Row

p - precipitation current not compensated for field currents.

* - significant correlation with displacement current.

Table 4.3

Fig. 4.1 shows plotted all the regression lines of comparable records taken at Sunniside. The records which had a correlation coefficient at 95% between ΔF and I were not included as these were those with appreciable displacement currents. It is quite clear that these lines do not conform closely to any one model regression line. This disturbing situation is enlarged upon in chapter five where the relation between precipitation current and field is examined in full.

The broken line in fig. 4.1 is the regression line computed from the centres of gravity of each record weighted according to the number of observations in the record. Although not much importance can be attached to a line representing such a widely scattered set of data it is encouraging that the line computed is of the same form as the accepted line. The regression equation is

$$I = 1.76 \times 10^{-11} - 0.0405F \times 10^{-11} \; Am^{-2}$$

4.6 Effective Number of Observations

It is essential in the use of standard elementary statistical tests that the observations be independent. Observations are said to be independent if the selection of one observation from the population does not bias the chance, for or against, of selection of any other for inclusion in the sample. In records of atmospheric phenomena a "memory" is often observed. If the time intervals between observations are less than this memory then the observations cannot be independent. In such a situation the effective number of
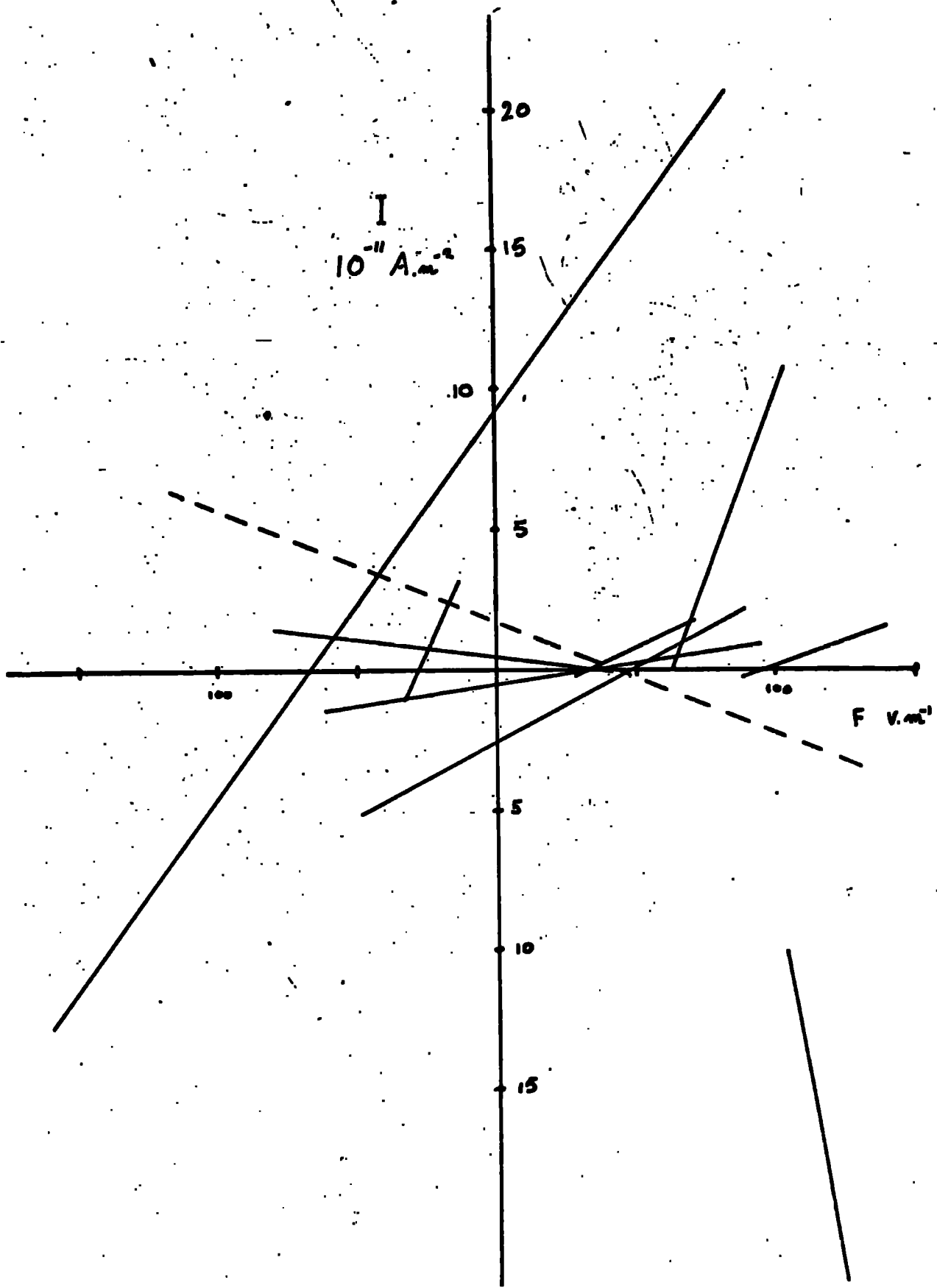
Fig. 4.1 Regression lines of comparable records

independent observations is less than the actual number of non-independent observations which would cause errors to be underestimated. Such under-estimation could very easily lead to erroneous conclusions concerning the significance of observed differences.

A record can be said to have a memory if there exists a significant autocorrelation coefficient (see section 5.2). The duration of the memory can be estimated using the method of AWE (1964) who defined an autocorrelation length or interval, L, to be the interval of time within which there exists correlation between the members of a time series. Pairs of values which are separated by an interval greater than L are clearly uncorrelated and therefore independent. Awe was able to show that $L \simeq \int r^2(k)\, dk$ over the central maximum of the correlogram of $r(k)$ against k; $r(k)$ is the autocorrelation coefficient of the time series $f(t)$ with $f(t+k)$. The integral must be found numerically.

A much simpler method (COLLIN, GROOM and HIGAZI 1966) is to take the correlation interval to be that lag which first gives a value of $r(k)$ which is not significantly different from zero at the 95% level of significance. Although this method has little theoretical justification it has been found to give good agreement with Awe's L.

Once the autocorrelation interval is known the effective number of observations can be calculated by dividing the actual number of observations by the autocorrelation interval.

In the present investigation the records were not long enough to obtain a reliable estimate of L. However, the results of COLLIN

(private communication) show that the autocorrelation length, calculated on the significance basis, in conditions of steady rainfall is between 4 and 24 minutes, the actual distribution is shown in fig. 4.2. Now clearly the best estimate of L is the shortest: since it is only during rapidly varying conditions that the true memory will manifest itself without being exaggerated by the existence of steady conditions.

The value for L of 5 minutes has been adopted in this investigation on the basis of Collin's results. All the significance tests have been conducted on the basis of the effective number of observations being one tenth of the actual number.
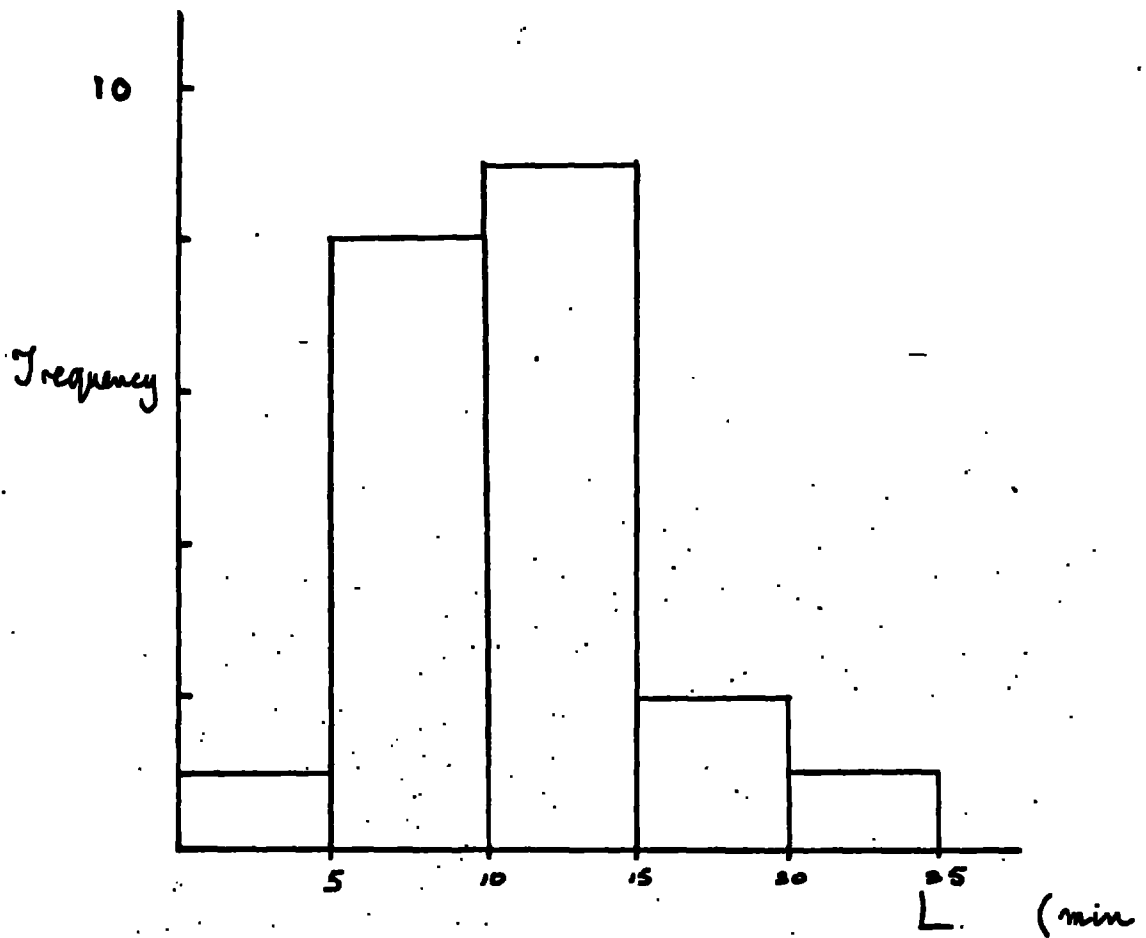
Fig. 4.2 Distribution of correlation intervals
during continuous rain; from COLLIN

CHAPTER 5

The Relation between Precipitation Current Density and Potential

Gradient

5.1 Introduction

The most obvious relation for the early workers in precipitation electricity to look for was one between their primary parameters, precipitation current density and potential gradient. ELSTER and GEITEL (1888) and BENDORF (1910) found the current density to be directly proportional to minus the potential gradient, fig. 5.1. The term "inverse relation" has been accepted for this relation. (It should be noted, as is pointed out by CHALMERS (1965), that this is not a good description. An inverse relation would normally be interpreted as meaning that a parameter is directly proportional to the reciprocal of another. This is, however, a case where accepted usage outweighs precision of terminology). SIMPSON (1909) obtained results which showed during rain an excess of negative potential gradient coupled with positive precipitation charge.

Since these early reports a very large number of workers have found evidence of the inverse relation. SCRASE (1938) measuring the charge per unit volume of rain found the inverse relation to be operative over long periods of continuous recording. NOTO (1959) recorded opposite signs for precipitation charge and potential gradient in 85% of his 622 recording intervals. CHALMERS and LITTLE (1940) found positive rain currents and negative potential gradients
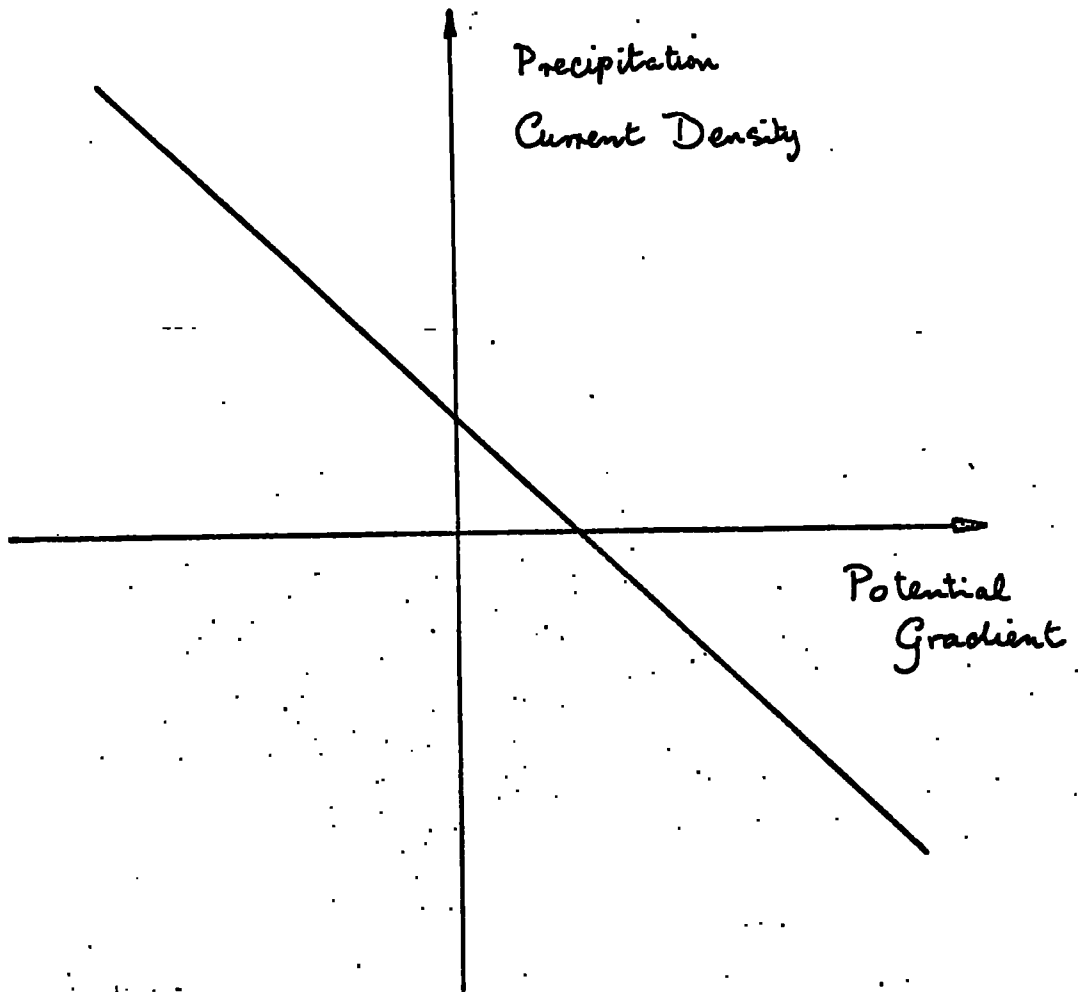
Fig. 5.1   The inverse relation.

during a long period of continuous rain.

The single drop observations of HUTCHINSON and CHALMERS (1951) confirm the existence of the inverse relation. So also do the observations of BANERJI and LELE (1952) made with their ingenious drop catching and recording system. MAGONO, ORIKASA and OKABE (1957) observed the relation for individual snowflakes as well as raindrops.

Mountain top measurements of KUETTNER (1950) on the Zugspitze, REYNOLDS (1954) in New Mexico and REITER (1965) in the Alps all showed the inverse relation to exist for solid and liquid precipitation.

When the electrical conditions are steady the inverse relation is very strong as has been found by SIMPSON (1949), SIVARAMAKRISHNAN (1957) and RAMSAY and CHALMERS (1960).

On the other hand, SCRASE (1938), in the same investigation, as quoted above, noted that there is no evidence for the inverse relation in stormy conditions. This is confirmed by the single drop measurements of GUNN and DEVIN (1953). Reiter, in the Alpine work quoted, found not an inverse, but a direct relation between the precipitation from very light showers and potential gradient. He also found a similar relation for very light precipitation from alto stratus cloud. Ramsay and Chalmers point out that the inverse relation is much more predominant in winter than in summer.

Scrase in his 1938 paper interprets the inverse relation by supposing that there is some process which gives a charge, usually

positive, to the rain. The opposite charge remains in the cloud, or air below, and produces a potential gradient at the ground with sign opposite to that of the rain.

The inverse relation described is not an exact functional relation but a statistical relation found to occur in most conditions. However, an effect has been found to occur in changing conditions which results in an exact relation. This effect observed by SIMPSON (1949), known as the mirror image effect, is said to occur when the records of current and potential gradient with time appear to be mirror images in the time axis of each other. The observations of the mirror image effect by SIVARAMAKRISHNAN (1957) led him to the same conclusions as Simpson had reached, namely that since the potential gradient and current change sign simultaneously, then the charge separation must take place close to the ground.

However, the observations of RAMSAY and CHALMERS (1960), showed that there could be quite considerable time lags in an otherwise normal mirror image effect. Such a lag in phase of current behind potential gradient, observed by OGAWA (1960), to be sometimes as much as 8 minutes, suggests that the charge separation is not always close to the ground.

OWOLABI and CHALMERS (1965) calculated the cross correlation coefficients between precipitation current and potential gradient records taken in mainly nimbo stratus rain. Their correlation diagrams, shown in OWOLABI (1965), showed that in general the

maximum cross correlation coefficient, R_k, occurred for some non-zero lag, k, of precipitation current behind potential gradient.

The reason for there being a lag (or lead) between precipitation current and potential gradient has been discussed by CHALMERS (1965) for different conditions of developing or moving cloud systems in the presence or absence of point discharge currents. Chalmers points out that the period of lag is not only dependent upon the electrical state of the cloud, but also upon other parameters. The height of the cloud together with the raindrop size controls the time of fall of the rain. This time along with the wind shear influences the lag.

The fact that the inverse relation is so well documented and readily explained leads one to wonder why it is quite often not observed even in non-stormy conditions. RAMSAY (1960), REITER (1965) and the current work have all found instances where the relation is not in evidence.

Since the inverse relation is observed as a statistical relation it is desirable to conduct the enquiry from a statistical view-point.

5.2 Statistical Terminology

It is not the purpose of this section to give a brief statistical text book. It is, however, necessary to clarify the meaning of statistical terms used and to set out a consistent scheme of notation. The scheme of notation adopted is chosen for its relevance to this Thesis and will not always coincide with accepted

statistical practice. This is unavoidable as current practice does not give an all-embracing scheme and so leads to ambiguities in notation.

The correlation coefficient, ρ, is used to give a standardised measure of the extent of the association between two parameters, say x and y. If n pairs of data are collected of the form (x_i, y_i) then the correlation coefficients is defined as

$$\rho = r(x, y) = \frac{\sum_{i=1}^{n} (x_i - \bar{x})(y_i - \bar{y})}{\left\{ \sum_{i=1}^{n} (x_i - \bar{x})^2 \sum_{i=1}^{n} (y_i - \bar{y})^2 \right\}^{1/2}}$$

This expression can also be written as

$$\frac{\text{covariance } (x, y)}{\left\{ \text{variance } (x) \text{ variance } (y) \right\}^{\frac{1}{2}}}$$

When a parameter, $x(t)$, varies with time there is said to be a time series. With a time series there is always some persistence. If the persistence is of less duration than the interval between observations it is of no consequence. However, if this is not the case then the observation taken at the $(i + 1)^{th}$ instant of time will be affected by that taken at the ith instant. There is thus a dependence of each observation upon the previous. The persistence can be measured by the autocorrelation coefficient which is defined as

$$\rho_k = r(x(t), x(t-k))$$

Now the auto correlation coefficient ρ_k will depend upon the value of the lag, k, which is taken. The extent of persistence will be indicated by the behaviour of ρ_k with k. For high persistence ρ_k will be larger for a particular value of k than it would be for low persistence.

It is of interest to consider a particular non-oscillatory type of variation. If the first auto correlation coefficient is ρ_1 then the observations will be of the form

$$x_{i+1} = \rho_1 x_i + \epsilon_{i+1}$$

i.e. each observation is composed of a part of the last observation, depending upon the persistence, and a random component ϵ. It can also be written that

$$x_{i+2} = \rho_1 x_{i+1} + \epsilon_{i+2}$$

Combining

$$x_{i+2} = \rho_1^2 x_i + \rho_1 \epsilon_{i+1} + \epsilon_{i+2}$$

Now the last two terms, being random, are independent of x_i so they will sum to zero over the whole series. Hence second auto correlation coefficient ρ_2 between x_i and x_{i+2} is ρ_1^2. It can similarly be shown that

$$\rho_k = \rho_1^k$$

A correlogram shows the variation of ρ_k with k and clearly in this case will be a decaying power series on either side of the maximum at k = 0 where clearly $\rho_0 = r(x(t),x(t)) = 1$. Fig. 5.2 shows two artificially generated time series with the same random

A

Long memory

B

Short memory

ρ_k 1·0

A

B

k
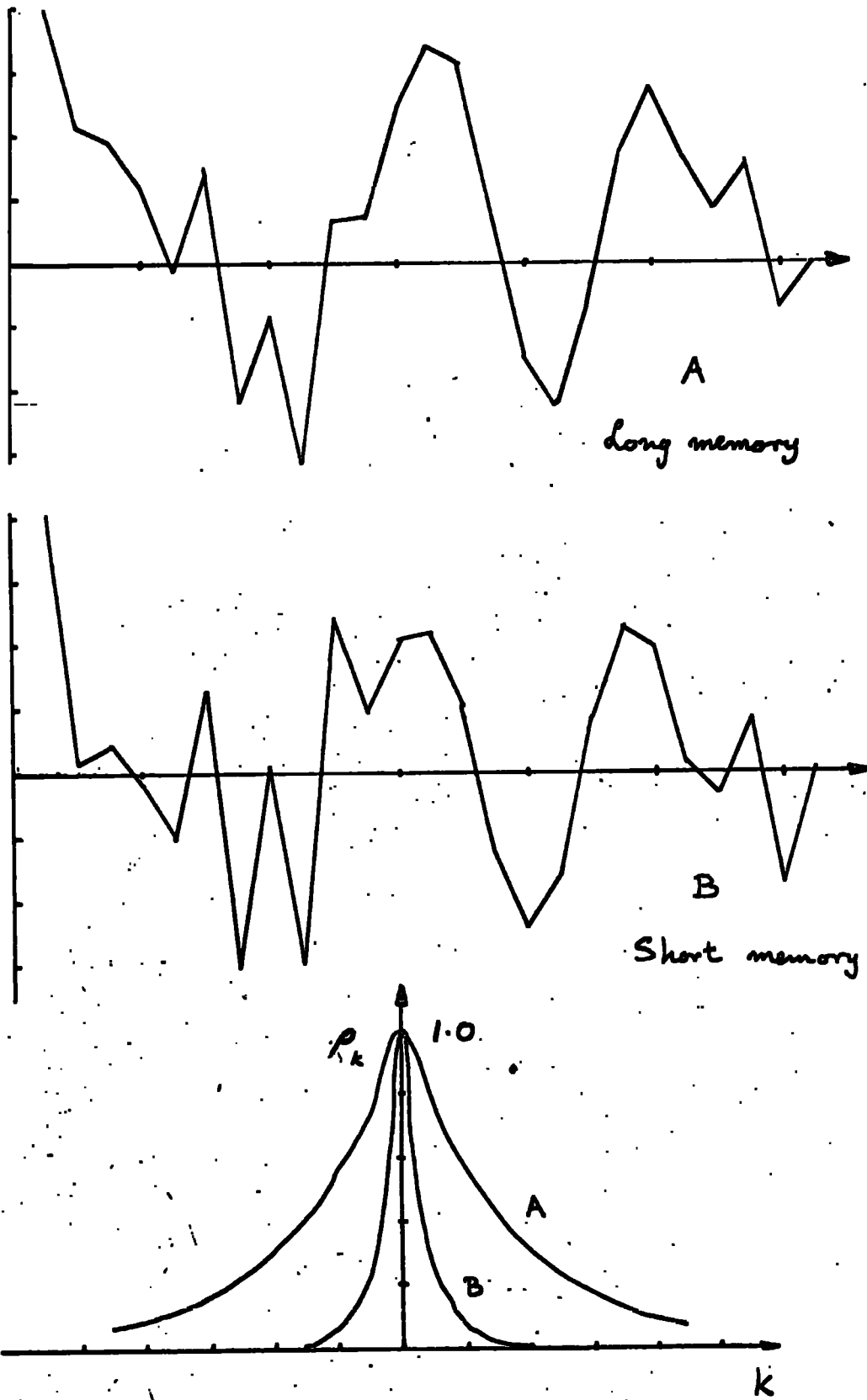
Fig. 5.2   Time series with long and short memories with their correlograms

components having high, A, and low, B, persistences together with their theoretical correlograms.

The idea of auto correlation between a series and itself can be extended to yield the cross correlation coefficient between two series. The cross correlation coefficient for a lag of k between the series $x(t)$ and $y(y)$ is defined as

$$R_k = r(x(t), y(t-k))$$

Note that the instantaneous cross correlation coefficient $R_0 = r(x(t),$ $y(t)) = \rho$. A cross correlogram of R_k vs k would show a maximum association at some, in general non-zero, value of k falling off on either side.

If the time series $x(t)$ and $y(t)$ have periodicity then the correlograms for auto- and cross-correlation will also exhibit periodicity.

It is useful at this stage to introduce a well known statistical relation between the correlation coefficient and slope of the linear regression equation for a set of pairs of observations of the form (x_i, y_i).

By the well known method of least squares the coefficients of the linear regression equation

$$y_i = a + b\, x_i$$

are given by

$$b = \frac{\sum (x_i - \bar{x})(y_i - \bar{y})}{\sum (x_i - \bar{x})^2} = \frac{cov(x,y)}{var(x)} \quad \ldots (1)$$

and $a = \bar{y} - b\,\bar{x}$

Now the correlation coefficient of x and y is given by

$$\rho = \frac{\sum(x_i - \bar{x})(y_i - \bar{y})}{\left\{\sum(x_i - \bar{x})^2 \sum(y_i - \bar{y})^2\right\}^{1/2}} = \frac{cov(x, y)}{\left\{var(x)\, var(y)\right\}^{1/2}} \quad \cdots (2)$$

It can be deduced by inspection of (1) and (2) that

$$b = \rho \left\{\frac{var(y)}{var(x)}\right\}^{1/2} = \rho\, \frac{\sigma_y}{\sigma_x} \quad \ldots (3)$$

Hence the behaviour of the slope of the linear regression line can be examined by considering the behaviour of the correlation coefficient. It is convenient to do this as the latter does not depend upon the units of x or y, being a dimensionless quantity.

It is clear from the work cited above, particularly Owolabi's, that the effect of a lag between current and potential gradient will be to reduce the value of the correlation coefficient, $(R_k > \rho)$ and so the slope of the regression line.

Of the infinite number of cross correlation coefficients only the maximum R_k is unaffected by the non-electrical factors which determine k. It would, therefore, seem that the most fundamental coefficient to consider would be R_k.

Now previous workers have all used the coefficient $R_o = \rho$, either actually or implicitly. As in general all the results will have been taken under different lags, comparison of one regression equation with another cannot be as valid as it would

appear unless the lag is known.

It is important to find out by how much R_o and R_k differ. It is only possible to analyse theoretically very simple cases. What follows is an analysis of an idealised situation.

5.3 Analysis of a Special Case

RAMSAY (1960) observed periods of almost sinusoidal variations of current and potential gradient. The analysis will be made of the case where the potential gradient and current vary sinusoidally with the current lagging by a phase angle ϕ . It should be noted that this is not an attempt to build a physical model. It is an attempt to make a mathematical model of the idealisation of experimental results.

The potential gradient, F, seen by a ground observer is supposed to vary with time as $F(\theta) = \bar{F} + f \sin \theta$. Where f is the amplitude of the potential gradient excursion from the mean $\bar{F}$, and θ is the time dependent phase angle of the oscillation. The precipitation current density, $j(\theta)$ is supposed to be functionally related to $F(\theta - \phi)$ i.e. lagging in phase behind $F(\theta)$ by ϕ .

i.e. $\qquad j(\theta) = c(F(\theta - \phi) - c')$

where c and c' are constants. (c will be negative for the inverse relation). Substituting for $F(\theta - \phi)$

$$j(\theta) = c \ (\bar{F} + f \sin (\theta - \phi) - c') \qquad (4)$$

$$\therefore \quad j(\theta) = \bar{j} + c \ f \sin (\theta - \phi)$$

It should be noted that the case under consideration is a form of the mirror image effect since the values of the parameters are changing with time.

Now the relation is not as precise as has been taken but $j(\theta)$ and $F(\theta - \phi)$ are associated with a/correlation coefficient R_k. *cross*

Now using the notation of section 5

$$= r(j(\theta),\ F(\theta)) = \frac{\text{cov}\ (j(\theta),\ F(\theta))}{\sigma_j \quad \sigma_F}$$

and

$$\text{cov}\ (j(\theta),\ F(\theta)) = \frac{\int (j(\theta)-\bar{j})(F(\theta)-\bar{F})\ d\theta}{\int d\theta}$$

$$(j(\theta)-\bar{j})(F(\theta)-\bar{F})\ d\theta = \int_0^{2\pi} cf \sin (\theta - \phi)\ f \sin \theta\ \ d\theta \text{ integrating}$$

over one cycle.

$$= cf^2 \int_0^{2\pi} \sin (\theta - \phi) \sin \theta\ \ d\theta$$

$$= cf^2 \left\{ \cos\phi \int_0^{2\pi} \sin^2\theta\ d\theta - \sin\phi \int_0^{2\pi} \sin \theta \cos \theta\ d\theta \right\}$$

$$= cf^2\ \pi \cos \phi\ .$$

So
$$\rho = \frac{cf^2 \pi \cos \phi}{\sigma_j \sigma_F\ \int d\theta}$$

Now the serial correlation coefficient, R_k, for maximum association, which can be called R_ϕ, is given by

$$R_\phi = r(j(\theta + \phi),\ F(\theta))$$

$$= \frac{\int (j(\theta + \phi) - \bar{j})(F(\theta) - \bar{F})\ d\theta}{\sigma_j \sigma_F\ \int\ d\theta}$$

On substitution of

$$j(\theta + \phi) = \bar{j} + cf \sin\left[(\theta + \phi) - \phi\right]$$

$$\text{and } F(\theta) = \bar{F} + f \sin \theta$$

the numerator becomes for integration over one cycle

$$\int_0^{2\pi} (cf \sin \theta)(f \sin \theta)\, d\theta$$

$$= cf^2 \int_0^{2\pi} \sin^2 \theta\, d\theta = cf^2 \pi$$

$$\therefore \quad R_\phi = \frac{cf^2 \pi}{\sigma_j \sigma_F \int d\theta}$$

So

$$\rho = R_\phi \cos \phi$$

5.4 Discussion

Morgan (1960) has shown how the coefficients of a regression equation can be calculated when both the variables are subject to error. His demonstration shows that if the ratio of the relative errors of x and y, $\frac{e_x}{\sigma_x} / \frac{e_y}{\sigma_y} = D$ is less than unity the slope of the line obtained will be less than that when $D = 1$. Also if D is greater than unity the slope is greater than the $D = 1$ case. Fig. 5.3 from Morgans paper shows this variation in slope.

How the effect of Morgan's ideas can be examined. The slope of the true regression line, as can be seen in fig. 5.3, must always be greater (in magnitude) than, or equal to, the slope of the regression of y on x. (That which assumes x free from error). Thus the relation (3) can be reformulated as

$$b \geqq \rho \frac{\sigma_y}{\sigma_x}$$
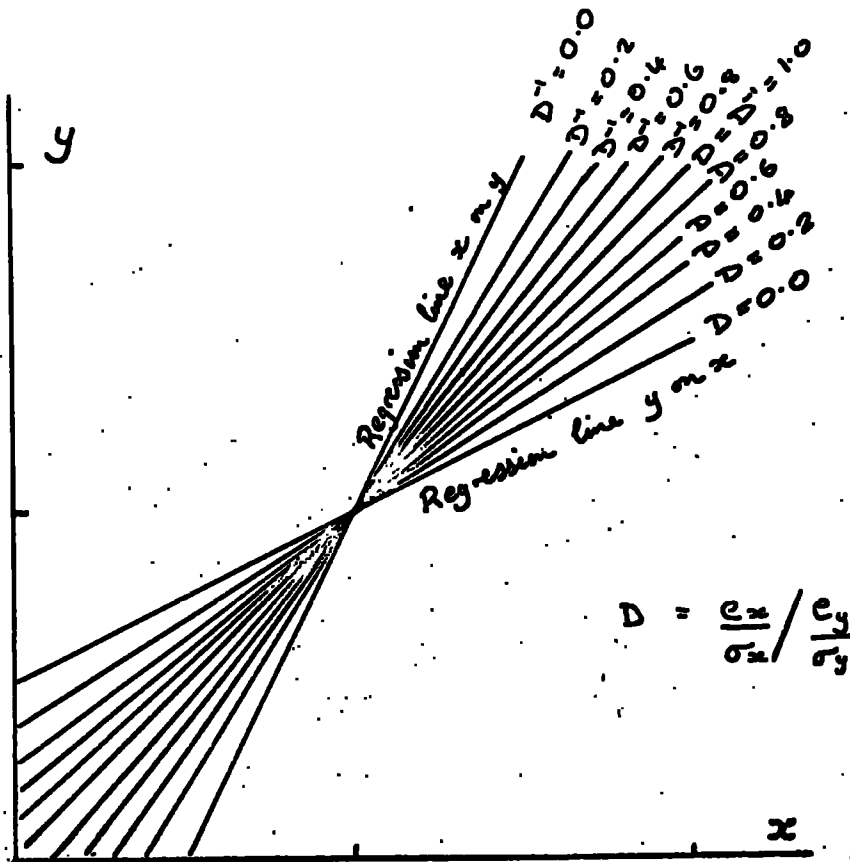
Fig. 5.3 Lines of best fit for $\rho = 0.5$ from MORGAN (1960)

and the conclusions of the previous section lose no generality for the change. (Clearly the actual value of the slope is changed by Morgan's considerations but the correlation coefficients will still bear the same relation to each other).

Now from this result some tentative conclusions can be made to assess the importance of the ideas given above, using the results of workers who report lags in the mirror image effect.

RAMSAY (1960) reports the lags of about a quarter of a period during approximately sinusoidal variations. This, of course, gives a value of $\pi/2$ for ϕ which gives zero for the correlation coefficient even if the association is perfect. So it can be seen that from (3) the estimate of regression coefficient b will yield zero.

OGAWA (1960) found phase lags to occur in the mirror image effect on 23 occasions out of 129; of the rest 60 were classified as indistinct and 46 as having zero lag. Although not specifically stated, it appears that the indistinct classification refers to those cases with a lag of less than 1 min. The average duration of a sign, that is to say, a half period, Ogawa found to be 17 mins. for the cases where there was a definite lag. The lags observed were from 1 to 8 min. giving ϕ values of $\pi/17$ to $8\pi/17$. Such values of ϕ would cause ρ and R_ϕ to differ by a factor of from 0.98 to 0.067. Taking the 60 indistinct cases as being of lag $\frac{1}{2}$ min. the factor becomes 0.99 which is not serious.

Now if the author is correct in assuming the coefficient of greatest importance to be that associated with maximum association,

the consequences of lags are occasionally serious. It has been shown that on occasions for Ramsay's and Ogawa's results that the regression slope for the instantaneous *pairing* reduces to almost zero because of the lag. It would seem then that there is a way of explaining why the inverse relation is not always in evidence. As soon as there is a lag which is of the order of a quarter period of the variation the instantaneous pairing $(j(\theta), F(\theta))$ will not show any association. For even greater lags the association $(j(\theta), F(\theta))$ would be of the opposite sense to the inverse relation.

All the work which has discussed the reasons for there being any lag has attributed it to time of fall of precipitation combined with the delaying effect of wind shear. It is clear that in precipitation from high clouds the possibility of lag will be greater. This will naturally account for the observations that the inverse relation is less prominent in summer. Also the observation by REITER (1965) of a direct relation with precipitation from alto stratus could be easily accounted for by a lag of half a period.

5.5 Physical Conditions for the Models Validity

Unfortunately there is insufficient data at hand for a more quantitative look at the problem of the non-appearance of the inverse relation.

It would be useful exercise to point out what would be necessary to give a physical backing to the mathematical model which has been erected.

It would clearly first be necessary to justify equation (4)
which was:
$$j(\theta) = c(F(\theta - \phi) - c').$$
The precipitation charge is assumed to be separated at one specific
level, say by melting. The precipitation current at the charging
level is assumed to depend upon the potential gradient at that
level. If no further charge separation takes place the current will
not vary with height so that the current can be expressed as
$$j(\theta) = A(F'(\theta - \phi) - B)$$
where F' is the potential gradient which prevailed in the cloud
when the charge separation responsible for j took place. A and B
are constants associated with the charging process. It is now
assumed that F' in the cloud is linearly related to F at the ground.
(They will certainly not be the same because of the space charge
on the precipitation). So by adjustment of the constants A and
B to facilitate this change equation 4 is obtained.

5.6 Further Discussion

Now in general the variation in the cloud would not give rise
to a sinusoidal pattern. However, it would always, in principle
at least, be possible to perform the analysis on a series of
sinusoidal Fourier components.

The above account implicitly assumes that the rain all falls
at the same velocity. In practice, there is a spread in the spectrum
of raindrop sizes. Fig. 5.4 shows two such spectra plotted from
BEST's (1950) relation
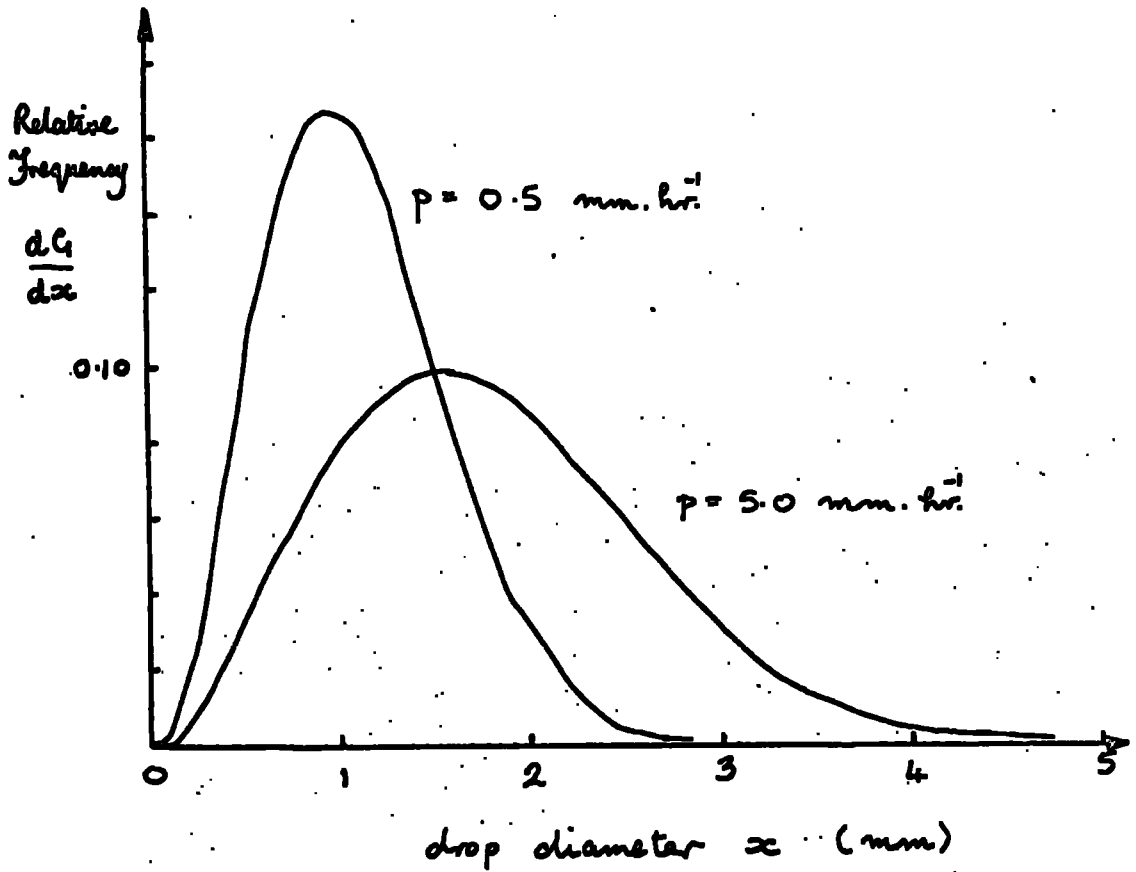
Fig. 5.4   Raindrop size spectra for differing rates of rainfall

$$G = 1 - \exp (- x/ \alpha p^\beta)^n$$

where G is the fraction of liquid water composed of diameter drops

of less than x mm falling at a rate of p mm hr^{-1}. α, β and

n are constants the average values of which were experimentally

determined. Such a spread of size lead, directly to a spread of

terminal velocities.

To attempt an analysis of a model which is close to the

physical situation involves the immense complication of a multiple

summation over a drop size spectrum, which varies with rainfall

rate, and a set of Fourier components.

The author would not suggest that this be done having himself

been baulked by the complexity of the problem. A constructive

suggestion the author would make is that the cross-correlation

analysis be attempted to find the lag for maximum association. Such

is desirable as it will only be possible to determine the lag by

visual inspection of records when the mirror image is very pronounced.

Once this maximum coefficient of association is known the

physically more meaningful regression lines can be derived, with

confidence that a freak lag will not reduce the significance of

a "lagging association" to a low level.

The above model would require for the steady state a Fourier

analysis. However, it is possible to consider the effects of lag

for such a situation without such complications.

Suppose that both records are randomly varying time series

which are correlated at a lag k with a cross correlation coefficient

of R_k.

Now for lags, i, greater and less than k, R_i will fall off with $|i-k|$. A cross correlation diagram, like Owolabi's, can be drawn. The sharpness of the peak of the diagram will depend upon the auto correlation of the two series. If the series have a long "memory" (COLLIN, GROOM and HIGAZI, (1966)) then the cross-correlation coefficient diagram will have a broad maximum. Thus if the lag is of the same order as the memory the instantaneous comparison will yield a strong association. While if the memory is short compared with the lag the instantaneous comparison will be between two uncorrelated series so the association will be weak.

CHAPTER 6

Further Discussion

6.1 "Lissajous Plots"

If the mirror image effect is not obviously apparent in a record the duration of a lag or lead cannot be estimated by inspection. If also the data are insufficient for reliable cross ~~auto~~ correlation analysis then some other way of establishing the existance of a lag or lead must be found.

In consideration of the effect of lag or lead in his records RAMSAY (1960) noted if consecutive points on the scatter diagrams of I and F were joined a kind of Lissajous figure was formed. Ramsay obtained ellipses with both clockwise and anticlockwise rotations for records with well defined mirror image effects. These "Lissajous plots" are interpreted by considering the intervals between the maxima of the current-time and the potential gradient-time records. (The maximum potential gradient is here taken as being the negative peak). Fig. 6.1 shows three ideal cases of (i) there being a lead of F's maxima before that of I; (ii) there being no lag or lead between the maxima and (iii) there being a lag of F behind I. In the absence of a well defined constant lag the Lissajous plot will not show a regular geometrical shape. However, if there is a definite, although not necessarily constant, lag or lead the plot will have a tendency to either clockwise or anticlockwise rotation.

Lissajous plots for records 3.0 and 4.0 are shown in fig. 6.2. Both records clearly show a clockwise rotation. However, the examples

(i)

Lead of F   Clockwise

(ii)

No lag or lead   Neutral

(iii)

lag of F   Anti clockwise
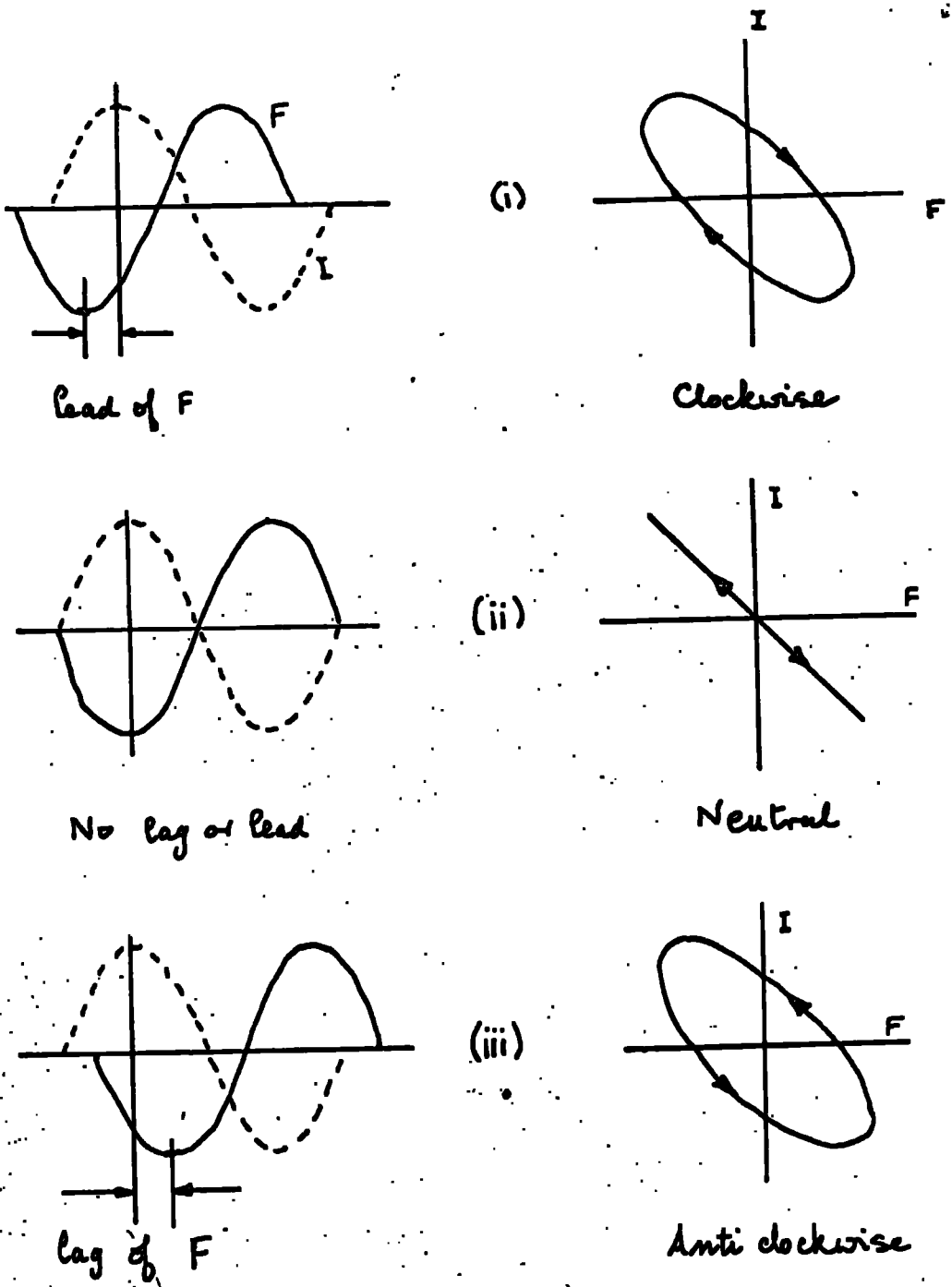
Fig. 6.1   Three cases of Lissajous plots
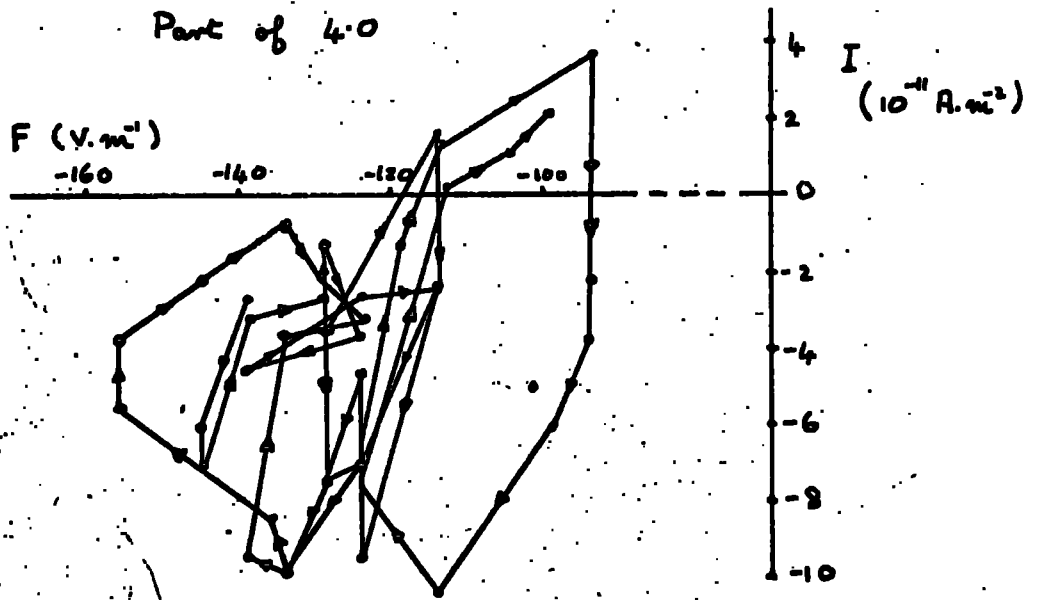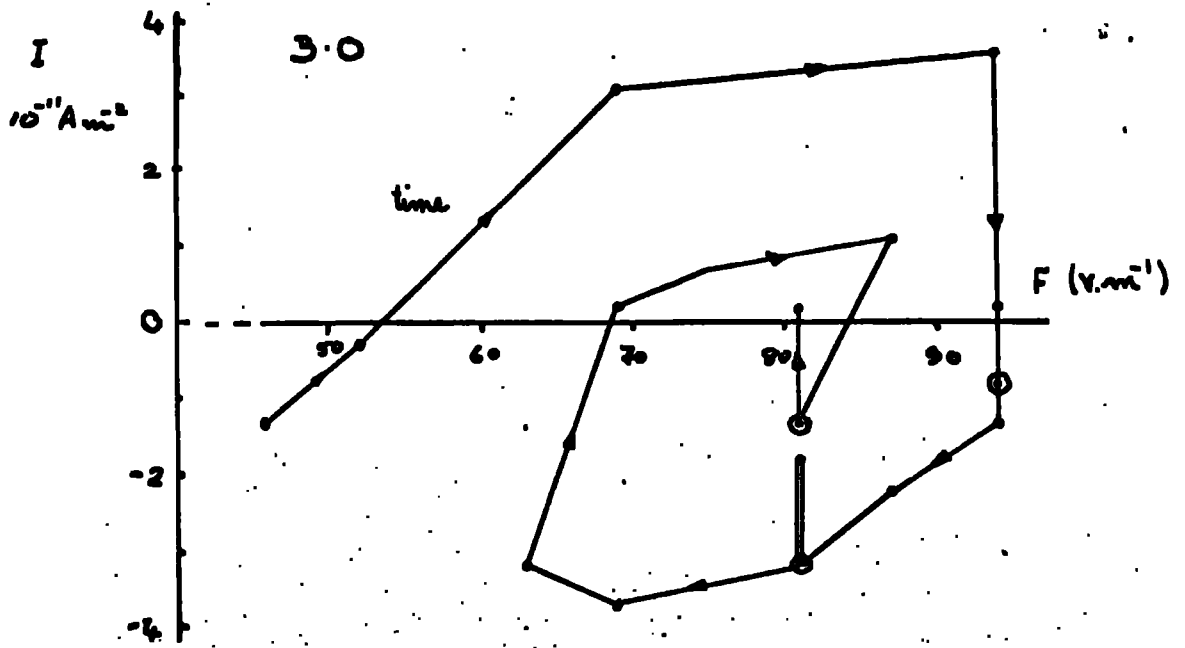
Fig. 6.2   Lissajous plots with clockwise rotation

were chosen for their clarity; in most plots there was no obvious trend towards clockwise or anticlockwise rotation. It was thought to be desirable to produce some quantitative measure of the rotation, preferably one to which a test of significance could be applied.

If the line joining consecutive pairs of points was considered as a vector then the total moment about the centre of gravity of the scatter diagram would give a measure of the rotation. However, the centre of gravity is the mean over the whole distribution, so would not be stationary as the record progressed; its position would change as each new point was entered. This difficulty could only be overcome if the moments were taken about a moving centre of gravity. Such a procedure would lead to computational difficulties so it was not attempted.

The procedure adopted was very much simplified. Each three consecutive points were considered as defining a change of direction in either a clockwise or anticlockwise sense. The case of all three points being on one straight line was considered neutral, as was the trivial case where two successive points had the same position. The ratio of the number of clockwise turns to the total number of non-neutral turns gave a measure of the extent of the clockwise rotation in the record. A value less than 0.5 clearly indicated an anti-clockwise rotation.

This measure of rotation is not all that might be desired as it in no way takes into account the extent of the turns. However, it was felt that in longish records errors would probably cancel

themselves out. The ratio proved convenient to handle and a
significance test was quite easily made as will be shown later.

A qualitative discussion of sinusoidal variation is sufficient
to show that the turning ratio gives a measure of the lag or lead.
If there is no lag or lead then the Lissajous plot will be of the
form of case (ii) in fig. 6.1. Whether a turn is clockwise or
anticlockwise is determined by chance alone. If there is a slight
lead in F before I the plot takes the form of narrow clockwise ellipse
as in case (i) of fig. 6.1. In this case each turn will be clockwise
unless the random component causes reversal. However, over the
record the random effects will be uniform so a ratio greater than
0.5 is obtained. Now if the lead of F becomes greater the ellipse
becomes less narrow and so the turns become even more pronounced
in a clockwise sense. It is thus less likely that the random
components will be able to reverse the turn. Hence the value of the
ratio will be greater. It is thus apparent that the greater the
lead then the greater will be the ratio.

In this sinusoidal case the greatest ratio will occur when the
lead is $\pi/2$. For greater leads the ellipse narrows from the circular
case at $\pi/2$ allowing the random effects to increase proportionately.
Difficulty is encountered with any analysis when the lead or lag
is greater than $\pi/2$ for the situation becomes ambiguous. Outside
the theoretical periodic cases the problem of ambiguity seldom arises.
It must be noted that if and when it does arise there is no direct
way of resolution.

In fig. 6.3 the procedure for determining the directions of the turns is given. The three consecutive points are (x_1,y_1), (x_2,y_2), (x_3,y_3). In essence the process is to transform the axes so that the origin becomes (x_2,y_2) and the point (x_1,y_1) lies on the negative x-axis of the new axes XY. Now if p is above the new X-axis (positive) an anticlockwise turn has been made in going from (x_1,y_1), (x_2,y_2) to (x_3,y_3). If p is below the new X-axis (negative) a clockwise turn has been made.

A program was written to calculate the value of p and to count the number of times it was <0, >0 and $=0$. Precautions had to be built into the program to allow for the trivial neutral points. For each record the number of neutral, n_N, clockwise, n_c, and anticlockwise, n_a, turns was calculated together with the ratio n_c/n_c+n_a.

The significance test was devised from calculating the probability of getting the particular ratio obtained or a more clockwise one, on the basis of chance alone. This is done very simply as the distribution of the number of clockwise and anticlockwise turns is Binomial. If chance alone operates the probabilities of getting either clockwise or anticlockwise turns are equal. If the neutral turns are excluded then

$$p(C) = p(A) = 0.5.$$

Thus the probability of getting n_c clockwise turns out of $N = n_c+n_a$ non-neutral turns is given by

$$P(n_c) = (0.5)^N \frac{N!}{n_c!\,(N-n_c)!}$$
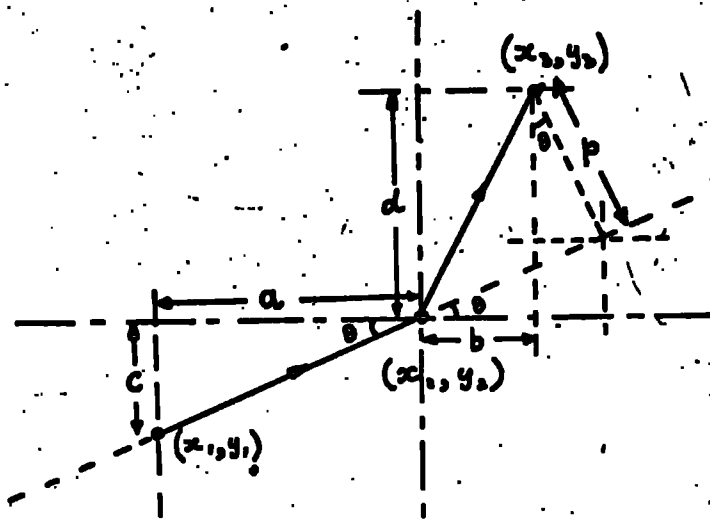
$$b = q \cos\theta - p \sin\theta$$

$$d = q \sin\theta + p \cos\theta$$

$$\therefore d\cos\theta - b\sin\theta = p(\cos^2\theta + \sin^2\theta) = p$$

$$\boxed{p = d\cos\theta - b\sin\theta}$$

$$\theta = \tan^{-1}(c/a)$$

$$a = x_2 - x_1$$

$$b = x_3 - x_2$$

$$c = y_2 - y_1$$

$$d = y_3 - y_2$$

Fig. 6.3 Determination of turning ratio

So that the probability of getting at least n_c clockwise out of N non-neutral turns is

$$P = P\left(\text{at least } n_c\right) = \sum_{r=n_c}^{N} \frac{(0.5)^N \; N!}{r! \; (N-r)!} \; .$$

This latter expression was computed and is shown together with results of the ratio program in table 6.1. A ratio is here said to be significantly clockwise at a particular level if the probability of obtaining that ratio, or a higher one, by chance where both directions are equally probable is less than the chosen level. A ratio is said to significantly anticlockwise, similarly, if $(1-P)$ is less than the chosen level.

The ratios for records 4.0 and 6.0 are in fact significantly clockwise at 0.05%. The probabilities are given as 0.000 because the fourth figure has been 'rounded' off.

Comparison with table 4.2 shows that of the six records with significantly clockwise ratios at some level four have significant correlation coefficients of ΔF with I. Suppose the potential gradient, F, varies sinusoidally as

$$F = F_0 \sin \omega t$$

then the displacement current is proportional to

$$\frac{dF}{dt} = \omega F_0 \cos \omega t.$$

Thus the displacement current lags behind the potential gradient by $\pi/2$ and so a Lissajous plot of F and I where I has a large displacement current component will be clockwise.

Lissajous Running Ratios

Record No.	n_N	n_c	n_A	Ratio $\dfrac{n_c}{n_c+n_A}$	P
2.0	11	10	12	0.455	0.738
2.1	13	37	27	0.578	0.130
3.0	6	10	2	0.833	0.019 **
4.0	12	94	37	0.718	ϕ 0.000 **
6.0	21	112	27	0.806	ϕ 0.000 **
7.0	80	37	35	0.514	0.453
7.1	15	0	1	0.000	ꜟ
8.0	16	45	46	0.495	0.583
9.0	65	23	34	0.404	0.944 o
10.0	38	15	10	0.600	0.212
11.0	30	14	8	0.636	0.143
13.0	4	2	1	0.667	ꜟ
13.1	8	6	4	0.600	0.377
14.0	10	18	8	0.692	0.038 **
15.0	21	6	1	0.857	0.062 *
16.0	10	22	12	0.647	0.061 *
17.0	13	3	8	0.273	0.967 oo
18.0	7	1	3	0.250	ꜟ
19.0	48	22	15	0.595	0.162
20.0	18	2	2	0.500	ꜟ

** Significantly clockwise ratio at 5%.

*   "   "   "   " 10%.

oo   "   anticlockwise   "   " 5%.

o   "   "   "   " 10%.

ϕ P < 0.005

ꜟ   insufficient observations for meaningful test

Table 6.1

Of course the converse is not true as is snown by record 14 where the correlation coefficient between ΔF and I is virtually zero (-0.06). Even after rejecting those records where the displacement current is evident there are still records having rotations which must be otherwise explained. Physically the rotations signify a lag or lead between the current and potential gradient records.

CHALMERS (1965) has explained qualitatively that one would expect in the absence of point discharge a lead of potential gradient when an unchanging cloud system is approaching an observer. While there would be a lag in the potential gradient record if a stationary cloud system were developing. Thus an approaching system would be clockwise while a developing system would be anticlockwise.

With only one recording station it is difficult to decide which process is predominant as both will usually exist side by side. However it is obvious that a fast moving cloud will have a larger "approaching component" than will a slow moving cloud. As a very rough indication of the cloud speed the reciprocal of the isobar separation on the Daily Weather Report maps was taken.

The values of ratio against the cloud speed for the significant ratios are plotted in fig. 6.4. Although very little importance can be attached to a graph containing only four points two tentative conclusions can be drawn. The two clockwise observations are associated with high cloud speeds while the two anticlockwise observations are associated with lower cloud speeds. It thus seems that both the cases postulated by CHALMERS (1966) have been operative. The developing
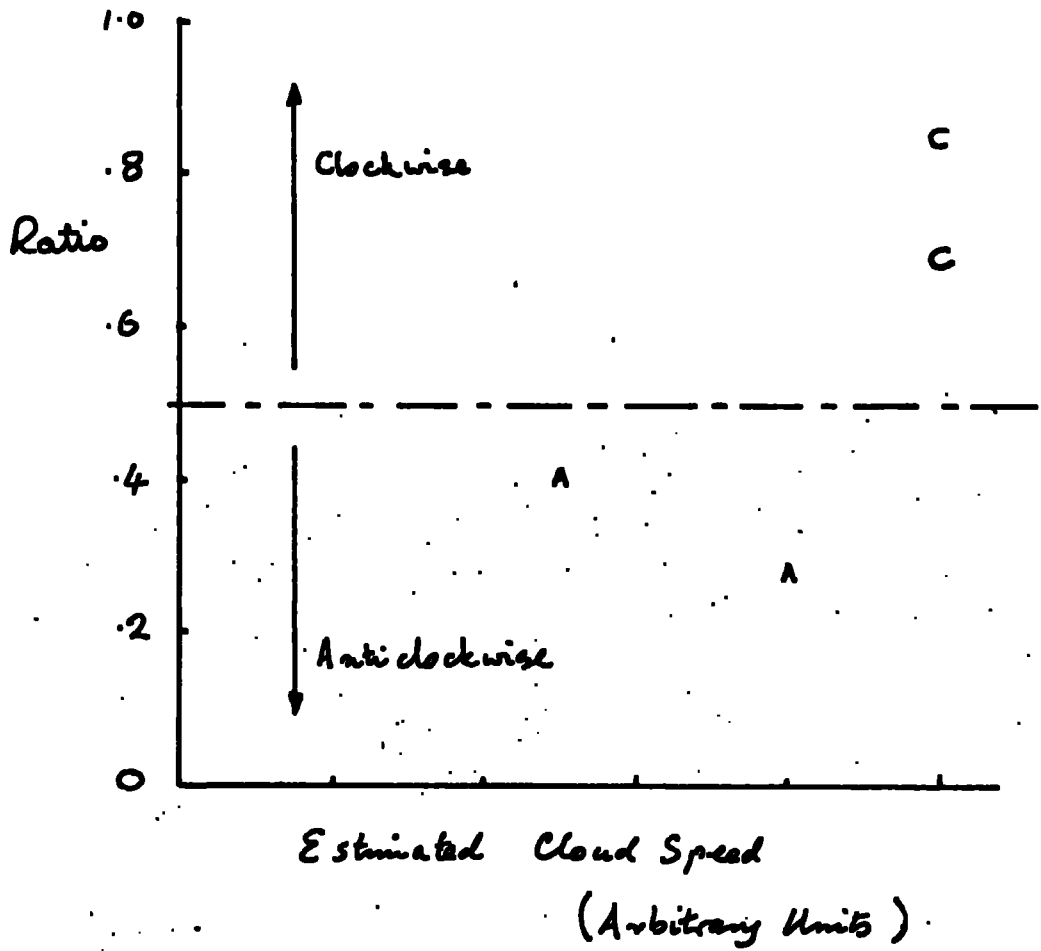
Fig. 6.4   Landau ratio against cloud speed

situation being evident at low cloud speeds and the approaching
situation evident at high cloud speeds. It must be emphasised that
these conclusions are drawn on very scanty evidence.

6.2 Measurements at different levels

On four occasions records were taken at Sunniside immediately
before or after a record was taken at a lower level. This was done
in an attempt to find information about the vertical profile of I
and F. The pairs of records 2.0 and 2.1, 13.0 and 13.1, 14.0 and 15.0,
19.0 and 20._ show that the time separation between the levels
varied from 16 to 33 minutes.

Examination of tables 4.1, 4.2 and 4.3 shows that there was
in general a difference in the relation between I and F as well as
in the actual values of I and F. However, there was no consistent
pattern to the changes.

It would seem that the assumption of the quasi-steady state was
not always justifiable. There was no way of telling whether or not
there had been a change in conditions with the horizontal displace-
ment and/or the interval of time between observations. In view of
this uncertainty any explanation of the changes with level would
be quite meaningless.

6.3 Suggestions for further work

Many of the uncertainties of the present work have arisen from
the inability of a single station to resolve spatial and temporal

effects. If the work could be extended to having more than one
simultaneously recording station many uncertainties would be
eliminated. A synoptic network would be ideal but this would at
present be beyond the scope of, at least, a University department.

A minimum sufficient requirement would be a stationary
observation point and a mobile van, as used by the author, which could
take its position at a point along the wind direction drawn through
the fixed station. Such a pair of stations would be able to
establish the relative importance of the development and motion of
a cloud system. It would be of immense value to measure the vertical
wind profile during each record taken by the pair. Such a measure-
ment would remove large errors when analysis involving the cloud
speed is attempted.

If records taken by the pair of stations were sufficiently long
cross correlation analysis as used by OWOLABI and CHALMERS (1965)
would prove a powerful tool in analysis. For this to be used to its
full potential an automatic recording system, perhaps like that
described in chapter 10, would be almost indespensible.

If a realistic investigation of the vertical profiles in
nimbo stratus conditions is to be made the author feels that it
would be necessary to have several stations, like REITER (1965),
distributed with small horizontal separation and large vertical
separations. It would thus be possible to take simultaneous
observations at different levels. There are so many changing influences
in this type of weather that a single station could only hope to get

representative readings over a few, perhaps many, years of continuous recording. To solve the vertical profile problem, which this investigation has failed to do, one of the above two approaches would be necessary.

If similar apparatus were to be used it would be desirable to develop a less critical method of displacement current compensation. It would also be desirable to render the collector surface more natural by covering with grass for example. This would avoid any unnatural splashing effects. Such were not noticed but may nevertheless have been present.

PART II

Chapters 7 to 10

Minor Topics

CHAPTER 7

Space Charge Measurements

7.1 Introduction

It was felt that measurements of space charge density in disturbed weather may have made a useful contribution to the understanding of the results of the main investigation. It was thought that the most suitable method would be that of filtration. ORLENSKY (1925) was the first to use a filtration method of measuring space charge. The collection efficiency of his steel wool filter may well have been insufficient to trap a large proportion of small ions. VONNEGUT and MOORE (1958) have discussed the problem of collection efficiency which they find increases as the fibre diameter of the filter medium decreases.

MOORE, VONNEGUT and MALLAHAN (1961) have used with success a filter of a glass asbestos medium (the Cambridge Filter Corporation's "Absolute Filter"). BENT (1964) conducted tests on the small ion collection efficiency of this filter, whose fibres are of diameter about 0.5 micron, compared with 50-100 micron diameter fibres comprising steel wool. Bent found that less than 0.2% of small ions avoided capture in this filter.

It was feared by BENT (private communication) that if the filter material became saturated with water it may suffer permanent damage. Such saturation is very likely to occur if a collector is operated in wet weather as was invisaged by the author. It was,

therefore, decided to construct a space charge filter without employing the expensive filter packets used by VONNEGUT and MOORE (1958) and BENT (1964). Dr. C.B. Moore was kind enough to give the Durham group a large quantity of the glass asbestos filter paper of the type used in the commercially manufactured filter packets. A collector was designed which ~~only~~ used a small piece of this filter paper. The filter holder was arranged to be readily removable so that the filter paper could be replaced when damaged.

7.2   The bad weather space charge collector

Figure 7.1 shows a diagram of the space charge collector. The diagram shows the collector dismantled for replacement of the filter paper. The filter paper is held between two gauzes for mechanical support, shown by broken lines. The filter holder is screwed into the cartridge by screw threads CC'. The cartridge is held to the insulated inner case by threads BB'. The exhaust cone is joined to the body of the collector by threads AA'. A filter paper can be replaced quite easily in five minutes.

The filtration properties were tested following the procedure of BENT (1964). The apparatus shown schematically in fig. 7.2 was set up in a sealed room. The out put of the conductivity chamber was recorded with and without the filter holder's presence in the space charge collector. The AC voltage supply to the fan was adjusted so that the fan drew air at the same rate in both cases. The flow was monitored with a standard gas meter.
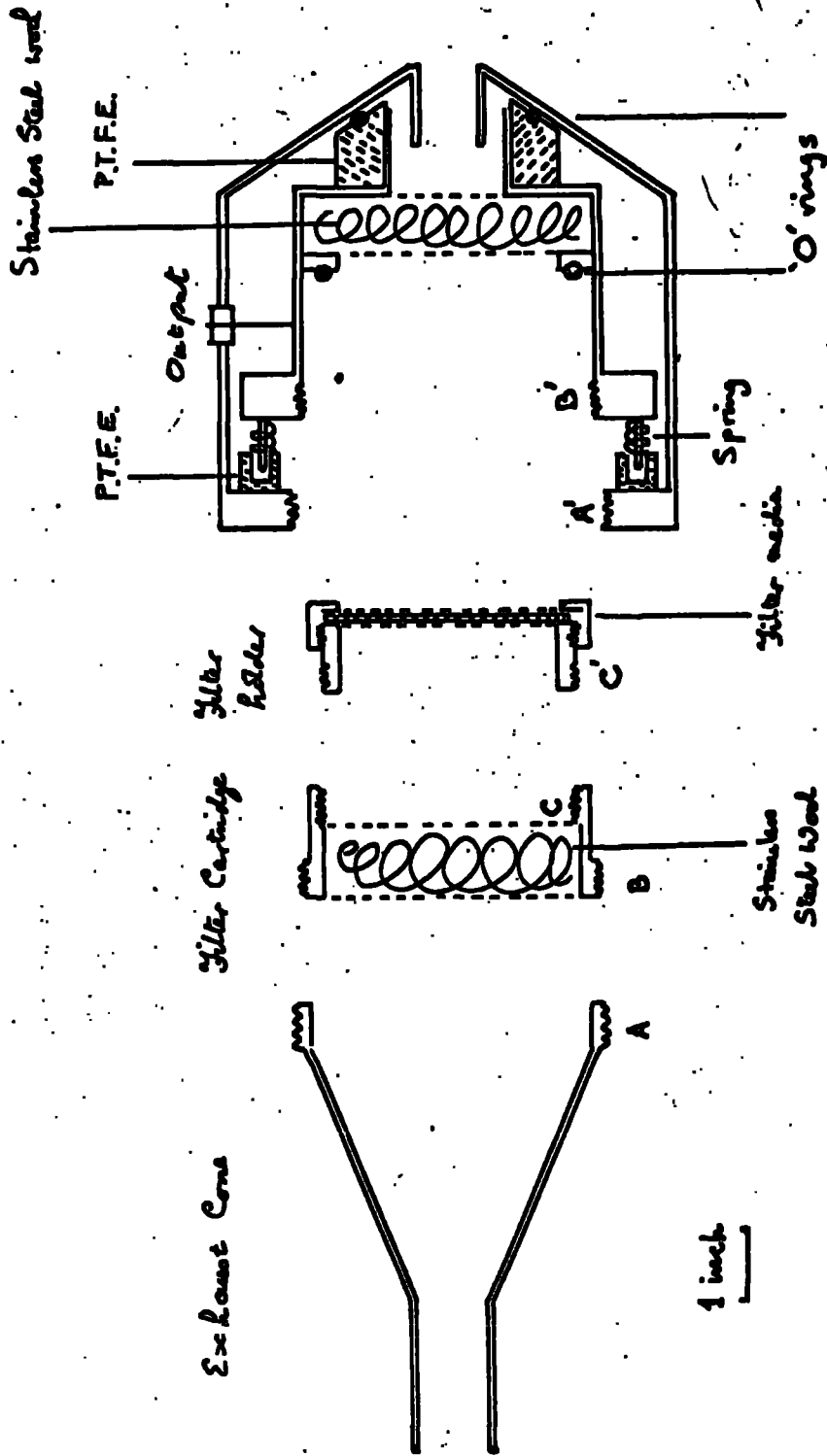
Fig. 7.1   The bad weather space charge collector
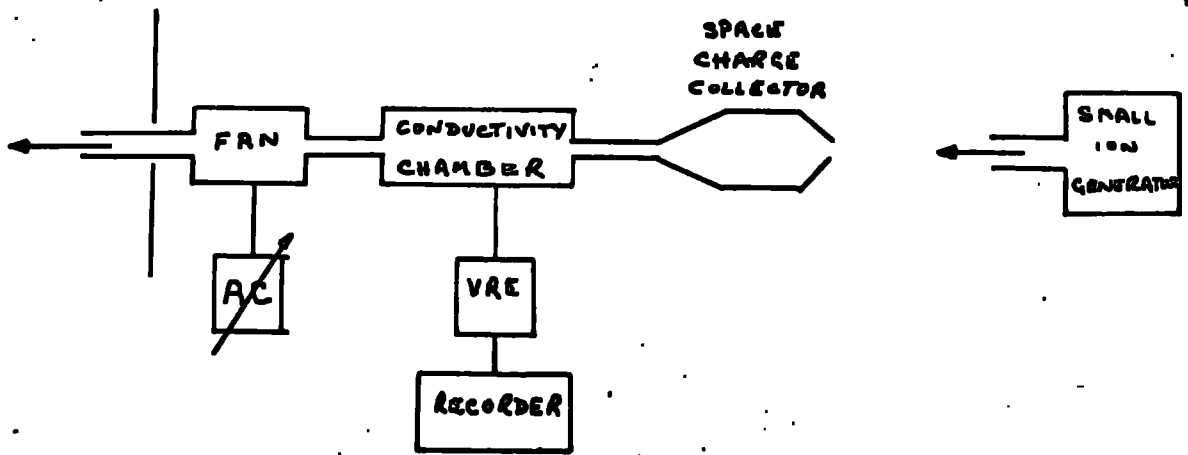
Fig. 7.2   Test of filtration efficiency
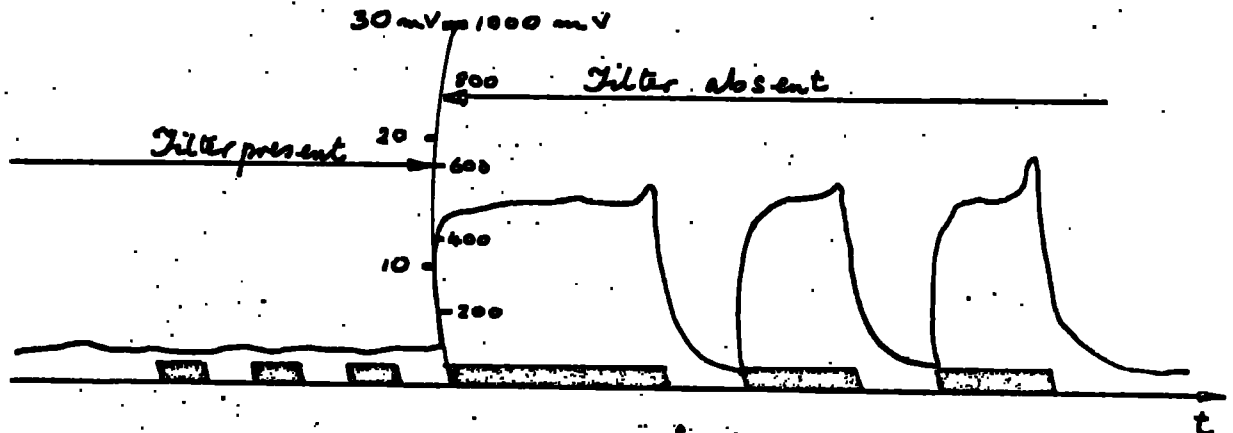
Fig. 7.3   Record of efficiency test

A tracing of the record obtained is shown in fig. 7.3. The shading in the lower portion shows when the polonium small-ion generator was on. The record shows that in the presence of the filter, no change in the recorded conductivity can be detected. The smallest detectable change above the noise level would have been about 1 mv. Now in the absence of the filter the VRE registered 500 mv so that the filtration can be seen to have removed all but less than 1 part in 500 of the small ions. Thus the filtration is better than 99.8% for ions contributing to the conductivity of the air. This figure shows that the bad weather collector was as good in its filtration properties as was Bent's collector.

There was one serious drawback to the collector constructed. The area of the filter was very much less than that of the Cambridge filter. There was a considerable pressure drop across the filter which necessitated using a powerful extractor fan. Whilst this was no problem in the laboratory tests, difficulty was found in obtaining a sufficiently powerful fan to run off the van's limited power supplies. This problem was not solved in the time allotted to the project, so the bad weather collector was not operationally used. It has, however, been used in a laboratory investigation by Mr. L.N. Rogers who found it to function satisfactorily.

It has been mentioned earlier that Mr. Ogden was conducting a fine weather space charge investigation using the van. Although the aim of wet weather measurements could not be realised some measurements over melting snow surfaces were attempted in collaboration with Mr. Ogden.

7.3 The Ogden space charge collector

This collector was built with minor modifications on the
BENT (1964) pattern using a Cambridge filter. As will, no doubt,
be fully described in Mr. Ogden's Thesis, an adequate flow could
be achieved with the Cambridge filter.

7.4 Space charges over melting snow

Observations of electrical effects associated with blowing
snow made by SIMPSON (1919) in the Antartic formed the basis of a
theory of thunderstorm charge separation, SIMPSON and SCRASE (1937).
The space charge distribution in the lower 3 m of the atmosphere
was inferred from potential measurements by MAGONO and SAKURAI (1963).
They found negative space charge upto the first metre and postive
thereafter.

Direct measurements of space charge at two fixed levels by
BENT and HUTCHINSON (1965) showed that in certain conditions over
melting snow the space charge was negative at 1 metre while positive
at 2 m. These conditions were found to persist in conditions of
strong mixing. Their explanation was that there was a separation
of charge at the surface liberating negative charge to the air. The
upper positive charge was thought to have been produced by the blowing
of snow at sub-zero temperature on the high moors from which the wind
was blowing. It was thought by Bent and Hutchinson that the process
of charge separation involved may have been the same as that
described by DINGER and GUNN (1946). Bent and Hutchinson found that

no such charge separation occurred when the wind speed was considerably less than 1 m s^{-1}.

It was proposed with the mobile apparatus to try and verify the observations of Bent and Hutchinson. The plan was to measure vertical space charge profiles over snow surfaces at sites above and below the 0°C isotherm.

To measure the profiles the space charge collector was pivoted at its centre of gravity and an inlet pipe fitted so that the height of the intake could be varied from 0 to 2 m in as many steps as desired.

It was felt that a profile of closely spaced vertical soundings may have been able to detect the effect in conditions where the two fixed level measurements lacked sufficient sensitivity.

7.5 Results and comments

Several profiles were measured in the winter 1965-66 but the results were not found to be reproducible. The lack of success was attributed to the fact that the inlet pipe was made of rubber. The rubber was thought to have had static charges on its walls. The field set up by these charges would attract small ions of the opposite sign to the walls. As there would have been static charges of both signs on the walls, it seems that the rubber tube would act as an efficient, although undesirable, small ion trap. It has been noted, unfortunately too late, that this effect was found by NOLAN and KENNY (1953) for condensation nuclei.

The rubber inlet was replaced by cardboard but a satisfactory method of fixing the tube was not found.

The eventual solution of raising and lowering the whole space charge collector was decided upon. There have been no suitable conditions for the experiment since the last solution was implemented. It is hoped that Mr. Ogden will be able to get some satisfactory results in the winter of 1966-67.

CHAPTER 8

Charge Separation at Power Lines in Fog

8.1 Introduction

Observations at Kew Observatory from 1933-1936 (B.N.R.) showed long periods of negative potential gradient in the absence of precipitation. CHALMERS and LITTLE (1947) found in Durham negative conduction currents and potential gradients when the two nearest meteorological reporting stations reported mist. Also they noted that there were no such reports on the occasions when they observed normal positive values. Their conclusion that the negative potential gradient was associated with the mist was supported by the observations of CHALMERS and HUTCHINSON (1949). The latter workers noted negative potential gradients in the presence of "high hanging fog".

Such observations suggest a process of charge separation which is not connected with precipitation. This hypothesis was verified by CHALMERS (1952) using a portable field measuring device. In conditions of mist or fog, Chalmers made journeys to the east of Durham making regular measurements of field. The source of the charge separation was found to be high tension electricity lines where negative space charge is liberated at the rate of some microamperes per pylon. This of course assumes the liberation to be at the pylons, from whence comes the maximum hissing noise in mist or fog.

MÜHLEISEN (1953) has detected this effect at distances of up to 7 km down wind of a power line. BENT and HUTCHINSON (1965)

detected an excess of negative space charge at Durham Observatory
when the nearest mist was upwind on the coast at a distance of 14 km.

To investigate this phenomenon further it is first necessary
to establish the validity of the assumption that the charge separation
takes place at the pylons, rather than uniformly along the power
lines.

8.2 Relevant apparatus

The effect can be examined by observing the potential gradient
due to the liberated space charge. If the wind direction is known
the source of the charge separation can be easily pinpointed. The
van is eminently suitable for such an investigation as it is movable
and is fitted already with a field mill.

It was found, as it was · by CHALMER (1952), that no useful
readings could be taken within about 30 metres of the pylons, as
the 50 c/s signal was picked up and amplified. No 50 c/s discrimina-
tion had been built into the field mill amplifier, nor was it thought
to be worthwhile for this minor investigation. All observations were
made at a distance of 40 m from the power line.

A simple wind vane was constructed and was observed visually
to get the wind direction.

8.3 Results

The experiments were conducted in a field at Whitwell near
Durham by kind permission of the farmer. The site was chosen because

it had a power line crossing from roughly North to South and a pylon
in such a position that it was approachable from both East and
West, fig. 8.1.

Runs round the path ABCD were made with continuous monitoring
of potential gradient and wind direction. The results, which were
quite reproducible, were taken on mornings when there was mist or
fog in late October 1965.

A typical morning's (19.10.65) results are shown in fig. 8.2.
In all cases the wind speed was very low (less than 1 m s^{-1}). The
wind direction fluctuated considerably but was in general perpendicular
to the power line.

It can be seen quite clearly in the downwind runs that the
maximum depression of potential gradient occurs when the wind blows
from the pylons to the field mill.

8.4. Discussion

The experiment showed quite conclusively that the charge
separation does, in fact, take place at the pylons to a greater
extent than it does along the lines.

A much more elaborate experiment would be required to detect
if any separation takes place between the pylons. It would be
necessary to make observations simultaneously at several points up
and down wind of the line before one could be sure that the depres-
sion observed was not due to that at the pylon. Also the simultaneous
observations would eliminate errors due to changes of potential
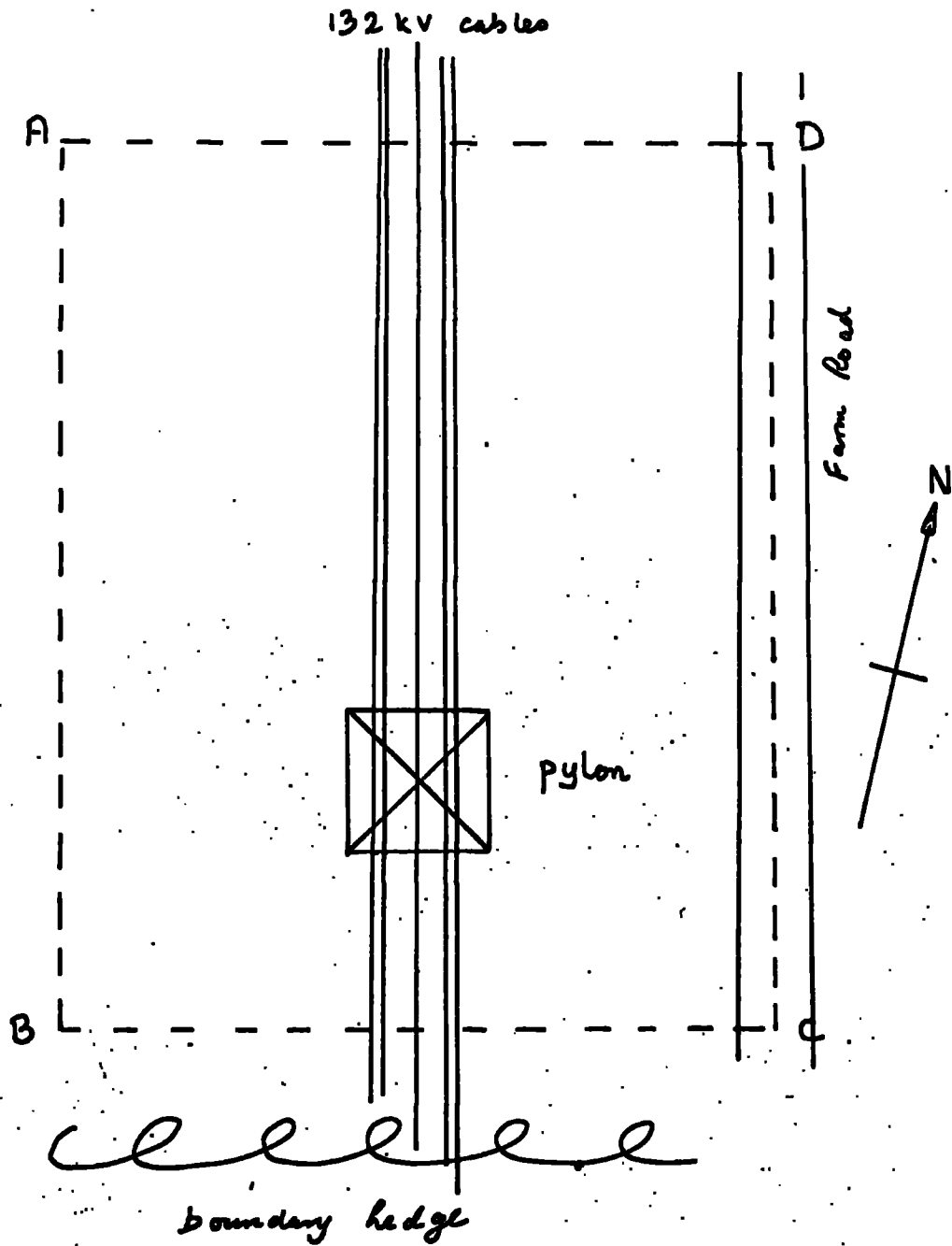
Fig. 8.1 Sketch of experimental site
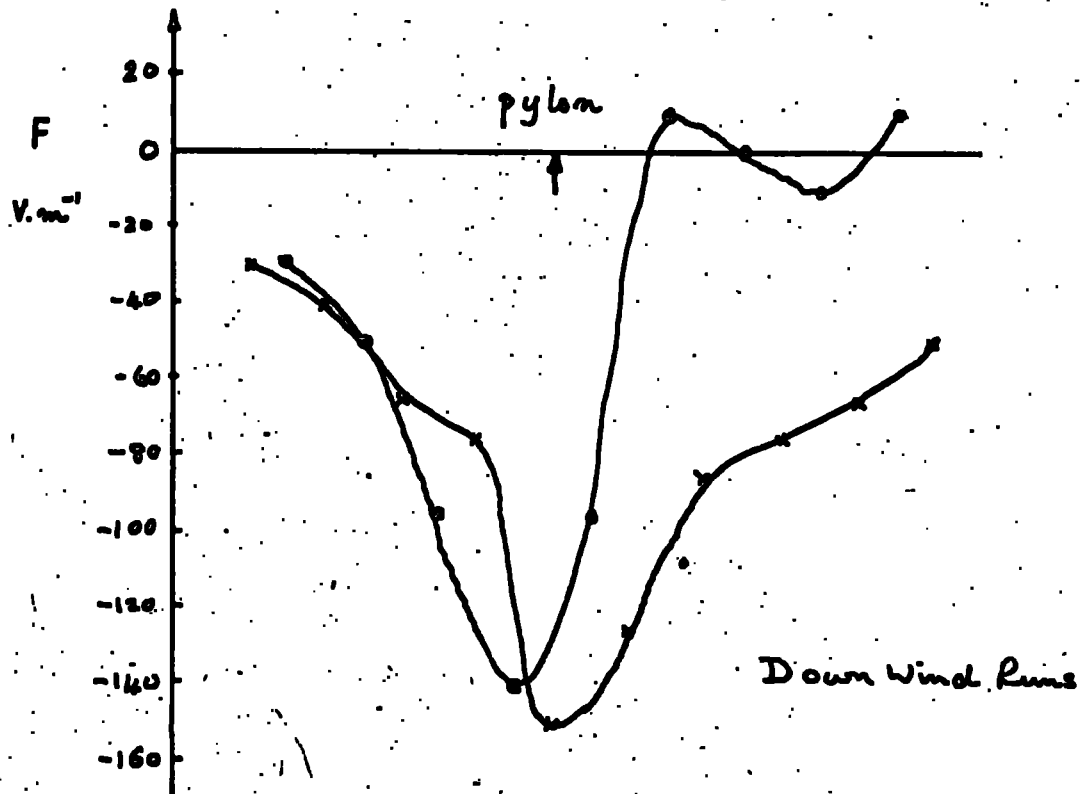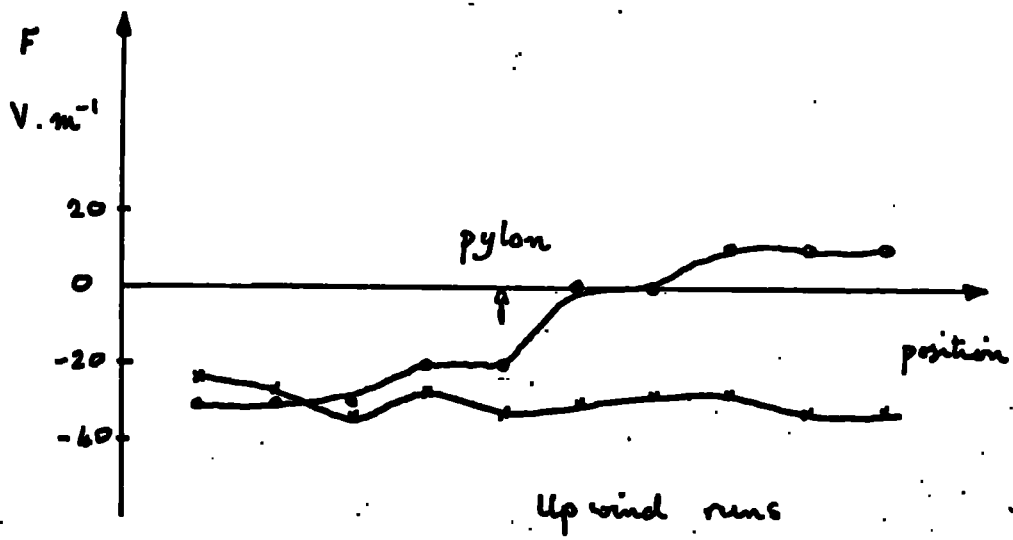
Fig. 8.2   Pylon effect in fog   19.10.65.

NOTE

There are two errors on pages 90/91. Their effect is not critical but the following modifications are necessary.

For electrons liberated at the negative peak voltage their distance of travel will be composed of two parts that while free and that while a small ion. Since the free life is small the distance travelled as a small negative ion will be that travelled in $\frac{1}{4}$ of a cycle i.e. $d/2$. The condition for escape has to be modified. Escape is achieved if the electron while free, can travel a distance greater than $d/2$.

The value 132 kV taken for the peak voltage is in fact the r.m.s. voltage so a correction must be made here also. Everywhere 132 kV appears the value should be $132\sqrt{2}$ kV.

(i) The value of d should read 0.14 m instead of 0.1 m.

(ii) At the peak voltage F/p = 196 V.m^{-1}/mm Hg not 140.

(iii) Thus the drift velocity is 16×10^3 m s^{-1}

(iv) So the electrons travel 0.16 m in their lifetime.

Now as $d/2$ = 0.07 the condition that the electrons travel further than $d/2$ is easily satisfied.

Similar modifications render the proportion 27.8% an underestimate.

gradient with time.

The cause of the charge separation is likely to be due to insulation breakdown. This results in currents flowing across the surface of the insulators producing ionization in the air nearby. Now since the potential of the line alternates the attraction and repulsion of each sign of ion will also alternate. The negative particles produced by ionisation will be electrons, although these will soon become attached to neutral molecules to form ions of molecular size. However, in the time before attachment, the electrons have vastly greater mobility than the molecular sized ions.

Thus, in the negative phase of the alternating voltage, electrons will be repelled from the line. Now the distance they will reach will depend upon how long the electron remains free. When attachment takes place the velocity will be greatly reduced due to the relatively low mobility of the larger ion.

8.5 Quantitative discussion

Whether or not negative space charge can be liberated by this process depends upon how far the electrons travel before their capture. If this distance is greater than that which a small ion will travel in half a cycle the negative small ions formed by electron capture will not be drawn right back to the line in the subsequent positive half cycle, so will contribute to the atmospheric space charge.

The critical distance, d, which a small ion can travel in a half cycle is given by

$$d = \int \mu F \, dt$$

integrating over half a cycle. Where μ is the small ion mobility and F the maximum local potential gradient. To a first approximation F can be taken as the quotient of the line voltage, V, and the length of the insulator, l. The expression for d is then

$$d = \int_0^{0.01} \frac{\mu \, V_o \sin 100\pi t}{l} = \frac{2\mu \, V_o}{100\pi l}$$

Substituting for

$$\mu = 1.5 \times 10^{-4} \, m.s^{-1}/V.m^{-1}$$

$$V_o = 132 kV$$

and $l = 1.25 \, m$

$$d = \frac{2 \times 1.5 \times 10^{-4} \times 132 \times 10^3}{100\pi \times 1.25} = 0.1 \, m$$

MUHLEISEN (1961) citing LENARD (1913) has stated that in moist air the lifetime of free electrons is increased from the usual 10^{-8} sec to about 10^{-5} sec. Now those electrons which are produced at the instant of the peak voltage will travel the greatest distance. At the peak voltage the ratio F/p in $V.m^{-1}/mm.Hg$ is $\frac{132 \times 10^3}{1.25 \times 760} = 140$. The experimental data of NIELSEN and BRADBURY (1937) show that the electron drift velocity is $14 \times 10^3 \, m.s^{-1}$ in air for such F/p. So in their lifetime of 10^{-5} sec these electrons will travel 0.14 m, which is greater than the critical distance of 0.1 m.

NOTE

Assuming a constant electron mobility an estimate of the proportion of escaping electrons can be derived.
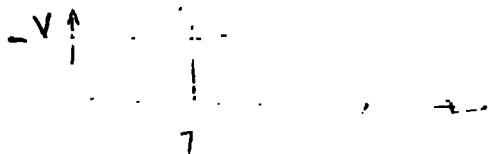
$$\theta = 2\pi ft = 100\pi t$$

$$\phi = 100\pi T$$

All electrons liberated before T will escape.

At T we have

$$\mu_e T \; \frac{V_o \sin\theta}{d} + \int_\phi^\pi \frac{\mu V_o \sin\theta \; d\theta}{100\pi \, d} = \int_o^\pi \frac{\mu V_o \sin\theta \; d\theta}{100\pi \, d}$$

So $\quad \mu_e T \sin\phi - \int_o^\phi \dfrac{\mu \sin\theta d\theta}{100\pi} = 0$

Thus $\quad \mu_e T \sin\phi - \dfrac{\mu}{100\pi} (1 - \cos\phi) = 0$

Now μ_e, electron mobility $\sim 10^{-1}$; μ, small ion mobility $= 1.5 \times 10^{-4}$

τ, electron lifetime $\sim 10^{-5}$ hence $\dfrac{\mu}{100\pi} \simeq 5 \times 10^{-7}$

So we have $10^{-6} \sin\theta - 5.10^{-7} (1 - \cos\phi) = 0$

i.e. $\quad 2\sin\theta - 1 + \cos\phi = 0$

Solution of which gives $\quad \cos\theta = 1 \quad$ or $\quad -0.6$

$$\theta = 0 \quad \text{or} \quad 127^o$$

Thus fraction of liberated electrons escaping in each cycle is

$$127/360 = 35.3\% \simeq \tfrac{1}{3}.$$

Electrons will escape at voltages below the peak as long as the drift velocity is sufficient for electrons to exceed the critical distance in their lifetime. The critical drift velocity is clearly $d/10^{-5} = 10^4$ m s^{-1}. The data of Neilsen and Bradbury show that this is equivalent to a critical E/p of 90 V.m^{-1}/mm.Hg. This value is achieved in the present circumstances by a line voltage of 85.5 kV.

It is a trivial matter to show that the alternating line voltage is more negative than 85.5 kV for $^1/3.6$ of a cycle. Thus it can be seen that 27.8% of electrons produced by ionisation travel further than the critical distance and so contribute to the atmospheric space charge on capture and formation of small ions.

Now clearly the actual estimate of 27.8% is not highly accurate depending as it does upon a first order approximation. However, it does serve to show that the mechanism suggested is adequate for explanation of the phenomena. The precise proportion of escaping electrons depends upon the local maximum field. The proportion is not quite independent of the actual line voltage because the electron mobility is not quite independent of E/p.

3.6 The next steps

A remaining question of interest would be to examine the ion spectra with distance from the pylons. This would presumably change as the small ions initially produced become attached to larger neutral particles forming large ions. It surely must have

been the large ions which we.e observed, at considerable distances
from pylons by BENT and HUTCHINSON. (1965) and MÜHLEISEN (1953).

In the hope of determining ion spectra a Gerdien tube was
installed in the van (see Chapter 9). However, the Gerdien could
only be run on the VRE which was, at that time, in use for the main
investigation. In fact, there were no suitable fog occasions during
the few weeks that the Gerdien was installed.

In collaboration with Mr. T.L. Ogden, a method of measuring
the large and small ion contributions of the total space charge was
evolved. A one inch diameter tube, about 1 foot in length, was
mounted in front of Mr. Ogden's space charge collector (see Chapter 7).
A potential of 240 volts was applied to an electrode coaxial with
the tube. This system serves to remove all the small ions. Their
mobility is such that, with the flow rate employed, they would all
migrate to the walls or electrode before they could have reached
the end of the tube.

Thus the space charge collector will only receive large ions.
If readings are taken with and without the potential applied to the
central electrode, the contribution of large and small ions to the
total space charge can be deduced. At the time of writing, no
observations have been made in fog with this apparatus but it is
hoped that Mr. Ogden will be able to complete the work.

CHAPTER 9

The Measurement of Atmospheric Conductivity in Disturbed

Conditions

9.1 The Gerdien apparatus

Conductivity has been measured at Durham by Dr. K.A. Higazi (HIGAZI and CHALMERS 1966). One of the chambers he used was borrowed for the few conductivity measurements made in this investigation.

The chamber was made following the design developed by GERDIEN (1905). The chamber, whose important dimensions are shown in fig. 9.1, consists of a cylindrical conductor containing a coaxial rod conductor. The inner electrode is highly insulated from the outer cylinder with P.T.F.E. insulation. The two electrodes were made of brass cleaned finally in chromic acid, to render the surfaces clean and similar to obviate contact potentials which could have a great influence on the results. (An error of 1 part in 6 would not be an outrageous estimate of the effect).

When a potential difference is applied between the conductors, a current composed of small ion carriers flows along the potential gradient. The ionic current of appropriate sign arriving at the central electrode is amplified and measured with a vibrating reed electrometer. If the whole arrangement is not shielded then movements of charged bodies e.g. the observer, will cause a displacement current to flow through the V.R.E. As this would clearly give
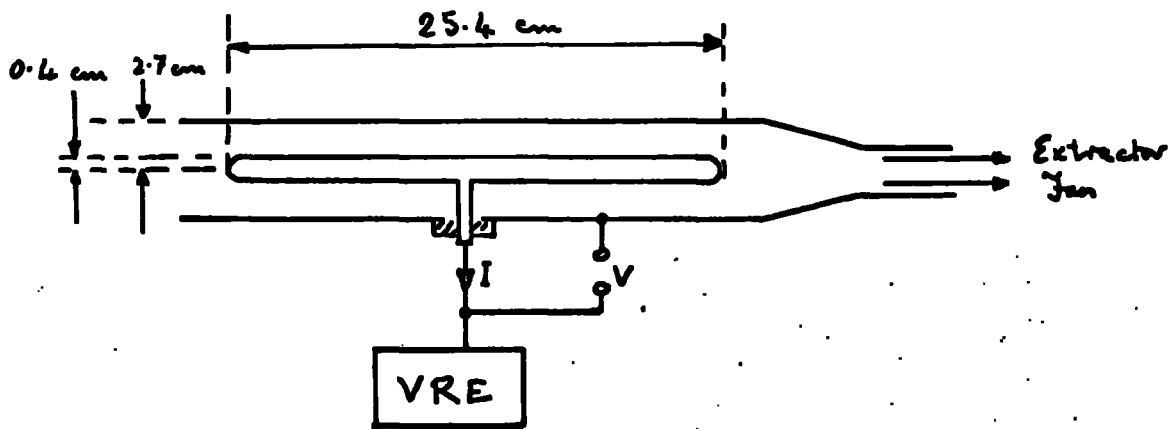
Fig. 9.1   The Gerdien chamber
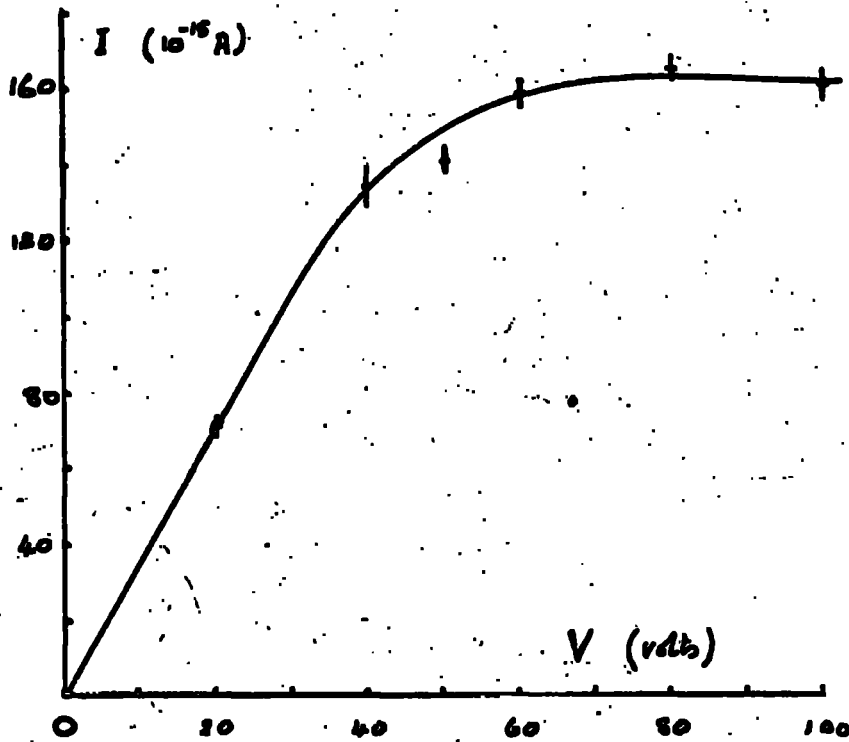
Fig. 9.2   The current-voltage characteristic

spurious readings the whole Gerdien system is mounted inside an earthed aluminium box. The air in the tube is continuously replaced by a suction fan to avoid reducing the conductivity of the air by removing the charge carriers. SWANN (1914) has shown that this rate of flow need not be constant over the cross section of the tube. In view of this, no complex fluid dynamics need be considered.

In Higazi's work a vacuum cleaner fan was used. In the van there was insufficient A.C. power to drive the fan so the AC motor was replaced by a 12v DC motor, as used in automobile heater fans. This arrangement of the DC motor, coupled with the vacuum cleaner fan blades, was capable of drawing 2 litres or air per second through the Gerdien tube.

To make conductivity measurements from the Land Rover the Gerdien tube was placed on the floor of the van and a 0.5m cardboard tube was used as an inlet pipe. Cardboard is a good material to use for this kind of task as it is a bad enough conductor not to distort the potential gradient; whilst it is not a good enough insulator to hold any residual charge, which would equally distort the potential gradient round the tube. When the apparatus was used during precipitation the cardboard tube never got wet enough to surfer damage. The spare tube kept at hand as a replacement was not called upon.

The finite length of the apparatus, together with the chosen rate of air flow and potential difference, impose a lower limit upon the mobility of ions which can always contribute to the ionic current. CHALMERS (1957)($70) has shown that the time t taken for

ion of mobility ω to get from the outer cylinder to the inner cylinder under the influence of a potential difference V is

$$t = \frac{(a^2 - b^2)}{2} \frac{\ln(a/b)}{\omega V}$$

where a and b are the outer and inner radii respectively of the Gerdien tube and ln represents natural logarithms to the base of e.

Equating this time to that taken for air flowing at velocity U to pass through a tube of length L will yield the minimum value of mobility ω which will always be captured. If the apparatus is to measure conductivity and not just count ions this minimum value for mobility for certain capture should be greater than the typical value for small ions which L contribute to the ionic current namely 1.5×10^{-4} (MKS). For air flowing at a rate R the velocity will be $U = R/\pi(a^2 - b^2)$ giving:

limiting mobility $\omega = \dfrac{(a^2-b^2) \ln(a/b) R}{2 \; V \; \pi(a^2-b^2) \; L} = \dfrac{R \ln(a/b)}{2\pi \; V \; L}$

$$= \frac{2 \times 10^{-3} \times \ln 6.8}{2\pi \; 6 \times 25.4} = 4 \times 10^{-4} \, m^2 v^{-1} s^{-1}$$

In the above calculation the potential difference has been taken as 6v. This value was chosen as it is well on the ohmic part of the current-voltage characteristic of the Gerdien tube. An experimental current-voltage characteristics is shown in fig. 9.2. The figure clearly shows the transition from an ohmic regime through an ion collection regime to saturation when all the ions available are carrying current to the central electrode.

There are a few practical points to be discussed with respect to this Gerdien apparatus.

Piezoelectricity will always rear its head when currents of 10^{-13} amperes are being measured. The piezoelectric currents set up in the cable from the head unit to the Gerdien tube due to vibration can be immense compared with the signal currents. They are, however, easily removed by the employment of coaxial cables with solid outer conductors.

In exact measurements of conductivity at a particular level it is necessary to apply a potential to a conducting ring on the end of the cardboard tube air intake. This potential is equal to that of the surroundings and serves to eliminate distortion of the potential gradient (HIGAZI 1965). However in this investigation where the tube protrudes from the Land Rover - a conducting box - such a correction would be irrelevant compared with the distortion of the potential gradient due to the Land Rover itself.

The high humidity conditions of precipitation could also be a cause of trouble. The P.T.F.E. insulators are run without heaters in the Gerdien tubes, they may have failed with respect to the 10^{12} ohm input resistor employed. Because of this risk the chamber was operated in a room at a temperature of $21^{\circ}C$ and 100% relative humidity. These conditions were maintained by boiling a kettle for one hour and there was no indication whatsoever of an insulation failure.

There would, in the conditions of fog and precipitation proposed for investigation, be a large number of water-borne charges.

These can be considered as large or super-large ions depending upon their droplet size. They will clearly have very small mobility so will not contribute to the conduction current in the Gerdien tube. However, the central electrode will catch some large ions by impaction. The contribution of this source of current to the central electrode will depend upon the out of balance large ion distribution. The current due to this source can be determined by running the Gerdien tube without any potential difference (the small ions can be filtered out electrostatically) and the impaction current measured. It was found experimentally that the contribution of impaction current was measurable but small.

9.2 Results in snow

The only results of interest taken with the Gerdien chamber were obtained on 26.11.65 in conditions of steady continuous snowfall. Readings of positive and negative conductivity together with potential gradient were taken at Sunniside and the Observatory. As only one chamber was installed in the van the positive and negative conductivities had to be recorded consecutively. The potential gradient was observed all the time. The readings at Sunniside and the Observatory were separated in time by 25 minutes and in distance by 13 km.

The results obtained are given in the order that they were taken, being exhibited in table 9.1. The subscripts 1 and 2 refer to the low level and high level results respectively.

Parameter	Units	Value	Notes
At Sunniside			
Negative conductivity, λ_2^-	10^{-14} ohm^{-1} m^{-1}	0.216	Mean over 15 min.
Positive conductivity, λ_2^+	10^{-14} ohm^{-1} m^{-1}	0.515	Mean over 15 min.
Potential gradient, F_2	V m^{-1}	+ 500	Mean over 30 min.
Air temperature, T_2	$^{\circ}$C	− 2	
At Observatory			
Positive Conductivity, λ_1^+	10^{-14} ohm^{-1} m^{-1}	1.38	Mean over 5 min.
Negative Conductivity, λ_1^-	10^{-14} ohm^{-1} m^{-1}	2.30	Mean over 5 min.
Potential Gradient, F_1	V m^{-1}	− 100	Mean over 10 min.
Air temperature, T_1	$^{\circ}$C	+ 1	
Precipitation Rate, R	mm of equivalent water.hr^{-1}	2.5	Mean over two hours of fairly constant snowfall.

Heights of recording stations above sea level:

Sunniside 300 m

Observatory 100 m

Table 9.1

Throughout the experiment the snow fell at an apparently constant rate at both sites. This subjective observation was supported by scrutiny of the observatory's precipitation record which shows a linear rise in precipitation amount over a period of two hours which includes the experiment.

At the upper level, the snow was observed to be dry with a flake diameter of about 5mm. At the lower level the snow was wet with larger flakes of about 1.5-2 cm diameter.

The total ionic current density, j, a level is given by:

$$j = (\lambda^+ + \lambda^-) F$$

Applying this equation to the results gives ionic current densities at the two levels of

$$j_1 = -3.68 \times 10^{-12} \text{ A.m}^{-2}$$
$$\text{and } j_2 = +3.65 \times 10^{-12} \text{ A.m}^{-2}.$$

9.3 Discussion

If it is assumed that a quasi-steady state prevails, it is possible to deduce a value for the current generator producing the change of ionic current with height. In a quasi-steady state the figures represent a current generator equivalent to 7.33 pico Coulombs per second over a 1 m^2 column between the levels. That is an average charge separation rate of 3.66×10^{-14} C $m^{-3} s^{-1}$.

The only likely source of charge separation would seem to have been the partial melting which occurred. If the vertical temperature gradient was uniform between the levels, then the charge separation rate in the melting region would have been 1.1×10^{-13} C $m^{-3} s^{-1}$.

This compares with the figure of 1.6×10^{-11} C $m^{-3} s^{-1}$ for a thunderstorm.

Now the value of these results cannot be rated as very high in view of the manner by which they were obtained. There are alternative explanations of the results which do not involve the assumption of a steady state. For example, the results could reflect a change with time of the situation which took place while the van was being taken from Sunniside to the Observatory. Or, there may have been a spatial change in conditions, so that the implicit assumption that the measurements taken reflect the true vertical profile was false.

Criticisms such as the above could be satisfied by having a wide network of stations. These would be able to resolve spatial and temporal changes and allow a vertical profile to be confidently built.

It would be of great interest to measure simultaneously the ionic and precipitation currents in, below and above the melting region. Such measurements would tie in nicely with the work being done on the melting of individual snow flakes in Japan by KIKUCHI (1965) and MAGONO and KIKUCHI (1963). Such a combined attack would perhaps establish quite definitely the widely held belief that the melting process plays a predominant part in precipitation electricity.

Unfortunately, time and weather did not allow repetition of this experiment, before the VRE was restored to the precipitation current apparatus of the main investigation.

CHAPTER 10

Appendix   The Automatic Recording of Data

10.1 Introduction

Earlier in this Thesis, especially chapter 2, references have been made to a proposed automatic recording system. Although no system was ever operationally used the author spent a good deal of time in designing and developing a prototype system. For completeness this appendix gives a brief description of the system. The reader will not be troubled by the electronic details. Only a description of the logic is given in terms of "black box" elements.

The requirements of an automatic recording system were taken as being as follows. It must be possible to record several inputs on a single track; each input being sampled in turn. The sampling cycle may be weighted so as to give more frequent readings of the more important parameters. It must be possible to allow the system to run for considerable recording periods without attention. The accuracy of the recorded parameters must not be limited by the quality of the recording system; that is the parameter must be able to be recorded as accurately by the system as it could have been without. It should be possible to get the data eventually onto a punched paper tape suitable for entry as a data tape into a computer.

Clearly, it would not be feasible to carry a paper tape punch
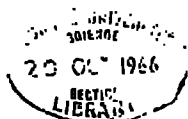
in the van because of the power and space limitations. Thus the
system invisaged was of two stages: a recording onto magnetic tape
and a subsequent play-back onto punched paper tape.

10.2 Recording

Each input in the form of a DC voltage level is selected in
turn and converted into a pulse chain whose frequency is proportional
to the voltage level. The voltage to frequency converter used is
that described by DE'SA and MOLYNEUX (1962). Each pulse chain is
admitted for a fixed time interval, so that the number of pulses
recorded is fundamental, thus allowing the subsequent output to
be independent of the tape speed. To synchronise later playback
and counting each recorded 'bit' of data is preceded by a single
trigger pulse. Two bits of recorded data would appear on the tape
as shown in trace H or fig. 10.1.

The circuitry necessary to achieve the above is indicated in
the block diagram fig. 10.2. FR1 is a free running multivibrator
which controls the speed of operation of the system. The period
of this element, 500 ms, is shown on the diagram, as are periods
of all the elements. Trace A in fig. 10.1 shows the wave form
emitted by FR1. The positive spikes, trace B, produced by the
differentiating element initiate three actions by triggering three
one shot multivibrators, OS1, OS2 and OS3. The output of OS3 supplies
the trigger pulse to the tape. OS2 causes a delay while OS1 provides
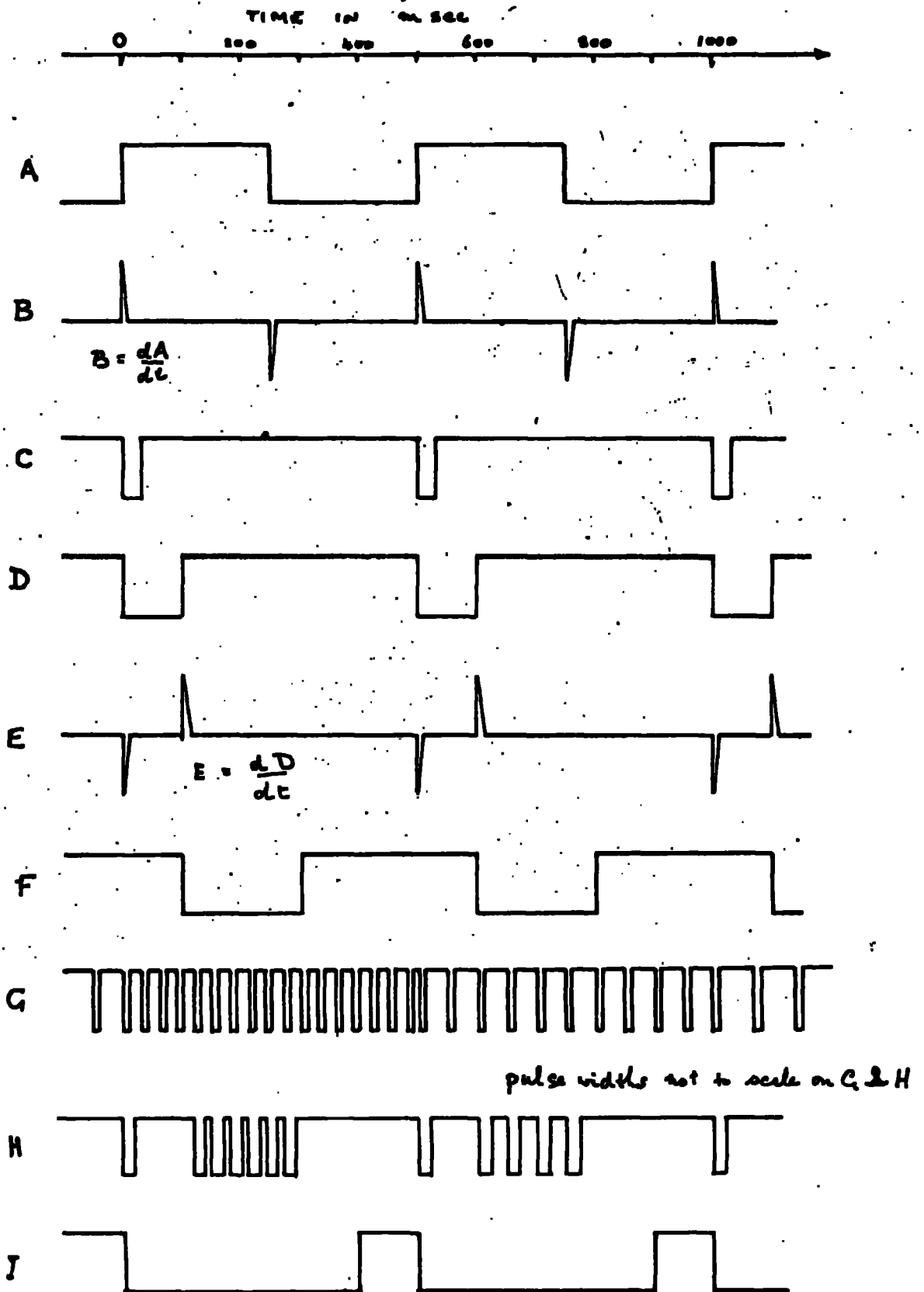
Fig. 10.1 Wave forms in automatic recording system
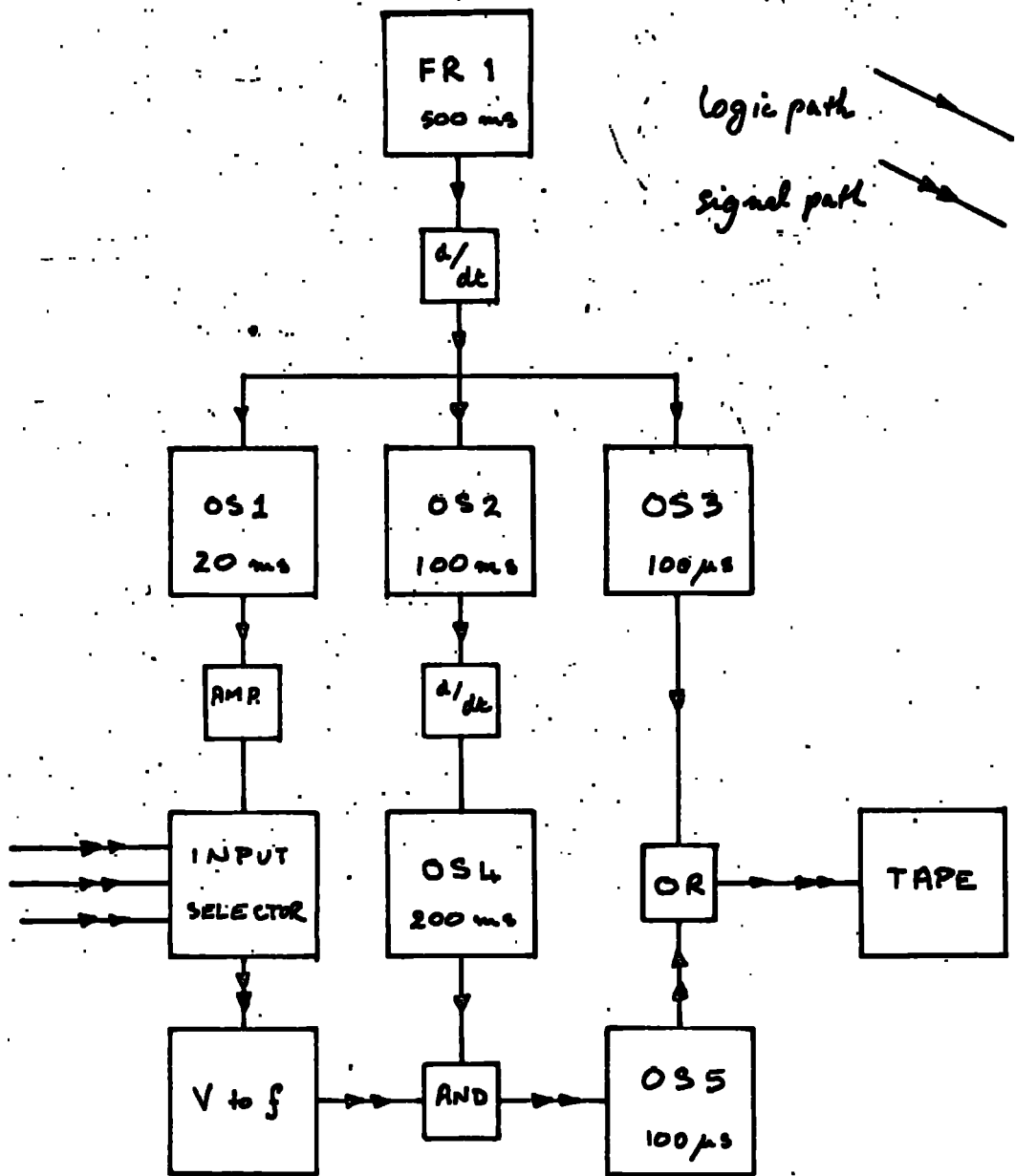
Fig. 10.2 Block diagram of recording system

a pulse which, after amplification, causes the input selector to choose the next input.

The input selector consists of a rotary relay described in connection with the rainfall recorder in section 2.3.

At the end of the delay due to OS2, trace D, the spike produced by differentiation, trace E, triggers OS4. OS4 gives a pulse, trace F, which is fed into the AND gate for a fixed period. When, and only when, the pulse from OS4 and pulses of the pulse chain from the voltage to frequency converter (V to f) are present do pulses pass out of the AND gate into OS5. OS5 is present to produce a pulse of the same standard size as those produced by OS3.

The trigger pulse from OS3 and the signal pulses from OS5 are all fed into the OR element. This element gives out a pulse when either input is supplied. Thus, the output of the OR element, which is put onto the magnetic tape, is as shown in trace H.

A prototype of this design was built and operated successfully for long periods with up to twelve voltage inputs. Without modification 48 inputs could be applied, each would be sampled once per cycle of 24 seconds. In practice, it is more likely that only a few inputs would be present with a more rapid repitition rate.

10.3 Playback

The response of a normal tape recording head to a 'square' pulse is in effect to attempt a Fourier analysis of the pulse. However, as there is an upper limit to the frequency which can be

recorded, the analysis is not complete. The result is that the recorded pulse is not clearly defined on playback. It is thus necessary to employ a pulse shaper before attempting to decode the recording.

The playback procedure is simply to note the trigger pulse and count all the pulses between one trigger pulse and the next. The clock diagram fig. 10.3 shows the elements by which this is done.

Standard sized pulses from the pulse shaper are applied to Gates 1 and 2. It is arranged that the first pulse to appear on a tape is a trigger pulse. Hence the trigger pulse will be accepted by Gate 1 which is normally open and rejected by Gate 2 which is normally closed.

Having passed through Gate 1 the trigger pulse enters the one shot multivibrator OS6. The output of OS6 is a pulse of 400 ms. Note that 400 ms from a trigger pulse is a period which includes all the signal pulses and ends before the next trigger pulse. The trace I in fig. 10.1 shows the output of OS6. The output is used to reverse the state of gates 1 and 2. Thus for 400 ms following a trigger pulse gate 1 is closed while gate 2 is open. Now the signal pulses which follow the trigger pulse will all pass through gate 2 into the counter.

The counter would be some such arrangement as used by BRAY (1964a) and COLLIN (1966) which will produce a punched paper tape output of a count by decatron tubes.
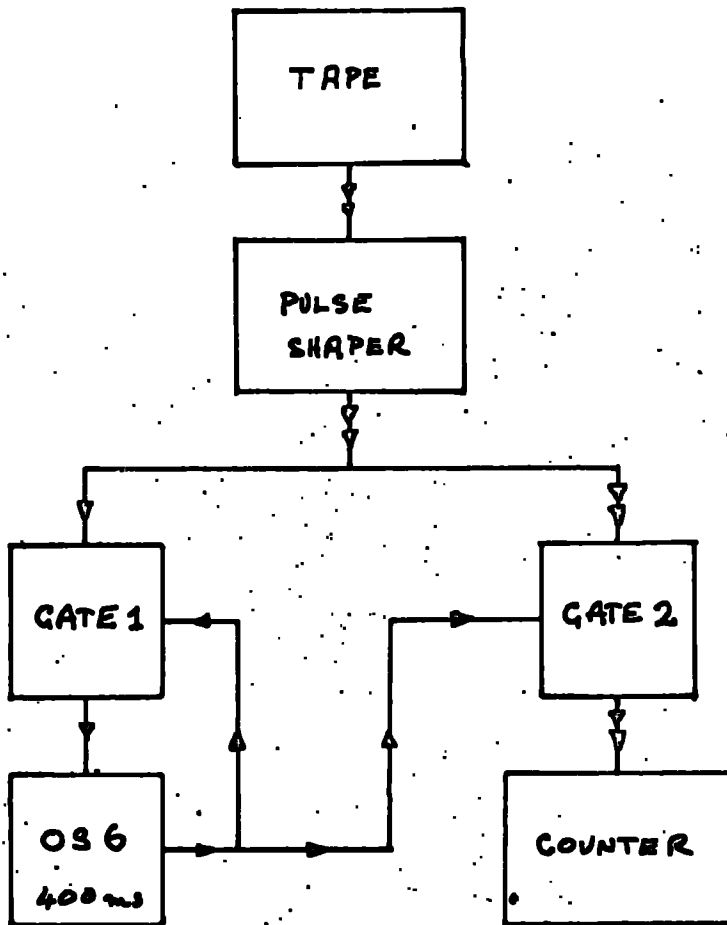
Fig. 10.3 Block-diagram of playback system

The prototype of the playback system was not completed by the author. It is hoped that a recording system may be built by a future research student, perhaps on lines similar to those laid down here. Perhaps another approach would be to adopt lines similar to those used in radiosonde equipment.

Acknowledgements

The author would like to take this opportunity to express his thanks to all the people who gave assistance in the course of the work described herein.

First and foremost to Professor J.A. Chalmers whose constant advice and encouragement were of inestimable value.

Secondly to Professor G.D. Rochester whose department provided facilities for the research. Thanks are also due to the United States Office of Naval Research from the funds of which money was made available for the purchase of equipment and payment of the author's salary.

To the technical staff of the Physics department, especially Messrs. Eric Lincoln and Denis Jobling for their advice also Mr. Jack Moralee for his assistance with the construction of apparatus.

Particular thanks are due to Drs. J.M. Breare and M.C.A. Hutchinson and to all the author's fellow research students whose advice through the medium of informal friendly conversations is deeply appreciated.

Finally a word of thanks to Miss Pat Stewart for the efficiency with which she typed this thesis.

L. N. G.
September 1966.

REFERENCES

ADAMSON, J.   1960   The compensation of the effects of potential
                                gradient variations in the measurement
                                of the atmospheric air earth current.
                                Quart. J. R. Met. Soc. 96, 252-258.

ADKINS, C.J.   1959   A rate of rainfall recorder.
                                Quart. J. R. Met. Soc. 85, 419-420.

AWE, O.   1964   Errors in correlation between time series.
                                J. Atmosph. Terr. Phys. 26, 1239-1255.

BANERJI, S.K. and
  LELE, S.R.   1952   Electric charges of raindrops.
                                Proc. Nat. Inst. Sci. India 18, 93-124.

BENNDORF, H.   1910   Luftelektrischer Beobachtungen au Graz.
                                S.B. Akad. Wiss., Wien 119, 89-110.

BENT, R.B.   1964   The testing of apparatus for ground fair-
                                weather space-charge measurements.
                                J. Atmosph. Terr. Phys. 26, 313-318.

BENT, R.B.   1964(a) Ph.D. Thesis, Durham.

BENT, R.B. and   1965
  HUTCHINSON, W.C.A.   Electrical space charges over melting snow
                                on the ground.
                                J. Atmosph. Terr. Phys. 27, 91-99.

BERGERON, T.   1935   On the physics of cloud and precipitation.
                                Gen. Ass. Int. Un. Geod. (Lisbon), 156-170.

BEST, A.C.   1950   Empircle formulae for the terminal velocity
                                of water drops falling through the atmosphere.
                                Quart. J. R. Met. Soc. 76, 302.

"BNR"   British National Report on Terr. Mag. and
                                Atm. Elec. (1936-1939).

CHALMERS, J.A.   1952   Negative electric fields in mist and fog.
                                J. Atmosph. Terr. Phys. 2, 155-159.

CHALMERS, J.A.   1953   The agrimeter for continuous recording of
                                the atmospheric electric field.
                                J. Atmosph. Terr. Phys. 4, 124-128.

BENT, R.B. and
HUTCHINSON, W.C.A.   1966   Electric space charge measurements and the
                                electrode effect within the height of a 21 m mast
                                J. Atmosph. Terr. Phys 28, 53-73.

CHALMERS, J.A.   1956   The vertical electric current during
                            continuous rain and snow.
                            J. Atmosph. Terr. Phys. 9, 311-321.

CHALMERS, J.A.   1957   "Atmospheric Electricity".
                            Pergamon Press.

CHALMERS, J.A.   1959   The electricity of nimbo stratus clouds.
                            Recent Advances in Atmospheric Electricity,
                            Pergamon Press, 309-315.

CHALMERS, J.A.   1962   The measurement of the vertical electric
                            current in the atmosphere.
                            J. Atmosph. Terr. Phys. 24, 297-302.

CHALMERS, J.A.   1965   The relation between precipitation current
                            and potential gradient.
                            J. Atmosph. Terr. Phys. 27, 899-905.

CHALMERS, J.A. and
  HUTCHINSON, W.C.A. 1949 Negative fields in the atmosphere.
                            Nature, London 164, 68.

CHALMERS, J.A. and
  LITTLE, E.W.R.   1940   The electricity of continuous rain.
                            Terr.Mag.Atmos.Elect. 45, 451-462.

CHALMERS, J.A. and
  LITTLE, E.W.R.   1947   Currents of atmospheric electricity.
                            Terr.Mag.Atmos.Elect. 52, 239-260.

CHERRY, E.M.   1963   An engineering approach to the design of
                            transistor feedback amplifiers.
                            J.Brit.I.R.E. 25, 127-144.

COLLIN, H.L.   1966   Ph.D. Thesis, Durham (to be published).

COLLIN, H.L.,
  GROOM, K.N. and
  HIGAZI, K.A.   1966   The "memory" of the atmosphere.
                            J. Atmosph. Terr. Phys. 28, 695-697.

COLLIN, H.L. and
  RAISBECK, I.A.   1964   Errors in recorded precipitation current
                            caused by splashing.
                            J. Atmosph. Terr. Phys. 26, 1107-1113.

CROZIER, W.D.   1963   Measuring atmospheric potential with passive
                                antennas.
                                J. Geophys. Res. 68, 5173-5179.

DE'SA, O. and
   MOLYNEUX, L.   1962   A transistor voltage-to-frequency convertor.
                                Electronic Engng. 34, 468-469.

DINGER, J.E. and
   GUNN, R.   1946   Electrical effects associated with a change
                                of state of water.
                                Terr.Mag.Atms.Elect. 51, 477-494.

DOLEZALEK, H.   1956   Free air insulator with a resistance of
                                more than 10^{14} ohms for all climates.
                                Technical Note 5, Contract No. AF61(514),
                                640.

ELSTER, J. and
   GEITEL, H.   1888   Uber eine Methode die elektrische Natur
                                der atmospherischen Niederschlage zu
                                bestimmen.
                                Met.Z. 5, 95-100.

FORSYTHE, G.E.   1957   J. Soc. Indus. Appl. Maths., 5, 74.

GERDIEN, H.   1905   Demonstration eines apparatus zur absoluten
                                messung der electrischen Leitfahigkeit der
                                Luft.
                                Phys. Z. 6, 800-801.

GLOSSARY OF METEOROLOGY
                       1959   Am. Met. Soc. Boston, Mass., U.S.A.

GUNN, R. and
   DEVIN, C.   1953   Raindrop charge and electric field in
                                active thunderstorms.
                                J. Met. 10, 279-284.

GSCHWEND, P.   1920   Beobachtungen uber die elecktrischen
                                Ladungen einzelner Regentropfen und
                                Schneeflocken.
                                Jb. Radioact. 17, 62-79.

HIGAZI, K.A.   1965   Ph.D. Thesis, Durham.

HIGAZI, K.A. and
CHALMERS, J.A.   1966   Measurements of atmospheric electrical
conductivity near the ground.
J. Atmosph. Terr. Phys. 28, 327-330.

HUTCHINSON, W.C.A. and
CHALMERS, J.A.   1951   The electric charges and masses of single
raindrops.
Quart. J.R. Met. Soc. 77, 85-95.

ISRAEL, H.   1957/1961   Atmospherische Elecktnzitat I/II
Leipzig.

KASEMIR, H.W.   1944   Die Zylinderfeldstarkenmulde mit kleinen
Segmenten.
Flugfunk-forschungsinstitut Oberpfallernhohen
E.V. Aussenstelle Grifelfirs B.K.F.
Ref. IIIA 1306.

KIKUCHI, K.   1965   On the positive electrification of snow
crystals in the process of their melting.
Proc. Int. Conf. Cloud Phys., 338.

KUETTNER, J.   1950   The electrical and meteorological conditions
in thunderstorms.
J. Met. 7, 322-332.

LENARD, P.   1913   Uber Elektrizitatsleitung durch freie
Elektronen und Trager, II.
Ann. d. Phys. 41, 71.

MAGONO, C. and
KIKUCHI, K.   1963   On the positive electrification of snow
crystals in the process of their melting.
J. Met. Soc. of Japan Ser.II, 41, 270-277.

MAGONO, C.,
ORIHASA, K. and
OKABE, H.   1957   The charge on precipitation elements and
surface electric potential gradient.
J. Fac. Sci. Hokkaido Univ. (7), 7-20.

MAGONO, C. and
SAKURAI, K.   1963   On the electric charge on drifting snow
pellets.
J. Met. Soc. Japan 41, 211-217.

MATHIAS, A.   1926   Fortschritte in der Auflarung der
Gewistereinfluxe auf Leitungsanlagen.
Elektrizitatswirkshaft 25, 297-300.

MOORE, C.B.,
 VONNEGUT, B. and
 MALLAHAN, F.J.   1961   Airborne filters for the measurement of
atmospheric space charge.
J. Geophys. Res. 66, 3219.

MORGAN, W.A.   1960   Determination of the straight line of best
fit to observational data of two related
variates when both sets of values are
subject to error.
Quart. J. Roy. Met. Soc. 86, 107-113.

MUHLEISEN, R.   1953   Die luftelektrischen Elemente in
Grossstadtbereich.
A. Geophys. 29, 142-160.

MUHLEISEN, R.   1961   Uber die elektrische Aufladung von Aerosol
und Dunstteilchen.
Geofisica pura e applicata 50,

NIELSEN, R.A. and
 BRADBURY, N.E.   1937   Electron and negative ion mobilities.
Phys. Rev. 51, 69-75.

NOLAN, P.J. and
 KENNY, P.J.   1953   Anomalous loss of condensation nuclei in
rubber tubing.
J. Atmosph. Terr. Phys. 3, 181-185.

NOTO, H.   1939   Some studies of thunderstorms part IV
The relation between the sign of the
potential gradient and that of the charge
on rain and snowflakes.
Jap. J. Astro. Geophys. 17, 107-118.

OBOLENSKY, W.N.   1925   Uber elektrische Ladungen in der Atmosphare.
Ann. Phys., Lpz. 77, 644-666.

OGAWA, T.   1960   Electricity in rain.
J. Geomagn. Geoelect. 12, 21-31.

CHALABI, I.E.   1965   Ph.D. Thesis, Durham.

OGOLABI, I.A. and
  CHALMERS, J.A.   1965   Correlations of precipitation currents.
                            J. Atmosph. Terr. Phys. 27, 303-308.

RAISBECK, I.A.   1963   M.Sc. Thesis, Durham.

RAMSAY, M.   1960 * Ph.D. Thesis, Durham.

RAMSAY, M.W. and
  CHALMERS, J.A.   1960   Measurements of the electricity of
                            precipitation.
                            Quart. J.R. Met. Soc. 86, 530-539.

REITER, R.   1965   Precipitation and cloud electricity.
                            Quart. J.R. Met. Soc. 91, 60.

REYNOLD, S.   1954   Compendium of thunderstorm electricity.
                            U.S. Signal Corps research report
                            (Socorro M.).

ROWSON, R.B.   1960   Inverted triode voltmeter.
                            Wireless World 66, 403-404.

SCRASE, F.J.   1933   The air earth current at Kew Observatory.
                            Geophys. Mem. London 58.

SCRASE, F.J.   1938   Electricity on rain.
                            Geophys. Mem. London 75.

SIMPSON, G.C.   1909   On the electricity in rain and its origin
                            in thunderstorms.
                            Phil. Trans. A 209, 379-413.

SIMPSON, G.C.   1919   Brit. Antarc. Exped. 1910-13.
                            Meteorology (Calcutta) 1, 302-312.

SIMPSON, G.C.   1949   Atmospheric electricity during disturbed
                            weather.
                            Geophys. Mem. London 84, 1-51.

SIMPSON, G.C. and
  SCRASE, F.J.   1937   The distribution of electricity in thunder-
                            clouds.
                            Proc. Roy. Soc. A 161, 309-352.

* should read throughout (1959)

SIVARAMAKRISHNAN, M.V.
1957   Point discharge current, the earth's electric field and rain charges during disturbed weather at Poona.
Indian J. Met. Geophys. 8, 379-390.

SMITH, L.G.   1955   The electric charge on raindrops.
Quart. J.R. Met. Soc. 81, 23-47.

SWANN, W.F.G.   1914   The theory of electrical dispersion into the free atmosphere, with a discussion of the theory of the Gerdien conductivity apparatus, and the theory of the collection of radioactive deposit by a charged conductor.
Terr. Mag. Atmos. Elect. 19, 81-92.

TERMAN, F.E.   1928   Inverted triode voltmeter.
Proc. I.R.E. 447.

"TEXAS"   Very high input impedance amplifiers.
Texas Application Note 6.

VONNEGUT, B. and
MOORE, C.B.   1958   A study of techniques for measuring the concentration of space charge in the lower atmosphere.
Final Report to Geophys. Res. Div.,
AF 19(604), 1920.

WEISS, E.   1906   Brobachtungen uber Niederschlags elektrizitat.
S.B. Acad. Wiss. Wien 115, 1285-1320.

WILSON, C.T.R.   1908   On the measurement of the atmospheric electrical potential gradient and the earth-air current.
Proc. Roy. Soc. A 80, 537.

WILSON, C.T.R.   1916   On some determinations of the sign and magnitude of electric discharges in lightening flashes.
Proc. Roy. Soc. A 92, 555-574.

WILSON, C.T.R.   1950   Atmospheric electricity.
Dictionary of Applied Physics, Vol.3, 84-107.

WORMELL, T.W.   1953   Atmospheric Electricity: Some recent trends and problems.
Quart. J.R. Met. Soc. 79, 19.